NTNU – Trondheim
Norwegian University of
Science and Technology

Investigation of Adsorption of Surfactants onto Kaolinite and Relations to Enhanced Oil Recovery Methods

Trine Johansen

Chemical Engineering and Biotechnology
Submission date: June 2014
Supervisor: Gisle Øye, IKP
Co-supervisor: Meysam Nourani, IKP

Norwegian University of Science and Technology
Department of Chemical Engineering

Preface

This thesis was submitted for the degree of Master of Science (MSc) in Chemical Engineering at the Norwegian University of Science and Technology (NTNU). The study was conducted from the 24th of January to the 20th of June 2014, and the experimental work was carried out in the Ugelstad Laboratory.

This thesis is part of a research program carried out in collaboration with the Department of Petroleum Engineering and SINTEF Petroleum, and is sponsored by Det Norske Oljeselskap, GDF SUEZ, Lundin, Statoil and Unger Surfactants.

I would like to thank my supervisor, Professor Gisle Øye, for constructive advice and guidance throughout this project, and my postdoctoral co-supervisor, Meysam Nourani, for motivational assistance regarding the experimental work. During this project, I faced several challenges with the experimental work. Countless nights were spent in the laboratory analysing samples with a hope for consistent results, and I would like to thank my fellow student Ingrid Karlsen Hov for good cooperation and pleasant company during many of these nights throughout this entire semester.

I declare that this is an independent work according to the exam regulations of the Norwegian University of Science and Technology (NTNU).

NTNU, Trondheim, 20.06.14

Trine Johansen

Abstract

Surfactant flooding is a well-established enhanced oil recovery (EOR) technique, but the economic feasibility of this method is a major concern due to the substantial misplacement and loss of expensive surfactants to the reservoir rock. However, a new focus on combining the EOR techniques of surfactant flooding and low salinity waterflooding is believed to create beneficial synergies that reduce surfactant retention.

In this study, the effect of low salinity water on surfactant adsorption was investigated. The adsorption of the anionic surfactant sodium dodecylbenzenesulfonate (SDBS) on Na-kaolinite in brines with different compositions and ionic strengths was studied for this purpose. Several test experiments were conducted in order to establish a good experimental procedure, and the analyses were conducted using both an UV-vis spectrophotometer and a ring tensiometer. Because of the large time consumption of the latter technique, the spectroscopic method was considered as the best approach for this study.

The equilibrium adsorption of SDBS on Na-kaolinite was studied by static methods, and the results were presented as adsorption isotherms, which indicated increasing SDBS adsorption with ionic strength and when adding divalent ions. The shapes of the adsorption isotherms of SDBS in monovalent brine were unexpected. Both maxima and minima were observed, and there was not an adsorption plateau, but an indication of increased adsorption after the critical micelle concentration (CMC). Adsorption isotherms with a characteristic S-shape were obtained for studies in divalent brine, and it was suspected that the adsorption maximum in these isotherms was due to the formation of precipitate when SDBS interacted with divalent ions.

The SDBS adsorption isotherms were analysed by the Langmuir and Freundlich adsorption models. The Freundlich model described the experimental data best, and SDBS systems with high salinity or divalent ions had the best fit to the theoretical model.

Sammendrag

Surfaktant fløming er en veletablert teknikk for økt oljeutvinning (EOR), men den økonomiske gjennomførbarheten av denne teknikken kan være vanskelig på grunn av tap av dyre surfaktanter til reservoarsteinen. Det er imidlertid ett nytt forskingsområde som kombinerer EOR-teknikkene surfaktant fløming og vannfløming med lav saltkonsentrasjon, som antas å skape gunstige synergier og redusert tap av surfaktant.

I dette studiet ble graden av surfaktantadsorpsjon på kaolinitt undersøkt i løsninger med ulik elektrolyttsammensetning og ionestyrke. Den anioniske surfaktanten Na-dodesylbensen-sulfonat (SDBS) og Na-kaolinitt ble benyttet til dette formålet. Flere test eksperimenter ble utført for å oppnå en god eksperimentell metode. Et UV-vis spektrofotometer og et ringtensiometer ble benyttet for bestemmelse av surfaktantkonsentrasjon. På grunn av det store tidsforbruket tilknyttet sistnevnte teknikk, ble spektrofotometrisk metode ansett som den beste analysemetoden for dette studiet.

Likevektsadsorpsjon av SDBS på Na-kaolinite ble studert ved statisk metode. Resultatene ble presentert i form av adsorpsjonsisotermer, som indikerte økt SDBS adsorpsjon ved økende ionestyrke og ionevalens. Det ble observert uventede former på adsorpsjonsisotermene for SDBS i monovalent saltløsning. Både maksimumspunkt og minimumspunkt ble observert, og det ble ikke observert et adsorpsjonsplatå, men i stedet økt absorpsjon etter kritisk micelle konsentrasjon (CMC). Isotermene for SDBS-adsorpsjon i løsning med divalente ioner hadde en karakteristisk S-form. Adsorpsjonsmaksimumet i disse isotermene ble antatt å stamme fra kompleksdannelse mellom SDBS og divalente ioner.

Adsorpsjonsisotermene ble analysert med Langmuir og Freundlich adsorpsjonsmodeller. Freundlich-modellen beskrev best de eksperimentelle resultatene for SDBS-adsorpsjonen, og tilpasningen til den teoretiske modellen var best for SDBS i saltløsninger med høy ionestyrke eller divalente ioner.

Table of Contents

List of Abbreviations

ASP	Alkaline/surfactant/polymer
CAC	Critical association concentration
CMC	Critical micelle concentration
CPP	Critical packing parameter
EOR	Enhanced oil recovery
HMC	Hemimicelle concentration
HS	High salinity
HSE	Health, safety and environment
IFT	Interfacial tension
L/S	Liquid/solid ratio
LS	Low salinity
LS-LSS	Low salinity flooding-Low salinity surfactant flooding
MIE	Multicomponent ionic exchange
MS	Medium salinity
OOIP	Original oil in place
PV	Pore volume
PZC	Point of zero charge
RPM	Revolutions per minute
SDBS	Sodium dodecylbenzenesulfonate
Sorw	Residual oil saturation to waterflood
SPM	Shakes per minute
UV-vis	Ultraviolet/visible

1 Introduction

The world's energy resources are mainly fossil fuels, which include natural gas, oil and coal. Oil dominates fuel consumption, but has the least abundant reserves among the fossil fuels (Moulijn et al., 2000, p. 1-6). As a result, great measures are taken to produce more oil from existing reservoirs.

Crude oil production is usually divided into three stages: primary, secondary, and tertiary oil recovery. The fraction retrieved from the oil reservoir increases with each stage. Primary recovery is the oil production driven by the natural pressure of the reservoir, when the pressure drops from the interior of the reservoir to the production wells, it causes a spontaneous production of oil. About 10% of the reservoir's original oil in place (OOIP) is produced during primary recovery (U.S Department of Energy, n.d.). To gain a higher oil production, secondary recovery is normally applied. This stage includes water and/or gas injection with the intention of pushing the oil towards the production wells, in addition to maintaining the reservoir pressure. These techniques lead to an oil recovery of 20-40% of OOIP (U.S Department of Energy, n.d.). This relatively low oil recovery is a result of the properties of water and gas: they are immiscible with oil and do not alter any of the forces, such as interfacial tension and viscosity that act to keep the oil within the reservoir. Consequently, a large amount of oil resists displacement from the rock pores (Scott, 1999).

The final stage is tertiary oil recovery, also known as enhanced oil recovery (EOR). EOR are techniques applied to overcome the forces that trap the oil in pores and cavities in the reservoir. These methods may lead to an oil recovery of 30-60% of OOIP (U.S Department of Energy, n.d.; Scott, 1999). EOR techniques include surfactant flooding and low salinity waterflooding, which when combined, has been the subject of interest in this study. Surfactants are used in EOR because of their ability to lower the interfacial tension between water and oil, which increases the ability to displace the oil from the rock pores. It is still not known why low salinity waterflooding has been shown to improve oil recovery in sandstone reservoirs, and several different mechanisms have been suggested. However, there is a general agreement that low salinity water increases the water wetness of the clay surface, and in this way releases oil components (Lager et al., 2008).

In the early 1960s, Marathon Oil Company conducted the first study on chemical flooding (Schramm, 2000, p. 203), and the popularity of chemical flooding increased through the 1970s

and into the 1980s when several field tests were conducted. In 1986, the oil prices dropped with more than 60% (Regnier, 2007), and the majority of the oil companies agreed that the economic risk of surfactant flooding was too high. Consequently, the research declined severely. From the 1990s to the present day, the price of oil has risen, and surfactant flooding as an EOR method has once more gained interest (Sayavedra et al., 2013). The economic aspect of surfactant flooding must be evaluated before implementation. To provide a reasonable profit from the oil produced by this EOR technique, all the expenses related to the production, transport and usages of surfactants, must be considered. The cost of the surfactant can be expected to be the most expensive element in the total cost (Schramm, 2000, p. 122).

Low salinity waterflooding was used as a complementary method to surfactant flooding in the 1970s. The low salinity water was injected to pre-flush reservoirs with a high salinity concentration to avoid precipitation of surfactants (Byham, 1985; Lager et al., 2008). Since the 1990s, research has been conducted on low salinity waterflooding as a stand-alone technique for sandstone reservoirs. Jadhunandan and Morrow (1991; 1995) were two of the first to research and publish articles on how brine composition affected wettability, and consequently, oil production. After Yildiz and Morrow (1996) published their pioneer paper on the effect of brine composition on crude oil recovery by waterflooding, the interest in this method, both as a secondary and tertiary EOR technique, increased.

Today, there is a focus on a new technique that combines surfactant flooding and low salinity waterflooding. This hybrid technique is believed to create several beneficial synergies. Because of the high cost of surfactants, it is important to minimize the loss of surfactants during chemical flooding. The adsorption and loss of active material during this process has been studied over several decades, but surfactant adsorption in combination with low salinity water is a relatively new area. The aim of this study was to investigate the effect of brine composition and ionic strength on the quantity of surfactants adsorbed on kaolinite. Adsorption isotherms of the anionic surfactant sodium dodecylbenzenesulfonate (SDBS) in five different brines were created and compared, and the experimental results were fitted to Langmuir and Freundlich isotherm models. The surfactant depletion method was used to determine the amount of adsorbed surfactant, and the analyses were conducted with an UV-vis spectrophotometer and a ring tensiometer.

2 Theory

2.1 Enhanced Oil Recovery

Enhanced oil recovery (EOR) techniques are applied after secondary recovery in order to mobilize trapped oil and increase oil production. EOR may increase oil recovery by an additional 30% of the OOIP (U.S Department of Energy, n.d.; Scott, 1999). EOR methods are based on the alteration and manipulation of forces and phenomena in the reservoir. Among these are interfacial tension, wettability, capillary forces and viscous forces, which are given a short description in the following sections.

2.1.1 Interfacial Tension

Interfacial tension (IFT) is defined as the force per unit length at the interface between two different phases. IFT occurs in every system where immiscible phases coexist. In the case of a liquid/vapour interface, the IFT is often referred to as surface tension. IFT arises from an imbalance in the intermolecular forces acting on molecules at the interface. It can be described as a contractile force that tries to shrink the surface area (Mørk, 2004, p.48-50; Green and Willhite, 1998, p. 12; Hiemenz and Rajagopalan, 1997, p. 248).

Water-in-oil emulsions can be used as an example to describe the IFT phenomenon. In the water bulk solution, hydrogen bonds are formed between oxygen and hydrogen atoms of neighbouring water molecules. On average, the attractive intermolecular forces will be equal in all directions, and thus sum to zero. However, at the oil/water interface, the forces that act on the water molecules are unequal and not symmetrical. The intermolecular attractive forces between two water molecules are greater than between oil and water molecules, and consequently the water molecules at the interface are pulled by a net force towards the water phase in an attempt to minimize the interface.

Interfacial tension has great importance in EOR technology, and numerous parameters affect the IFT between the phases in a reservoir. The type and concentration of electrolyte, molecular weight and structure of the oil phase, the temperature and the age of the system all affect the

IFT (Sheng, 2011; Sharma and Shah, 1989). The EOR technique, surfactant flooding, increases oil production by manipulating the IFT between the oil and water phase.

2.1.2 Wettability

Wettability is a term used to describe a fluid's tendency to spread on a solid surface in the presence of another immiscible fluid. In other words, the wettability describes the surface's relative affinity for nearby fluid phases (Green and Willhite, 1998, p. 13; Alagic, 2010). In reservoirs, if the oil phase has a greater affinity towards the reservoir rock and thus greater spreading tendencies than water, then the reservoir is referred to as oil-wet, and vice versa.

Wettability is an important parameter in oil recovery processes. The effect of secondary waterflooding is highly dependent on the wetness of the reservoir rock. A water-wet system typically displays no oil production after water breakthrough. An oil-wet system is characterised by early water breakthrough and a long tail production with a high water cut (Alagic et al., 2011). The optimal condition in order to maximize oil recovery by waterflooding is a weakly water-wet surface (Jadhunandan and Morrow, 1995; Yildiz and Morrow, 1996).

The wettability of the reservoir depends on several parameters such as ageing time, temperature, initial water saturation, the crude oil's characteristics and most importantly, the brine composition and ionic strength (Yildiz and Morrow, 1996). In recent years, low salinity waterflooding has been used as an EOR technique to alter the wettability in order to increase oil production (Austad et al., 2010).

2.1.3 Capillary Forces and Viscous Forces

Capillary forces are defined as the directional forces acting on the liquid meniscus in a capillary. When a liquid is in contact with a solid surface, e.g., a liquid in a capillary, the system has three interfaces and hence three separate IFTs. The liquid's surface tension gives rise to forces that act on the liquid meniscus in the line of contact between the liquid and the capillary wall. Capillary forces play an important role in any system where capillaries, pores or porous structures are involved, e.g., a reservoir rock (Mørk, 2004, p. 59-64).

Capillary forces and viscous forces act to keep the oil trapped in pores and cavities in an oil reservoir. The capillary number is defined by Equation (1), which gives the ratio of viscous to capillary forces (Sharma and Shah, 1989).

$$N_c = \frac{\mu_w \varphi q}{\gamma_{o/w}} \quad (1)$$

Where:

N_c	:	The capillary number
μ_w	:	Viscosity per unit cross-section area of water
φ	:	Porosity of the reservoir rock
q	:	Flow rate per unit cross-section area of water
$\gamma_{o/w}$	:	Interfacial tension between oil and water

An increase in capillary number corresponds to easier displacement of trapped oil. Thus, achieving a high capillary number is desired when producing oil. After secondary oil recovery by waterflooding, the capillary number is usually between 10^{-7} and 10^{-6}. In order to produce 50% of the remaining oil, the capillary number must increase to somewhere between 10^{-4} and 10^{-3}. An oil recovery of 100% corresponds to a capillary number in the range of 10^{-2} to 10^{-1} (Schramm, 2000, p. 206-207; Sharma and Shah, 1989).

As shown in Equation (1), the capillary number can be improved by increasing the viscosity and/or flow rate of water. Thus, increased water viscosity may mobilize the oil trapped by capillary forces after a waterflood. Another alternative is to decrease the IFT between oil and water in the reservoir. These parameters are manipulated in the EOR technique, chemical flooding. Chemical flooding involves the injection of a chemical/water solution that flows through the porous rocks in order to reduce the oil-water IFT and/or increase the viscosity of injected water, which subsequently results in a more effective displacement process. The injected chemicals may be alcohols, caustics, polymers, carbon dioxide, surfactants or other substances that can increase the oil production (Austad et al., 1991b; Scott, 1999). The capillary number can be increased 3-4 orders of magnitude by altering the IFT with the use of surfactants (Sharma and Shah, 1989).

It is also possible to lower the viscosity of oil in order to increase oil production. Thermal recovery methods, such as steam injection and in-situ combustion, use heat to lower the oil viscosity. These methods leads to an increase in mobility, and consequently, the oil transportation to the producer wells increases (Scott, 1999).

2.2 Surfactants

Surfactants are amphiphilic molecules with hydrophobic alkyl chains and a polar head group. Surfactants are categorized in four main groups by the charge of their head group: anionic, cationic, zwitterionic and non-ionic. The anionic group is the largest, and accounts for about 60% of the total amount of surfactants. The alkyl chain may be branched, comprise phenyl groups, double bonds or be fluorinated. Some surfactants have more than one alkyl chain (Holmberg et al., 2002, p. 8-24).

The term *surfactant* was derived from *surface-active agent*, which describes to their ability to adsorb at the surface or interface between two phases and alter the properties of the interface. At a water surface, the polar head group will be directed towards the water phase, while the hydrophobic chain will face away from the water, giving the water surface a hydrophobic characteristic.

2.2.1 Micelle Formation

When the surfactant concentration increases, it eventually reaches the critical micelle concentration (CMC). At this concentration, the surface is fully loaded with surfactant monomers, and the monomers begin to form aggregates, also known as micelles. The hydrophobic chains of the surfactant molecules interact with each other, and generally form a spherical shape with the polar head groups pointing towards the water. Consequently, the hydrophobic core is shielded from the water phase. These spherical micelles can be compared to minimalistic oil droplets coated with polar groups. Several physical properties of the surfactant solution are concentration-dependent and will change dramatically when the CMC is reached. The concentration dependence of some of these physical properties is illustrated in Figure 1 (Holmberg et al., 2002, p. 41-43).

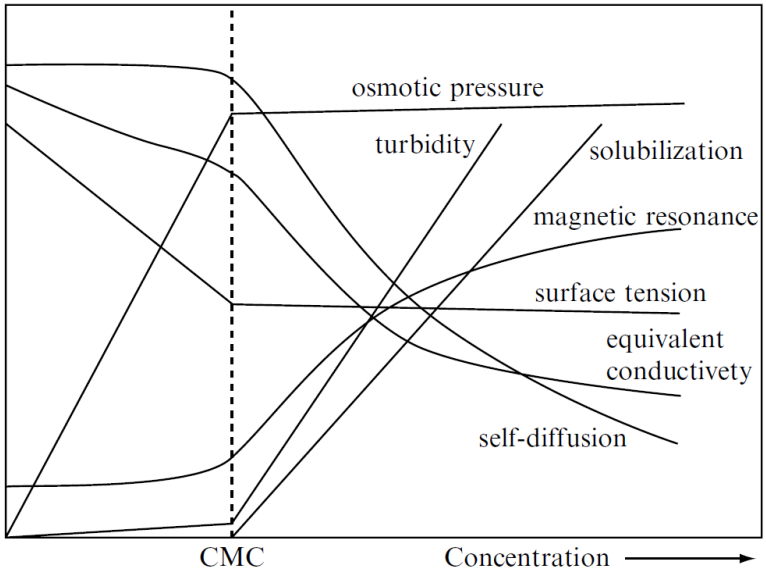

Figure 1. Graphic representation of the concentration dependence of physical properties for solution of an ionic micelle-forming surfactant (Holmberg et al., 2002, p. 42).

Several properties of surfactants influence the CMC, such as length or branching of the hydrophobic tails, charge of the head groups and valency of the counter ions. In addition, the CMC of ionic surfactants is strongly influenced by the presence of electrolytes. The addition of electrolytes dramatically lowers the CMC and the longer the hydrophobic chains, the greater the decrease. Furthermore, the effect depends strongly on the valency of the ions. Higher valency results in a greater decrease of the CMC. This reduction is due to a compression of the electrical double layer surrounding the hydrophilic head groups, which reduces the electrostatic repulsion between the surfactants. The electrical double layer is defined as a charged surface together with the thin film surrounding it containing free ions (Mørk, 2004, p. vii, Holmberg et al., 2002, p. 43-48). The electrical double layer is described in more detail in section 2.6.2.

2.2.2 Micellar Growth

When the surfactant concentration increases after the CMC, various surfactant systems will respond differently. In some systems, the micelles will remain small and spherical, but in other systems, the aggregation structure may change dramatically. The phase structure of the

surfactant solution determines several different physiochemical properties, viscosity being one of the most important.

The tendency towards micellar growth for ionic surfactants is related to several factors; it is promoted by long alkyl chains, a decrease in temperature, specific counterions, the addition of salt, and of course increased surfactant concentration (Holmberg et al., 2002, p. 70-71). When a surfactant system is altered by any of these parameters, the intermicelle repulsions become greater. This induces micellar growth in which the micelles become packed in a more energetically favourable manner (Alagic, 2010).

The critical packing parameter (CPP) provides a geometric characterisation of a surfactant molecule, and is helpful when predicting the type of aggregate structure that is most likely to occur. The CPP is expressed in Equation (2) (Holmberg et al., 2002, p. 60-61).

$$CPP = \frac{v}{l \cdot a} \qquad (2)$$

Where:

CPP	:	Critical packing parameter
v	:	Volume of hydrophobic chain
l	:	The extended length of hydrocarbon chain
a	:	Effective area per polar head group

Several different surfactant aggregates, and the CPPs that promote these structures are presented in Figure 2.

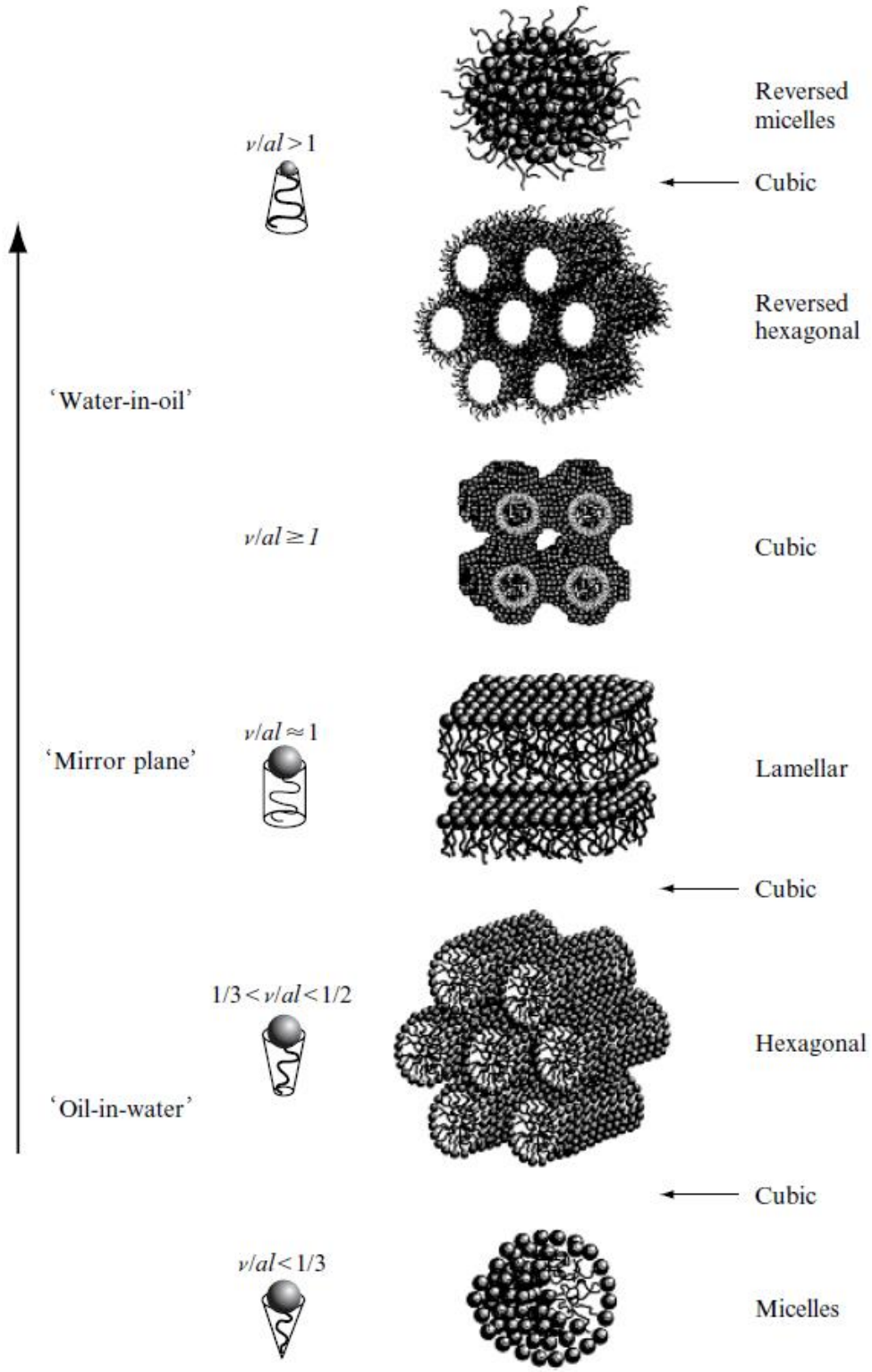

Figure 2. Surfactant aggregate structures and the CPPs that induce these structures (Holmberg et al., 2002, p. 91).

2.2.3 Surfactants in the Petroleum Industry

When surfactants are implemented in EOR techniques, it is important to reduce the loss of surfactants due to interactions with the reservoir rock. In the North Sea, there are mainly sandstone reservoirs. Sandstone has a negative surface, and in order to minimize surfactant adsorption, it is advantageous to use anionic surfactants. However, anionic surfactants will still adsorb to some extent on the negatively charged surface (Schramm, 2000, p. 128; Lv et al., 2011).

Sulfonates are common anionic surfactants used in EOR processes. Sulfonates are salts of sulfonic acids where a hydroxysulfonyl group is attached with a strong thermal and chemical bond between the sulphur atom and the hydrophobic chain. Sulfonates are water soluble and sensitive to water hardness, and these properties are both dependent on the molecular mass. With increased molecular mass, the sulfonates become less water soluble and more sensitive to hard water (Kosswig, 2012). Petroleum sulfonates, synthetic sulfonates and ethoxylates sulfonates are the three main groups of sulfonates applied in chemical flooding. Petroleum sulfonates are produced from refining products and are included in most surfactant formulations for EOR. Synthetic sulfonates are highly effective EOR surfactants, but are also more expensive. Alkyl benzene sulfonates were one of the first groups of synthetic sulfonates to be commercially applied. Ethoxylates sulfonates are often used in combination with petroleum sulfonates to increase the effect of the EOR process and increase the salinity tolerance (Sharma and Shah, 1989).

2.2.4 Sodium Dodecylbenzenesulfonate

In this study, a synthetic sulfonate surfactant, sodium dodecylbenzenesulfonate (SDBS), was used. This surfactant is an alkyl benzene sulfonate, and the chemical structure is shown in Figure 3.

There are several isomers of this surfactant, where the head group is attached to different carbon atoms in hydrophobic chain (Dick et al., 1973). Chou and Bae (1983) determined the CMC of SDBS to $1.7 \cdot 10^{-3}$ M in distilled water without co-solutes. Many adsorption studies have utilized this surfactant (Hanna and Somasundaran, 1979; Torn et al., 2003; Siffert et al., 1992; Sastry et al., 1995; Healy et al., 2003). In adsorption studies of surfactant on clay minerals, SDBS has

been shown to be superior to other linear alkyl sulphates due to its resistance to hydrolysis (Sastry et al., 1995).

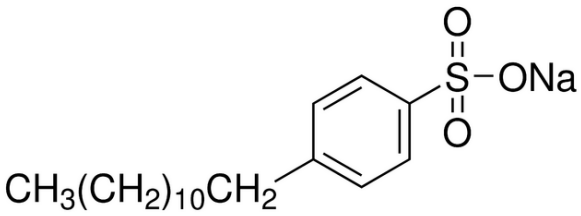

Figure 3. Sodium dodecylbenzenesulfonate (SDBS) (Sigma Aldrich, 2013).

2.3 Surfactant Flooding

Surfactants are used in a wide range of applications in the petroleum industry, and among them, several EOR techniques. These include classic micellar/polymer (surfactant) flooding, alkaline/surfactant/polymer (ASP) flooding, and foams. Surfactant flooding is based on the surfactants' ability to lower the interfacial tension between water and oil in a reservoir. This results in a reduction of the capillary forces that prevent trapped oil from mobilizing. In ASP, the interfacial tension is decreased to an ultralow level by the cooperation between alkali and surfactants, while polymers are controlling the mobility. This system effectively increases the oil production. Foam may lead to an increased oil production by increasing the sweep efficiency and controlling the mobility (Schramm, 2000, p. 121; Alvarado and Manrique, 2010).

2.3.1 Conventional Surfactant Flooding

Surfactant flooding is usually applied as an EOR technique near the end of a waterflood. The chemical process is illustrated in Figure 4.

Region 1 illustrates the residual oil saturation after waterflood (Sorw), which can be defined as the liquid that remains in an oil reservoir after a waterflood. After the waterflood, only an aqueous phase is flowing in region 1 (Schramm, 2000, p. 205; Green and Willhite, 1998, p. 7).

Injected micellar solution is specified by volume of primary slug, which is usually in the range of 3 to 30% of the flood pattern pore volume (PV). The IFT between the micellar solution and the residual oil is very low, and enables the gravity forces to displace the trapped oil. The mobilized oil forms an oil bank in front of the micellar slug, as illustrated by regions 2 and 3 in Figure 4 (Schramm, 2000, p. 205; Green and Willhite, 1998, p. 7).

The viscosity of the micellar solution may be adjusted with polymers to obtain a favourable mobility ratio between the micellar slug and the oil bank. Thus, both viscosity and capillary forces are altered to enhance oil recovery. Because of the high cost of surfactants, the volume of the micellar slug should not be too large, and a less expensive fluid is used to displace the slug. Water is not suitable because of its relatively low viscosity, which creates undesired mobility effects. Thus, the viscosity of the water is increased by adding polymers, and this solution is injected after the micellar slug, as illustrated by region 4 (Schramm, 2000, p. 205; Green and Willhite, 1998, p. 7).

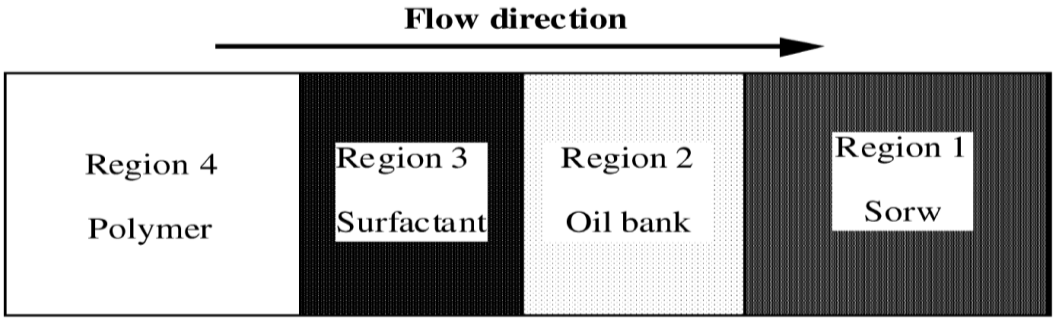

Figure 4. Phase position in a chemical flooding process (Schramm, 2000, p. 205).

2.3.2 Alteration of the Interfacial Tension

When surfactant flooding is introduced to a reservoir, the surfactants in the water phase will accumulate on the interface between oil and water. This will result in a reduced IFT and subsequently increase the capillary number according to Equation (1), as previously described. The IFT should be at an ultra-low level so that the work required to deform the oil droplets is reduced sufficiently to mobilize oil trapped in the porous structure. The effect of surfactant flooding is illustrated in Figure 5, which illustrates how the deformed oil drops are able to flow

through narrow pores. To obtain an ultra-low IFT, surfactants should adsorb and cover as much of the interface between the phases as possible (Sharma and Shah, 1989).

Several properties of surfactants affect the IFT between the phases in a reservoir. Among these are concentration, molecular weight, distribution and structure (Sheng, 2011; Sharma and Shah, 1989). As the surfactant concentration increases towards the CMC, the IFT between the aqueous phase and oil phase decreases and approaches its minimum value. At low surfactant concentration, there are two phases present—oil and aqueous, while at high concentration there is a third phase known as microemulsion (Sharma and Shah, 1989). A microemulsion is a thermodynamically stable colloidal system in which surfactants adsorbed on oil droplets (10-100 nm) are dispersed in an aqueous phase.

The IFT between the aqueous phase and the oil phase is strongly dependent on the salinity of the aqueous phase. There is an optimal concentration of salt where the IFT is at its minimum. This concentration is referred to as the optimal salinity. At this value, the amount of surfactants adsorbed at the interface is at its maximum, creating an ultra-low IFT (Sharma and Shah, 1989). If the salinity increases beyond the optimal salinity, the surfactants will prefer the oil phase rather than the interface. Similarly, if the salinity is below the optimal salinity, the surfactants will prefer the aqueous phase rather than the interface. Thus, by varying the salinity of the aqueous phase, the relative solubility of surfactants in the oil and water can be manipulated (Sharma and Shah, 1989; Sheng, 2011).

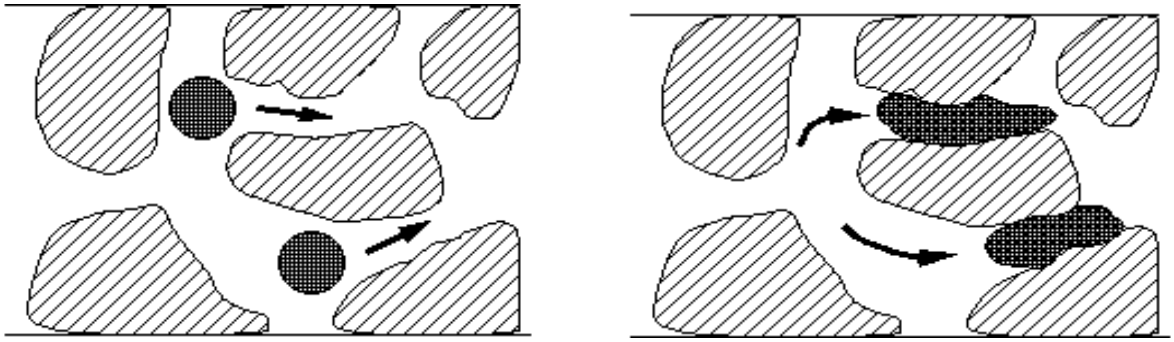

Figure 5. The effect of surfactant flooding, where a decrease in IFT results in the deformation of the oil droplets and mobilization of trapped oil (Sim Science, n.d.).

2.4 Low Salinity Waterflooding

In the last decade, there have been several laboratory studies on low salinity waterflooding, and some single well field tests. Low salinity flooding has been used both as a secondary and tertiary oil recovery method. In secondary recovery, low salinity water is injected after the core is restored from re-injection of formation water. When low salinity water is used as an EOR technique, low salinity water is introduced after the oil production plateau is reached by secondary waterflooding. The low salinity water usually has a salt concentration of 1000-2000 ppm, and is prepared by diluting the formation water with distilled water (Tang and Morrow, 1999; McGuire et al., 2005; RezaeiDoust et al., 2009; Austad et al., 2010).

Several studies (Tang and Morrow, 1999; McGuire et al., 2005) report an increased oil production when low salinity water is applied as an EOR technique in sandstone reservoirs. The low salinity flood has been shown to increase the oil production with about 5-20% of OOIP (RezaeiDoust et al., 2009). There is little documentation of increased oil production by low salinity water in carbonate reservoirs. In these reservoirs, seawater has shown to increase the oil recovery compared to formation water (RezaeiDoust et al., 2009).

Tang and Morrow (1999) and Larger et al. (2008) listed conditions necessary to obtain the EOR effect of low salinity waterflooding, and these conditions are widely acknowledged and have been referred to by several researchers (RezaeiDoust et al., 2009; Austad et al., 2010). Among these conditions are the necessity of polar components in the crude oil and divalent cations in the formation water.

The clay minerals in the reservoir act as cation exchangers, and especially divalent cations interact with the surface more readily. In addition, organic materials in crude oil, including both acids and bases, adsorb on the clay surface. On an oil-wet surface, the organic components are adsorbed directly on the surface in addition to binding to the adsorbed divalent cations creating organo-metallic complexes; in other words, divalent cations create a bridge between the clay and the organic molecule. At this stage, before the low salinity waterflooding, the formation water in the reservoir has a pH of about 5 due to dissolved H_2S and CO_2 (Austad et al., 2010; Lager et al., 2008).

There is broad agreement that introducing low salinity water will change the wettability of the clay minerals in the reservoir. However, there is still no consensus on the mechanisms behind

the EOR effect. There are four well-established theories: salting-in, migration of fines, decrease in pH and multi-ion exchange (Austad et al., 2010; RezaeiDoust et al., 2009).

The ions in brine water have no preference for the oil phase over the aqueous phase, and with increased salt concentration, the solubility of organic material in the water will decrease. This effect is known as salting-out. Consequently, if the salt concentration decreases, the solubility of organic material in the water will increase. This mechanism is referred to as salting-in, and has been suggested as the mechanism behind the increased oil recovery by low salinity waterflooding. The theory behind this mechanism is that the increased solubility of organic materials in water will lead to desorption of crude oil components from the clay surface and thus increase oil production (RezaeiDoust et al., 2009).

Tang and Morrow (1999) investigated the influence of brine composition and fines migration on oil recovery, and suggested a mechanism responsible for the EOR effect of low salinity flooding. The theory is based on the mobilization of fines in pores and cavities in the reservoir during waterflooding. The fines are stabilized on the solid surface by colloidal forces, and a balance between van der Waals attractive forces and electrostatic repulsion between the fine particles are established. Lowering the salinity leads to an expansion of the electrical double layer around the particles, consequently making it easier to mobilize fines. It was suggested that this mechanism resulted in increased water wetness of the surface and increased oil production. Larger et al. (2008) performed laboratory studies at reservoir conditions that showed enhanced oil recovery without the presence of fines, and was as a consequence sceptical of this theory.

Multicomponent ionic exchange (MIE) is a well-established adsorption theory that focuses on the competition between ions to adsorb on mineral surface exchange sites. Based on several studies that showed a decrease in Ca^{2+} and Mg^{2+} in the formation water after low salinity waterflooding, Larger et al. (2008) suggested that low salinity water promotes MIE mechanisms in the reservoir, and subsequently increase oil production. This proposal was explained in the following manner: Low salinity waterflooding leads to a change in the ionic exchange equilibrium, leading to a net desorption of adsorbed ions from the clay. The divalent ions in this new brine composition may exchange with cationic organic complexes adsorbed directly on the mineral surface or as organo-metallic complexes. Consequently, the concentration of Ca^{2+} and Mg^{2+} decreases, the mineral surface becomes more water-wet and the oil production increases.

During low salinity flooding, the pH in the reservoir increases, and the effluent water is usually measured 1-3 units above the formation water (Tang and Morrow, 1999). Austad et al. (2010)

suggested that the increase in pH results in precipitation of $Mg(OH)_2$ and consequently a decrease in Mg^{2+} concentration, and that the cation exchange suggested by Larger et al. was less dominant.

McGuire et al. (2005) suggested that low salinity flooding has the same effect as alkaline flooding, in other words, that the increase in pH is the dominant factor towards increased oil production. Alkaline flooding is known to decrease the interfacial tension between oil and water in addition to increasing the water wetness of the mineral surface. There has been some questioning of the effect of low salinity flooding as compared to alkaline flooding since in some studies, the pH is measured to have only increased by 1 (RezaeiDoust et al., 2009). In addition, one of the best low salinity results were obtained by coreflood with crude oil having a low acid number, which is known to give unsuccessful results with alkaline flooding (Lager et al., 2008).

Austad et al. (2010) recently proposed a new mechanism. This mechanism is based on the increase in pH in the area close to the clay surface. The pH increases as a consequence to an alteration of the brine adsorption-desorption equilibrium, which leads to the substitution of Ca^{2+} adsorbed on the clay with H^+ from the surrounding water. Austad et al. (2010) suggested that a subsequent reaction between OH^- and the adsorbed organic material takes place, resulting in desorption of organic material, and consequently a water-wet surface and increased oil production. This mechanism is based on the assumption that the composition of oil, the composition and pH of the initial formation water, and the properties of the dominant clay in the reservoir, have a large impact on the EOR effect of low salinity flooding. Figure 6 illustrates the principle of the model suggested by Austad et al. (2010).

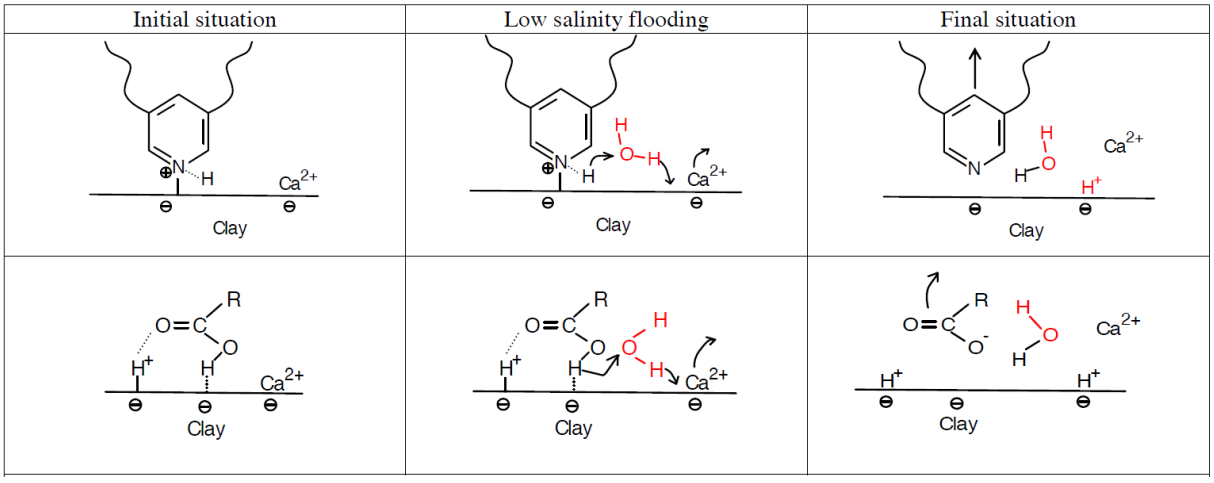

Figure 6. Mechanism of the low salinity EOR effect proposed by Austad et al. (2010). Upper: Desorption of basic material. Lower: Desorption of acidic material.

2.5 Combination of Surfactant Flooding and Low Salinity Waterflooding

The hybrid EOR process that combines low salinity waterflooding with surfactant flooding has very recently piqued the interest of some researchers. Notable are various articles on the subject published by UNI Research, Centre for Integrated Petroleum Research, several of which are part of a doctoral thesis written by Edin Alagic (2010).

In a low salinity/surfactant flooding (LS-LSS) process, low salinity waterflooding is followed by surfactant flooding at the same salinity. The idea is that a more efficient oil recovery process can be obtained by combining the two EOR techniques. Low salinity water is injected in order to destabilize and mobilize the oil layers, while the surfactants are then applied to create a low IFT environment that prevents re-trapping of the mobilized oil. Thus, combining the two stand-alone EOR techniques is believed to create beneficial synergies (Alagic et al., 2011; Sun et al., 2014; Alagic and Skauge, 2010).

There are several advantages to using surfactants in combination with low salinity water. First, the surfactant solubility is strongly improved in a low salinity environment. Second, efficient surfactants at low salinities are more commercially available and less expensive than equivalent efficient surfactants in high salinity brine. As a result, there are more surfactants to choose from, and also a greater range of environment-friendly surfactants (Alagic et al., 2011; Alagic and Skauge, 2010).

Alagic and Skauge (2010) preformed core flood experiments on outcrop sandstone cores in order to study the combination of low salinity brine and surfactant flooding. An anionic surfactant was used in low salinity water containing 0.50 wt% NaCl, in which the surfactant formed Winsor type I (oil-in-water) microemulsion. Results showed high oil recovery when surfactant flooding was applied in tertiary mode with a stabilized low salinity environment, but the oil recovery was significantly reduced when the surfactant solution was introduced into a high salinity environment. High salinity contributes to trapping the surfactant in the oil phase, which leads to a delay of the breakthrough. Paul and Froning (1973) investigated salinity effects on micellar flooding and reached a similar conclusion. The results pointed towards an increased oil production when introducing surfactants in an environment with similar brine composition.

The optimum salinity in the LS-LSS process is not usually equal to the optimal salinity for low salinity flooding or surfactant flooding as stand-alone techniques. The oil recovery in the LS step is higher with lower salinity (Austad et al., 2010), while the IFT between oil and water is

reduced by higher salinity in the LSS step (Tichelkamp et al., 2014). However, the salinity should be close to the optimal salinity with respect to surfactant flooding in order to give a sufficient low IFT in the LSS step. Sun et al. (2014) investigated how to optimize the salinity for a LS-LSS process in a North Sea field case and pointed out that loss of surfactant (retention) must be taken into consideration. Since high surfactant retention seemed to be a characteristic of ultra-low IFT systems, the optimum salinity in the LS-LSS process was arrived through a compromise between ultra-low IFT and surfactant retention.

Alagic et al. (2010) investigated the effect of surfactant concentration and slug size on the efficiency of the LS-LSS process. The results indicated that oil recovery was mainly dependent on surfactant concentration, but that the slug size had little influence on oil production.

The studies on the LS-LSS process to date shows promising results in terms of oil recovery. However, only lab scale experiments have been conducted and field application may give different results. The economic aspects should also receive more attention.

Parallel to the studies on the LS-LSS process, a hybrid process where low salinity water is used in combination with polymers has been investigated. Shiran and Skauge (2013) addressed the timing of low salinity waterflooding and the added benefit of polymer injection. The results of this study indicated that injection of small amounts of polymer further increased the oil recovery in a low salinity environment.

2.6 Adsorption of Surfactants on Solid Surfaces

During the surfactant flooding process, surfactants are misplaced and lost due to adsorption, chromographic effects, entrapment and partitioning in the reservoir rock, where adsorption is the dominating mechanism (Austad et al., 1991a; Figdore, 1982). From an economic point of view, it is important to minimize these interactions, and to do so an understanding of surfactant adsorption mechanisms is required.

During the adsorption process, surfactant molecules are transported from the bulk solution to the interface. Interactions and mechanisms like ion pairing, electrostatic attraction, hydrogen bonding, hydrophobic bonding, covalent bonding and ion exchange can contribute to the adsorption and desorption of surfactants on solids. The dominant mechanism may change when

the contact time between surfactants and solid is extended (Somasundaran and Krishnakumar, 1997; Lv et al., 2011; Austad et al., 1991b).

2.6.1 Influence of Surface Characteristics

Two main mechanisms contribute to surfactant adsorption. The first is the interaction between the surfactants and the solid surface, and the second is surfactant-surfactant interactions. The latter is referred to as the hydrophobic effect, the extent of which is highly dependent on the surfactants' structures. The effect becomes more dominant as the length and branching of the hydrophobic chains increases (Holmberg et al., 2002, p. 357).

Hydrophobic surfaces

On hydrophobic surfaces, the hydrophobic effect is the dominant adsorption mechanism. In these systems, the surfactants adsorb with the hydrophobic tails on the surface and the hydrophilic head groups towards the solution. This gives a more energetically favourable system as the hydrophobic tails are sheltered from the aqueous environment upon adsorption. This mechanism has several similarities to micelle formation, and the adsorption free energy of the surfactants at a hydrophobic surface is close to the micellisation free energy by the surfactants (Holmberg et al., 2002, p. 357-358). The surfactant structures formed on hydrophobic surfaces are presented in Figure 7.

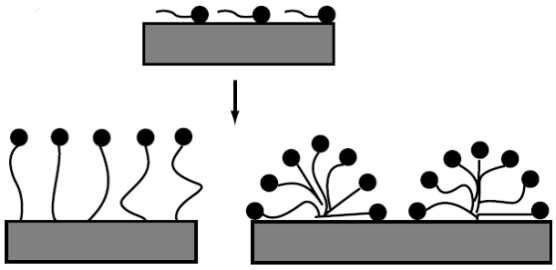

Figure 7. Surfactant adsorption on hydrophobic surfaces (Holmberg et al., 2002, p. 358).

Hydrophilic surfaces

In surfactant systems with hydrophilic surfaces, the surfactants adsorb with their polar head groups on to the surface. At higher surfactant concentrations, the surfactants either create surface aggregates or adsorb with their head groups onto the surface. The surfactant structures formed on hydrophilic surfaces are presented in Figure 8.

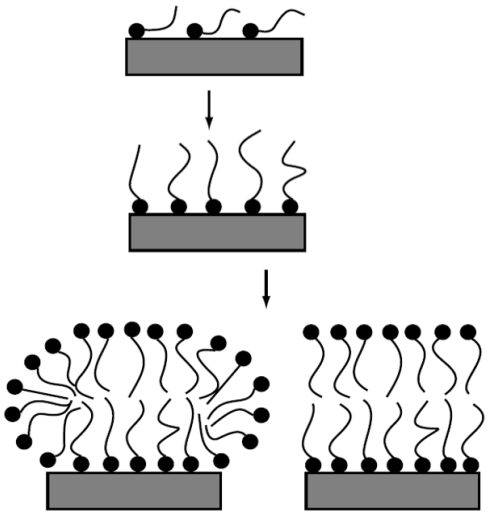

Figure 8. Surfactant adsorption on hydrophilic surfaces (Holmberg et al., 2002, p. 358).

In the first case (left side in Figure 8), the attraction between the polar head groups and the hydrophilic surface are relatively weak. The hydrophobic attraction between the surfactants are the dominant interaction, and leads to the formation of surface aggregates. In the second case (right side in Figure 8), there is strong attraction between the surfactant head group and the solid surface. This is typical for ionic surfactants that adsorb on oppositely charged surfaces. In these systems, a monolayer of surfactants is formed where the hydrophobic tails are pointed towards the solution, giving the surface a hydrophobic characteristic. This enables formation of bilayers where surfactants adsorb by hydrophobic interaction between surfactant-surfactant at increased surfactant concentrations (Holmberg et al., 2002, p. 357-358). Thus in these systems, electrostatic interactions between charged sites on the solid surface and the charged head groups of the surfactants, has a great significance for adsorption. Consequently, the electrical double layer at the solid/liquid interface is usually an important phenomenon for the adsorption of ionic surfactants (Paria and Khilar, 2004).

2.6.2 Surface Charge and Electrical Double Layer

Origin of charges at a surface

A charged surface may arise through several mechanisms. Among these are preferential adsorption of ions from the surrounding medium, and the ionization or dissociation of surface groups. Examples of the latter are deprotonation of silanol groups on the surface of quartz in aqueous solution, creating a negative charge, and elimination of hydroxyl groups on the surface of aluminium oxide based particles, leading to a positive charge. Isomorphic substitution of ions may also occur. In this process, one element replaces another in the crystal structure of the mineral. Examples are the replacement of Si^{4+} ions with Al^{3+} or replacement of Al^{3+} with Mg^{2+}, both of which result in a charged surface.

However, preferential adsorption is usually most common, and several mechanisms fall under this category. One of these mechanisms is the release of less preferential ions. Ionic compounds may emit different amounts of the ions they consist of and form an equilibrium distribution of potential determining ions between the surface and the solution. This mechanism indicates that the affinity towards the surface is stronger for some of the ions and those ions will be found in excess on the surface. The adsorption of ionic surfactants on the interface in aqueous solutions is another example of preferential adsorption. Ionic surfactants will dissociate in water and adsorb on hydrophobic interfaces with the ionic group directed towards the aqueous phase. Thus, a charged surface will be created (Hiemenz and Rajagopalan, 1997, p. 502-504; Mørk, 2004, p. 194-197).

The electrical double layer

One of the earliest models describing the adsorption of surfactant on solid was the electrical double layer theory. This theory was suggested by Helmholtz in 1879 and revised by Stern in 1924. When ions are present in a system with two or more phases, a gradient of electric potential will form across the interface. One side of the interface carries a positive charge, while the other carries an equal negative charge. These two charged portions of the interface constitute the electrical double layer (Hiemenz and Rajagopalan, 1997, p. 499; Schramm, 2000, p. 125-126).

Figure 9 displays a schematic representation of the electrical double layer. The Stern modification divided the counterions in the solution, opposite in charge relative to the surface, into two separate regions. The first region is the inner layer known as the Stern layer (δ). This layer consists of immobile ions adsorbed close to the surface. The Stern plane separates the

Stern layer from an outer diffuse layer of mobile ions, often referred to as the Gouy-Chapman layer. As illustrated in the figure, the potential decreases rapidly within the Stern layer from the surface potential (Ψ_0) to the potential at the stern plane (Ψ_δ), and this rapid decrease is due to a masking of the surface charge by the adsorbed ions. The potential decreases more gradually within the diffuse layer (Schramm, 2000, p. 126-127; Mørk, 2004, p. 206-211).

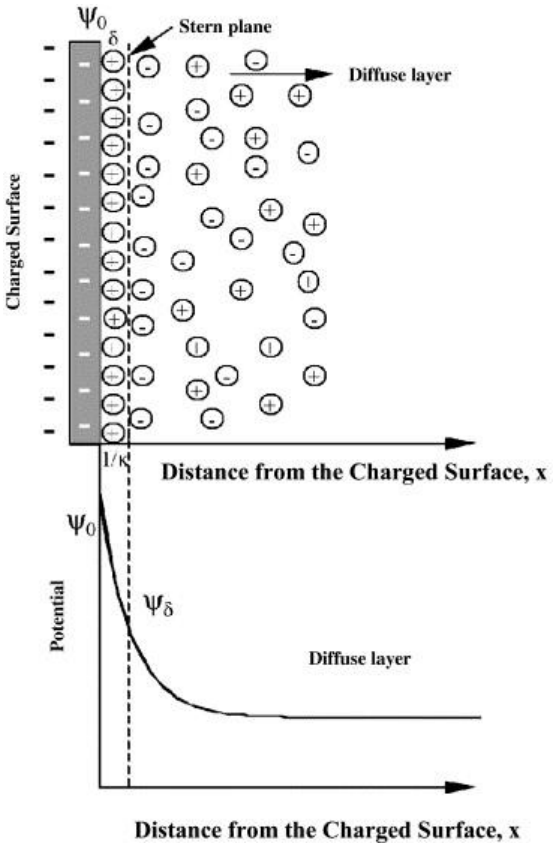

Figure 9. Schematic representation of the electrical double layer (Paria and Khilar, 2004).

The Debye length (κ^{-1}), Equation (3), describes the extension of the double layer, where most electrical interactions with the surface occur. The equation shows that the Debye length is inversely proportional to the valency of the ions and the square root of their concentrations. Thus, an increase in valency and concentration of ions leads to a decrease of the Debye length (Paria and Khilar, 2004).

$$\frac{1}{\kappa} = \sqrt{\frac{\varepsilon\varepsilon_0 k_B T}{1000e^2 N_A \times \sum_i z_i^2 c_i}} \quad (3)$$

Where:

κ	:	Debye-Hückel parameter
ε	:	Dielectric constant of the solution
ε_0	:	Dielectric constant in vacuum
k_B	:	Boltzmann constant
T	:	Absolute temperature
e	:	Elementary charge
N_A	:	Avogadro's constant
z_i	:	Valency of ion in solution
c_i	:	Molar concentration

At low electrolyte and surfactant concentrations, the charge of the electrical double layer surrounding the solid surface largely determines the surfactant adsorption. However, at higher surfactant concentrations, the development of self-assemblies must be taken into account and the electrical double layer model no longer applies (Somasundaran and Krishnakumar, 1997; Schramm, 2000, p. 126).

2.6.3 Depletion Method

Most adsorption studies have employed the surfactant depletion method, where the change in surfactant concentration after contact with the adsorbent is measured and assumed to be adsorbed. The concentration depletion gives the adsorption from Equation (4), and this equation may also be expressed with the particle specific surface area (Holmberg et al., 2002, p. 360).

$$\Gamma = \frac{(C_0 - C_e)V}{m} \quad (4)$$

Where:

Γ	:	Adsorption	mg/g
C_0	:	Concentration before adsorption	mg/mL
C_e	:	Equilibrium concentration (after adsorption)	mg/mL
V	:	Solution volume	mL
m	:	Mass of adsorbent/particles	g

2.6.4 Four-Region Adsorption Isotherm

The results from adsorption studies are usually presented as adsorption isotherms that represent the relationship between the amount surfactant absorbed versus the equilibrium surfactant concentration at a constant temperature. These isotherms are characterized by four regions with different mechanisms dominating in each region, as illustrated in Figure 10 (Somasundaran and Krishnakumar, 1997; Schramm, 2000, p. 129-130). This four-region isotherm shows the general trend for ionic surfactants when they are adsorbed on oppositely charged surfaces, but this trend has also been observed in other surfactant-solid systems (Austad et al., 1991a). The general mechanisms and characteristics of each region in Figure 10 are described below.

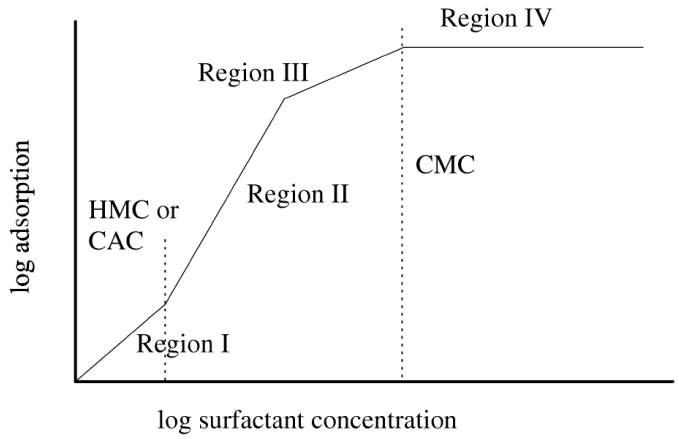

Figure 10. Typical four-region adsorption isotherm for a monoisomeric anionic surfactant (Schramm, 2000, p. 130).

Region I describes the adsorption at low surfactant concentrations. In this concentration range, the simple electrical double layer theory may be applied since adsorption is due to electrostatic interaction between the surfactant and the solid surface. In most cases, the adsorption obeys Henry's Law. In this region a monolayer of disassociated surfactant molecules are formed on the surface (Lv et al., 2011; Schramm, 2000, p. 129-130).

As the concentration of surfactants increases, the first surface aggregates are formed in region II. These aggregates are also known as hemimicelles and this concentration is often referred to as the hemimicelle concentration (HMC). These aggregates form due to lateral interaction between hydrocarbon chains. Thus, the adsorption in this region is due to both electrostatic attraction and hemimicelle association. The HMC may be manipulated in a similar manner as the CMC, and the addition of salt will lead to a decrease of the HMC for ionic surfactants

(Schramm, 2000, p. 130-131; Somasundaran and Krishnakumar, 1997; Somasundaran and Fuerstenau, 1966).

There are two main theories that describe region III. Scamehorn et al. (1982a) believed that the formation of bilayer began in region II, but that it developed at a slower rate in region III at surface sites with lower energy. Somasundaran et al. (1964; 1966) proposed that the surface became neutralized by the end of region II due to the surface sites being filled by surfactant ions, and that the adsorption in region III was the result of lateral attractions operating alone.

Region IV, plateau adsorption, generally begins at the CMC. In this region, there is no further adsorption of surfactants on the surface as the surfactant concentration increases (Austad et al., 1991a). This implies that there is no significant adsorption of micelles at the surface, and consequently, the pseudo-phase separation model is a good approximation for these systems. This model predicts that in addition to a constant monomer concentration, the concentration of micelles increases linearly with total surfactant concentration (Scamehorn et al., 1982a).

2.6.5 Isotherm Models

Adsorption isotherms are curves relating the amount of material adsorbed on a surface (Γ) to the remaining equilibrium concentration of the solution (C_e). There are several models for predicting the equilibrium distribution that enable a molecular interpretation of experimental results, and the obtained parameters from these models are useful when comparing adsorption behaviour of different systems. Langmuir and Freundlich are two of the most commonly observed isotherm models, and Figure 11 illustrates their typical shapes.

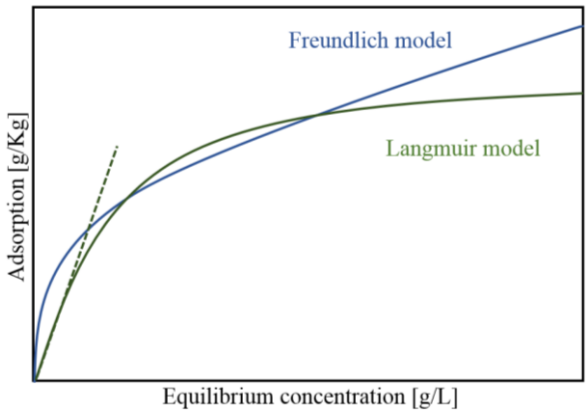

Figure 11. Illustration of Langmuir and Freundlich adsorption isotherms.

Langmuir Isotherm

Irving Langmuir developed a theoretical equilibrium isotherm in 1916, which describes the adsorption process (Langmuir, 1916). The Langmuir equation is presented in Equation (5).

$$\Gamma = \Gamma_{max} \frac{K_L C_e}{1+K_L C_e} \quad (5)$$

Where:

Γ	:	Amount adsorbed	g/Kg
Γ_{max}	:	Maximum adsorption capacity for forming monolayer	g/Kg
K_L	:	Langmuir equilibrium constant	L/g
C_e	:	Equilibrium aqueous concentration	g/L

The surface coverage, $\theta = \Gamma/\Gamma_{max}$, specifies the fraction of adsorbent surface covered by the adsorbed molecules at a given concentration. Two limiting cases are of particular interest. The first is achieved if the solution is highly diluted, $C_e \rightarrow 0$. Then $\theta = K_L C_e$, which shows that θ increases linearly with an initial slope of K_L, and thus the isotherm follows Henry's Law. The second case is achieved at high concentrations where $K_L C_e >> 1$. The surface then becomes completely saturated by a monolayer of adsorbate, $\theta = 1$ and $\Gamma = \Gamma_{max}$. Thus, a further increase in concentration would not provide any increase in the amount adsorbed (Hiemenz and Rajagopalan, 1997, p.331-333; Mørk, 2004, p. 174-175).

The Langmuir isotherm is based on the following assumptions:

- Monolayer coverage
- Adsorption takes place at specific homogenous sites in the adsorbent
- No solute-solvent or solute-solute interactions

Even though the assumptions are only approximations at best, it has been found that many experimental adsorption isotherms can be described relatively well by the Langmuir adsorption isotherm (Holmberg et al., 2002, p. 363).

In order to investigate whether a set of experimental data can be described by the Langmuir isotherm, the results can be plotted on a graph to give a straight line if the adsorption isotherm applies. The Langmuir equation can be linearized as presented in Equation (6).

$$\frac{1}{\Gamma} = \frac{1}{\Gamma_{max}} + \frac{1}{K_L \Gamma_{max}} \cdot \frac{1}{C_e} \quad (6)$$

If the experimental system matches the model, then the maximum adsorption capacity and the equilibrium constant may be obtained from the plot where the slope = $1/(\Gamma_{max}K_L)$ and intercept = $1/\Gamma_{max}$ (Muherei and Junin, 2009; Mørk, 2004, p. 174-175).

Freundlich Isotherm

Herbert Freundlich developed an empirical equation to describe the adsorption process in 1906 (cited by Ho et al., 2002). The Freundlich equation is presented in Equation (7).

$$\Gamma = k_f C_e^{\frac{1}{n}} \quad (7)$$

Where:

Γ	:	Amount adsorbed
k_f	:	Constant for a given system
C_e	:	Equilibrium aqueous concentration
n	:	Constant for a given system

The constant, k_f, is an indicator of adsorption capacity. A high k_f value equals a high maximum capacity. The constant, n, is usually in the range of 2-10, and is a measure of the intensity of adsorption. A high n gives a more favourable adsorption (Mørk, 2004, p. 175; Okeola and Odebunmi, 2010).

The Freundlich isotherm is based on the following assumptions:

- Multilayer adsorption
- Heterogeneous surface composed of different classes of adsorption sites
- The heat of adsorption decrease exponentially with the surface coverage

This isotherm is unsuitable at high surface coverage, because it does not include the possibility of a complete surface saturation. Thus, an infinite surface coverage by multilayer adsorption is mathematically approached. The isotherm does not reduce to Henry's Law at low concentrations (Muherei and Junin, 2009; Ho et al., 2002). A linearized form of the Freundlich isotherm is presented in Equation (8). The constants, k_f and n, are determined from the straight line's slope and its intersection with the ordinate.

$$\log \Gamma = \log k_f + \frac{1}{n} \log C_e \quad (8)$$

2.7 Adsorption of Anionic Surfactants on Kaolinite

2.7.1 Kaolinite

In the North Sea, most of the oil reservoirs are characterized by sandstone. The core of sandstone reservoirs is nonhomogeneous and built up of several individual minerals, of which quartz is the primary component. The reservoir core contains clay clusters, which include kaolinite, illite, feldspar, mica and calcium carbonate (Austad et al., 1991b; Schramm, 2000, p. 124; Lv et al., 2011). Kaolins and illitic minerals are the most common clay minerals in sandstone reservoirs (Beaufort et al., 1998). Kaolin refers to the different minerals of the kaolin group, such as kaolinite, dickite and nacrite. In this study, kaolinite was used in the experimental work.

The chemical formula of kaolinite is $Al_2(OH)_4Si_2O_5$, and one unit is built from one silica tetrahedral and one alumina octahedral sheet. The two sheets are connected by shared oxygen atoms at the edge of the silica tetrahedron and one of the oxygen atoms of the alumina octahedral sheet. Consequently, they form a joint layer (Schramm, 2000, p. 124). Hydrogen bonds connect the kaolinite units together (Austad et al., 2010). A site consisting of one aluminium atom and three hydroxyl groups, $Al(OH)_3$, is often referred to as a Gibbsite (Lv et al., 2011).

Kaolinite is a non-swelling clay, which means the volume of the clay is not dependent on the amount of water present. This reflects on the low surface area of 15-25 m^2/g (Austad et al., 2010). The research on specific surface area and pore-size distribution in clays and shales by Kuila and Prasad (2013) indicated that kaolinite is predominantly macroporous, and that micropores and fine mesopores are negligible or non-existent. The total pore volume was estimated to be 0.049 cm^3/g.

Kaolinite has a point of zero charge (pzc) around 4.5 (Schramm, 2000, p. 128). Thus, at this pH the surface has a net charge of zero. Therefore, at a pH greater than 4.5, kaolinite has a negative surface charge. The charged surface is caused by structural imbalances on the clay surface, and kaolinite is characterized as a cation exchange material (Austad et al., 2010; Lv et al., 2011). It should be mentioned that dissolution of kaolinite can occur above pH 4.7, and consequently yield a new Gibbsite. This Gibbsite has a pzc around 8.5–9.1, resulting in some positively charged sites on the clay surface below pH 9.1 (Lv et al., 2011). The amphoteric edges of

kaolinite behave differently than the surface due to protonation/deprotonation, and the charges of the clay edges may be positive, neutral or negative depending on whether the pH is below, equal or above 7, respectively. The formation water in the reservoir has a pH of about 5, giving the edges of kaolinite a positive charge and the surface a negative charge (Torn et al., 2003).

Several researchers (Shelton, 1964; Wilson and Pittman, 1977; Hancock and Tayler, 1978) have investigated the different modes of kaolinite in sandstone, which was found in cracks and cavities as pore filling material, in pore linings, along fractures, and as a replacement of quartz in grains of quartz, known as pseudomorphous replacement. The different modes of kaolinite in sandstones are illustrated in Figure 12. The most common occurrence of kaolinite is pore filling, followed by pore lining (Wilson and Pittman, 1977).

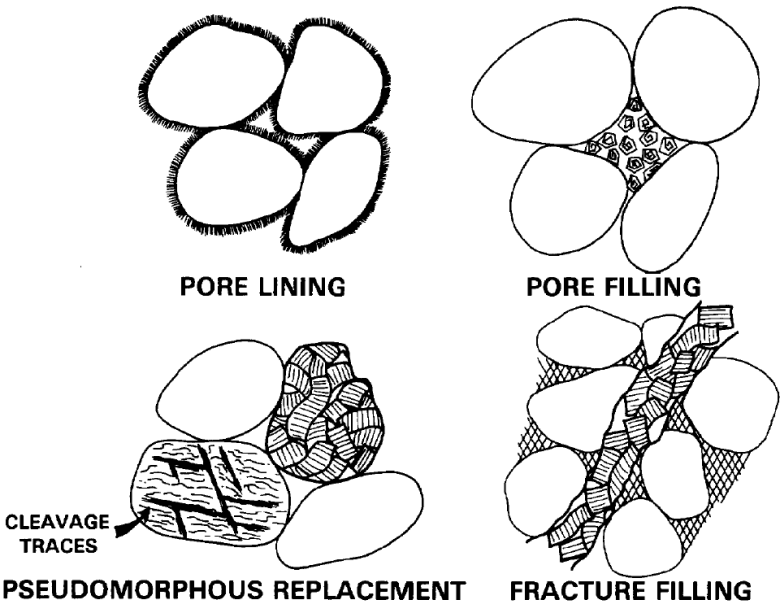

Figure 12. Modes of occurrence of kaolinite in sandstones (Wilson and Pittman, 1977).

2.7.2 Adsorption Mechanisms

The adsorption of anionic surfactants on kaolinite depends on several factors such as temperature, pH, salinity and surfactant concentration (Austad et al., 1991a; Torn et al., 2003; Lv et al., 2011). In addition, these properties can affect the dissolution of the minerals in the reservoir and consequently influence the precipitation of surfactants (Lv et al., 2011; Somasundaran and Krishnakumar, 1997).

Lv et al. (2011) and Scamehorn et al. (1982a) studied the adsorption of anionic surfactants on kaolinite, and the results of the adsorption studies were presented as adsorption isotherms. The shapes of the obtained isotherms was similar to the four-region isotherm presented in section 2.6.4, with the exception that region III was not observed.

At low surfactant concentration, adsorption is due to interactions between several carbon atoms in the alkyl chain and the surface, in addition to the adsorption due to electrostatic interaction between the head groups of the surfactant and positive sites on the kaolinite edges (Sastry et al., 1995; Figdore, 1982). As the surfactant concentration increases, surface aggregates are formed, and Lv et al. (2011) and Scamehorn et al. (1982a) proposed hemimicelle formation at the surface.

As the surfactant concentration increases beyond the CMC, the adsorption isotherms for negatively charged surfactants have occasionally shown an adsorption maximum when adsorbed on kaolinite. This provides a characteristic S-shape, as shown in the studies performed by Lv et al. (2011). This behaviour are likely a result of the precipitation of surfactant molecules when interacting with multivalent cations exchanged from the kaolinite surface, followed by redissolution of the precipitate by micelles as the surfactant concentration increases. The isotherm will have different shapes according to the surfactant in in the system, and is affected by factors such as the presence of co-solutes (Lv et al., 2011).

2.7.3 The Influence of Electrolytes

Several physicochemical processes may occur when kaolinite interacts with electrolytes. The most important of these are hydrolysis, ion exchange, electrostatic adsorption and dissolution of surface species (Hanna and Somasundaran, 1979).

Increasing the ionic strength will lead to a compression of the electrical double layer surrounding the charged kaolinite; this will make it easier for the surfactants to approach the surface and consequently may lead to increased adsorption (Figdore, 1982). Hanna and Somasundaran (1979) investigated the effect of salinity on the adsorption of SDBS on purified Na-kaolinite without pH adjustments, and the results indicated that the adsorption of SDBS on kaolinite increased as the salinity increased. The exchange of Na^+ with H^+ at the kaolinite surface caused a decrease in pH. The increase in pH might supersede the effect of electrolytes compressing the electrical double layer. H^+ and OH^- are considered potential determining ions

regarding the charged edges on kaolinite, meaning they will influence the surface potential. Thus, a decrease in pH will increase the number of positive sites on the clay surface, and this effect will contribute to increased adsorption of sulfonates on kaolinite as the pH decreases. Regarding other ions, kaolinite shows a stronger selectivity for Ca^{2+} over Na^{+} (Austad et al., 2010). Figdore (1982) observed that Ca^{2+} had a tendency to form complexes with RSO_3^- surfactants that adsorbed on kaolinite, resulting in a greater surfactant adsorption on kaolinite than with brine based only on NaCl.

2.8 Analytical Methods for Detection of Surfactant Concentration

2.8.1 UV-Spectroscopy

Spectroscopic methods of analysis are quantitative and qualitative. They can be used to determine the concentration of an analyte or to identify the chemical specie in a sample solution. This technique is known for its simplicity and accuracy, and takes advantage of the fact that chemical species adsorb light at characteristic frequencies of electromagnetic radiation; when the molecules absorb energy, a transition of electrons to orbitals with higher energy will occur (Skoog et al., 2004, p. 718-720; Thermo Spectronic, n.d.).

A cuvette, made from a transparent material such as glass, silica or plastic, is filled with the solution containing the analyte, and a beam at a specified wavelength is sent through the sample. The beam is emitted from a light source that may be a tungsten lamp, tungsten-halogen lamp, deuterium lamp, or a combination of these sources (Thermo Spectronic, n.d.). The intensity of the beam, the incident light, is reduced through the length of the cuvette due to absorption by the analyte. Hence, the higher concentration of analyte, the greater the reduction in incident light intensity. The transmitted light is then detected, amplified and displayed by a read-out system (Skoog et al., 2004, p. 718-720). Figure 13 illustrates the concept of spectroscopy.

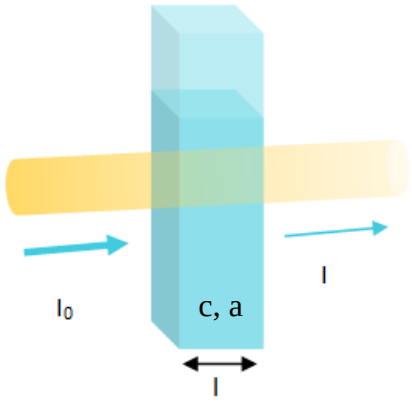

Figure 13. The concept of spectroscopy. I_0: intensity of incident light, I: intensity of transmitted light, c: concentration of analyte, a: absorbance of light, l: length of cuvette.

The transmittance of the solution is the ratio between incident and transmitted light, as shown in Equation (9).

$$T = \frac{I}{I_0} \tag{9}$$

Where:

T	:	Transmittance
I	:	Intensity/power of transmitted light
I_0	:	Intensity/power of incident light

Modern instruments automatically relate transmittance to absorbance (A) by Equation (10), and the computer software displays the absorbance for each sample at a specific wavelength, monochromographic light. It is also possible to analyse the sample over an interval of several wavelengths. The absorption is plotted as a function of wavelength to give an absorption spectrum, and in most instruments, this spectrum is created automatically (Skoog et al., 2004, p. 724).

$$A = -log\, T = log \frac{I_o}{I} \tag{10}$$

A positive error in the detection of absorbance by the analyte may arise due to impurities in the sample, or because the incident light is reflected or scattered by the cuvette itself. In addition,

the sample matrix may absorb and influence the intensity of the transmitted light. This is corrected by analysing a blank sample with the sample solvent at the same time as the analysis sample. The intensity of transmitted light from the blank sample replaces I_0 in Equation (10) as a practical value of the intensity of incident light (Skoog et al., 2004, p. 718-720; Thermo Spectronic, n.d.).

In this study, a spectroscopic method was used for quantitative analysis. Absorbance by chemical species is related to concentration by Beer's Law, Equation (11). It is evident that absorption is proportional to the concentration of the absorbing molecule and the length of the cuvette. The molar absorptivity is a proportionality constant.

$$A = \varepsilon \, l \, c \qquad (11)$$

Where:

A	:	Absorbance	
ε	:	Molar absorptivity	$L/mol\ cm$
l	:	Length of cuvette	cm
c	:	Concentration of the absorbing compound	mol/L

In this study, ultraviolet/visible (UV-vis) spectroscopy was used, which is a well-suited technique for analyses of unsaturated organic components. UV-vis radiation has a wavelength of 200-800 nm (Weckhuysen, 2004, p. 258). Chromophoric groups and molecules with halogens usually have one or several absorption maxima between 200-400 nm. In addition to organic components, salt of Co, Ni, Cu, V etc. absorb in the visible region. To avoid interference with the analyte spectrum and to achieve accurate results, the solvent should be transparent in the region where the analyte absorbs light. Furthermore, the analyte should have a high solubility in the solvent. The polarity of the solvent influences the absorption maxima of an analyte (Skoog et al., 2004, p. 786-793; Thermo Spectronic, n.d.).

UV-vis spectroscopy was used in this study to analyse samples containing the surfactant SDBS. The chemical structure of SDBS (shown in Figure 3, section 2.2.4) contains a phenyl group, and this group is the source of the highest peak in the absorption spectrum of SDBS at approximately 254 nm. Lv et al. (2011) and Torn et al. (2003) used UV-vis spectroscopy to determine the concentration of SDBS, and used wavelengths of 207 nm and 223.6 nm, respectively, to detect the phenyl group of SDBS.

2.8.2 Tensiometer

Surface tension is the force per unit length at the surface caused by an imbalance in the intermolecular forces at the air/liquid interface (Mørk, 2004, p. ix). There are several different techniques used to measure the surface tension, such as force-, optical- and bobble tensiometers (Biolin Scientific, 2011a). In this study, a force tensiometer was used, specifically, a Du Noüy ring tensiometer. This tensiometer can be used to measure the surface tension of a liquid solution, or the interfacial tension between two liquid phases with different densities. The tensiometer measures the force required to detach a platinum ring from a surface or from the interface between two liquids (Mørk, 2004, p. 72-73). The technique is described in Figure 14.

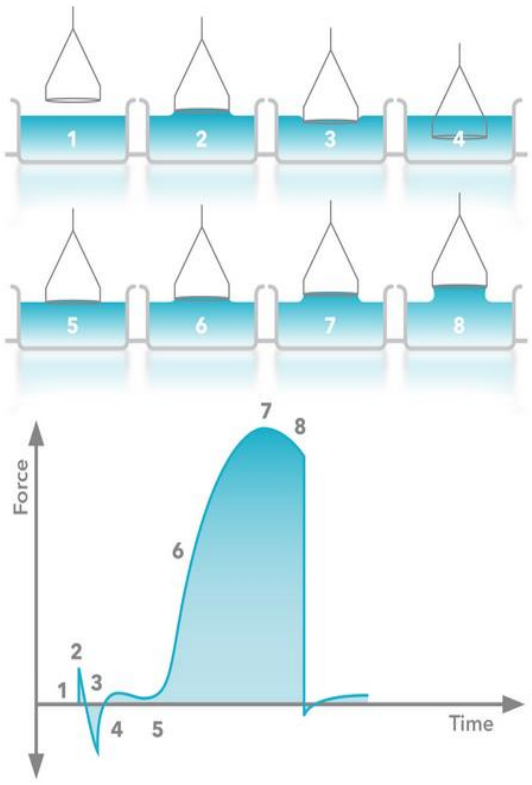

1. Ring is above the surface, there is no force pulling on the ring.
2. The ring is in contact with the surface, resulting in a pull downwards.
3. The ring attempts to break through the surface, the ring is lifted, thus, a negative force is measured.
4. The ring is in the fluid. The contact between the surface and the wires cause a small positive force.
5. The ring is lifted and the total force increases.
6. The force increases as the ring is lifted.
7. The ring is at the surface and the liquid surface stretches and pulls the ring down. The ring is completely wetted, and maximum pressure is achieved.
8. The liquid surface starts to loose contact with the ring and the force decreases.

Figure 14. Description and illustration of the ring tensiometer method (Biolin Scientific, 2011a).

The ring is lowered into the liquid and pulled upwards, while the force pulling on the ring is measured simultaneously. Only the maximum force—the force needed to overcome the surface tension and break the surface, is relevant for the calculations in this method.

At the maximum force, the ring is completely wetted and the theoretical relationship between force and surface tension at this point is given in Equation (12) (Mørk, 2004, p. 72-73; Biolin Scientific, 2011a; CSC Scientific Company, 2013).

$$F_t = W_r - b + 2(2\pi r\gamma) \quad (12)$$

Where:

F_t	:	Theoretical force
W_r	:	Wight of ring
b	:	Buoyancy
r	:	Ring average radius
γ	:	Surface tension

Modern instruments, as used in this study, correct for several factors when measuring surface tension. Ring buoyancy and weight are corrected by a reset of the instrument before use. Other factors, such as deviation from the vertical impact of surface tension during detachment, and complexity of the geometry of the meniscus are corrected by a correction factor. The corrected surface tension is automatically calculated from Equation (13) (Mørk, 2004, p. 72-73).

$$\gamma = K \cdot F/4\pi r \quad (13)$$

Where:

γ	:	Surface tension
K	:	Correction factor
F	:	Force, corrected for ring buoyancy and weight
r	:	Ring average radius

In this study, the tensiometer was used to measure the surface tension of surfactants in brine solution, and the measurements were subsequently related to surfactant concentration in order to create calibration curves and determine the CMC. When surfactants migrate to the surface, the surface tension decreases until the CMC is reached. Figure 15 describes the relation between surface tension and surfactant concentration.

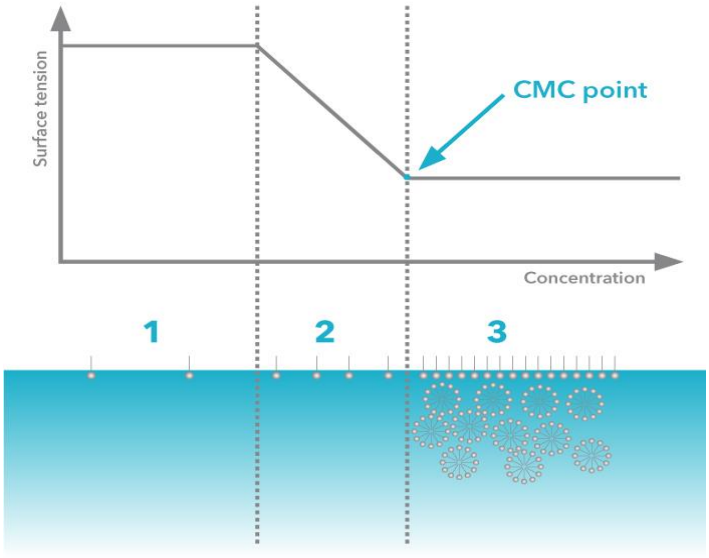

1. Low surfactant concentration does not influence the surface tension to any great extent.
2. The surfactant concentration has reached a certain value and the surface tension decreases.
3. At the CMC, the surface is fully loaded with surfactant monomers and the surface tension is constant.

Figure 15. Description and illustration of the relation between surface tension and surfactant concentration (Biolin Scientific, 2011b).

When measuring surface tension, it is important to avoid impurities in the sample solution. Impurities will affect the measurement significantly, and are one of the biggest and most common sources of errors. Another source of error is damage to the ring geometry. Surface tension can be measured with accuracy of 0.05 mN/m in samples without contaminations. The determination of surface tension in surfactant solutions may cause concentration effects near the ring surface, which could cause an error of up to 10 mN/m (Mørk, 2004, p. 72-73).

3 Materials and Methods

3.1 Materials

3.1.1 Chemicals

Sodium dodecylbenzenesulfonate (SDBS), $CH_3(CH_2)_{11}C_6H_4SO_3Na$. MW 348.48 g/mol. Technical grade. Aldrich Chemistry.

Kaolinite, $Al_2O_7Si_2 \cdot 2H_2O$. MW 258.16 g/mol. Natural. Fluka Analytical, Sigma Aldrich.

Sodium chloride, NaCl. MW 58.44 g/mol. For Analysis. Emsure, Merck.

Calcium chloride dihydrate, $CaCl_2 \cdot 2H_2O$. MW 147.01. For Analysis. Sigma Aldrich.

3.1.2 Instruments and Equipment

Tensiometer: Sigma 70, KVS Instrument. Du Noüy platinum ring

UV-vis Spectrophotometer: Shimadzu, UV-2401PC

Density/Concentration Meter: Anton Paar, DMA 5000 M

Zetasizer: Malvern Instruments, Nano ZS

Conductivity meter: Inolab Cond Level 2, WTW Wissenschaftlich-Technische Werkstätten

"Shaker": IKA Labortechnic, HS 501 digital

pH meter: Mettler Toledo, Seven Easy

Centrifuge: Eppendorf, centrifuge 5810

Analytical balance: Mettler Toledo, AB304-S/FACT

Acrodisc CR Syringe Filter: Life Sciences, 0.2 µm PTFE Membrane Ø 13 mm

Filter Paper Circles: Schleicher & Schuell, 589^3 Blue ribbon Ø 150 mm

3.2 Health, Safety and Environment (HSE)

A risk assessment was completed before the experimental work was conducted. The risk assessment included identification of activity hazardous to human health and the safety measures performed to avoid unwanted situations. The risk assessment is provided in Appendix A.

3.3 Pretreatment of Kaolinite

The kaolinite was pretreated into a purified sodium state, the purpose of which was to obtain equilibrium of the clay with a homoionic surface. Equilibration of kaolinite involves a fast ion exchange and/or electrostatic adsorption, and may also include the dissolution of aluminium species upon prolonged contact of kaolinite with water (Hanna and Somasundaran, 1979). Na-kaolinite was prepared according to the following procedure, a modification of a well-acknowledged procedure developed by Hanna and Somasundaran (1979):

1) Approximately 25 g kaolinite was gradually suspended in 500 mL MilliQ water while stirred with a magnet stirrer. The suspension was then stirred for 2 hours before it was left to settle for 2 nights. The supernatant was discarded with a peristaltic pump. This washing procedure was repeated four times.
2) The washed clay was re-agitated with a magnet stirrer, and gradually suspended in 500 mL 0.2 M NaCl solution. The suspension was then stirred for 2 hours before it was left to settle for 8-12 hours. The supernatant was discarded with a peristaltic pump. This procedure was repeated three times.
3) The NaCl-treated product was agitated with 50 mL 1 M NaCl for 15 minutes. The pH was adjusted with HCl to approximately pH 3 in order to remove $Al(OH)_2$ surface contamination. The product was diluted with 450 mL MilliQ water and stirred for 2 hours before it was left to settle for 8-12 hours. This procedure was repeated three times.
4) The washed product was agitated and gradually suspended in 500 mL 0.01 M NaCl solution. The suspension was then stirred for 2 hours before it was left to settle for 8-12 hours. The supernatant was discarded with a peristaltic pump. This procedure was repeated three times.

5) The Na-kaolinite product obtained was vacuum filtrated with a Buchner funnel. A 2.5 µm filter from Schleicher & Schuell was used. The product was dried at 60°C for 4 days.

The procedure was conducted at 25°C. The conductivity and pH were measured after each washing step outlined in points 1-4 above, and the entire procedure was repeated five times, resulting in a pretreatment of approximately 125 g kaolinite.

The treated kaolinite was compared to untreated kaolinite with regards to conductivity and surface tension. Approximately 0.3 g of pretreated clay was weighed directly in a centrifuge tube, and 30 mL of MilliQ water was added. An analogue sample was prepared with untreated kaolinite, and three parallels of both samples were prepared. The samples were mixed for 24 hours with an IKA Labortechnic shaker, and then centrifuged at 11 000 rpm for 60 minutes. Conductivity and surface tension of the supernatants were measured. Figure 16 displays a batch of pretreated kaolinite ready for use. The pretreated kaolinite was used in the adsorption experiments within two weeks after preparation, since stored Na-kaolinite is known to exhibit lower adsorption capacities (Hanna and Somasundaran, 1979).

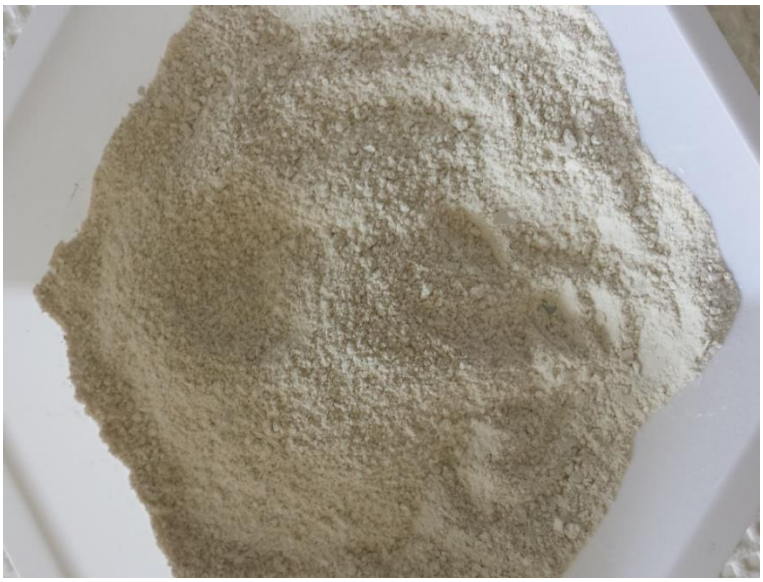

Figure 16. Pretreated kaolinite.

3.4 Preparation of Solutions

3.4.1 Preparation of Brine Standards

Five different brine standards were prepared in graduated flasks. The ionic strength and the concentration of NaCl and $CaCl_2$ of the five brine standards are given in Table 1. These salt compositions were used in all calibration solutions and adsorption samples, and are labelled as low salinity (LS), low salinity with $CaCl_2$ (LS w/Ca^{2+}), medium salinity (MS), medium salinity with $CaCl_2$ (MS w/Ca^{2+}) and high salinity (HS) throughout this report.

Table 1. Ionic strength and concentration of NaCl and $CaCl_2$ in brine standards for calibration solutions and samples.

Solution	**Notation**	**C $_{NaCl}$ [mM]**	**C $_{CaCl2}$ [mM]**	**I [mM]**
Low Salinity	LS	20.0	-	20.0
Medium Salinity	MS	80.0	-	80.0
High Salinity	HS	200	-	200
Low Salinity with $CaCl_2$	LS w/Ca^{2+}	18.8	0.417	20.0
Medium Salinity with $CaCl_2$	MS w/Ca^{2+}	75.0	1.67	80.0

3.4.2 Preparation of Calibration Solutions

Calibration solutions for measurements of both absorbance and surface tension were prepared. The ionic strength and concentration of NaCl and $CaCl_2$ in the calibration solutions are given in Table 1. The concentration of SDBS in calibration solutions for measurements of both absorbance and surface tension are presented in Table 2.

Table 2. Concentration of SDBS in calibration solutions for absorbance and surface tension measurements

Concentration of SDBS [M]	
UV-vis spectrophotometer	**Tensiometer**
$1.00 \cdot 10^{-5}$	$1.00 \cdot 10^{-6}$
$5.00 \cdot 10^{-5}$	$5.00 \cdot 10^{-6}$
$1.00 \cdot 10^{-4}$	$1.00 \cdot 10^{-5}$
$2.00 \cdot 10^{-4}$	$5.00 \cdot 10^{-5}$
$4.00 \cdot 10^{-4}$	$1.00 \cdot 10^{-4}$
$6.00 \cdot 10^{-4}$	$5.00 \cdot 10^{-4}$
$8.00 \cdot 10^{-4}$	$1.00 \cdot 10^{-3}$
$1.00 \cdot 10^{-3}$	$5.00 \cdot 10^{-3}$
$1.20 \cdot 10^{-3}$	$1.00 \cdot 10^{-2}$

3.5 Development of Method for Adsorption Studies

3.5.1 General Procedure

Static adsorption of SDBS onto kaolinite was determined by batch experiments. Approximately 0.3 g of kaolinite was weighed directly into centrifuge tubes, and 30 mL diluted stock solution was added. This resulted in a liquid/solid ratio (L/S) of 100. The adsorption of SDBS on kaolinite took place while mixing the adsorption samples with an IKA Labortechnic shaker in order to ensure good exposure of the kaolinite to the brine-surfactant solution. This instrument shook the samples back and forth, sideways. To ensure adsorption equilibrium, the tubes were shaken for 24 h at 300 shakes per minute (SPM), after which the adsorption samples were centrifuged for 30 min at 11,000 rpm in an Eppendorf centrifuge. The supernatant was then separated from the solid. The experiments were conducted at 25°C and without pressure or pH adjustments.

3.5.2 Improvement of the General Procedure

Several test experiments were conducted in order to improve the general procedure, and a short description of each experiment is provided in Table 3. All of the test experiments were performed with low salinity water.

Table 3. A short description of test experiments and the analysis method for detection of SDBS concentration.

Experiment	**Short description**	**Analysis method**
Test experiment 1	General procedure. Particle measurement.	UV-vis spectroscopy
Test experiment 2	Comparison of general procedure, additional centrifugation and filtration. Investigation of sample ageing.	UV-vis spectroscopy
Test experiment 3	General procedure with additional centrifugation and filtration. Comparison of different spectrophotometric baselines.	UV-vis spectroscopy
Test experiment 4	Comparison of general procedure and additional centrifugation.	Surface tension

Test experiment 1

The general procedure was carried out for samples with initial nominal SDBS concentrations of $1.00 \cdot 10^{-4}$, $5.00 \cdot 10^{-4}$, $1.00 \cdot 10^{-3}$ and $5.00 \cdot 10^{-3}$ M. The analytical samples were analysed with an UV-vis spectrophotometer. Furthermore, the particle size of two analytical samples, 0 and $5.00 \cdot 10^{-3}$ M SDBS, was measured before and after filtration with a 0.20 µm filter in order to investigate the necessity of filtration. The measurement of particle size was performed with a Malvern Zetasizer at 25°C.

Test experiment 2

The effects of filtration and further centrifugation on spectrophotometric analysis were studied. The general procedure was carried out for samples with initial nominal SDBS concentrations of $1.00 \cdot 10^{-4}$ and $5.00 \cdot 10^{-3}$ M. After the general procedure, the samples were split into three equal portions: one part was analysed with an UV-vis spectrophotometer without further treatment, the second part was filtrated with 0.20 µm filters before the analysis, and the last part was centrifuged once more for 60 min at 11,000 rpm before the absorbance measurements. The samples were stored for 4 days before the UV-vis spectrophotometric analysis was repeated.

Test experiment 3

The general procedure was carried out for samples with initial nominal SDBS concentrations of $1.00 \cdot 10^{-4}$, $5.00 \cdot 10^{-4}$, $1.00 \cdot 10^{-3}$ and $5.00 \cdot 10^{-3}$ M. In addition to the general procedure, the supernatants were centrifuged once more for 60 min at 11,000 rpm and filtered with 0.20 µm filters before being analysed by UV-vis spectroscopy. The absorbance measurements were carried out two times, once where the spectrophotometric baseline was created with pure low salinity water, and once where the baseline was created with a blank adsorption sample (a sample having undergone the same preparation as the adsorption samples, but without SDBS in the solution).

Test experiment 4

The general procedure was carried out for samples with initial nominal SDBS concentrations of $5.00 \cdot 10^{-6}$, $1.00 \cdot 10^{-5}$, $5.00 \cdot 10^{-5}$ and $1.00 \cdot 10^{-4}$ M. In addition to the general procedure, the supernatants were centrifuged once more for 60 min at 11,000 rpm. Density and surface tension were measured for all samples.

3.6 Adsorption Studies of Surfactant on Kaolinite

The equilibrium adsorption of SDBS on kaolinite was studied in brine with different compositions. Three or more parallels of each adsorption sample were prepared to ensure repeatability. The initial nominal SDBS concentrations were in the range of $5.00 \cdot 10^{-5}$ to $5.00 \cdot 10^{-3}$ M.

The adsorption studies were performed according to the general procedure described in section 3.5.1, with some additions. After the adsorption samples were mixed for 24 h, the clay particles were separated from the liquid by three centrifugation steps instead of one. First, the samples were centrifuged for 30 min at 11,000 rpm before the supernatant was separated from the solid and centrifuged once more for 30 min at 11,000 rpm. In the last step, the supernatant was centrifuged in smaller centrifugal tubes for 15 min at 11,000 rpm. A spectrophotometric analysis was conducted within four hours after the mixing was completed, and the pH of the adsorption samples was measured.

This procedure was conducted for samples of SDBS in the five different brine standards presented in Table 1. In addition, an experiment where the supernatant was further filtered with 0.20 µm filters was carried out for samples with SDBS in low and medium salinity brine.

3.7 Analyses of Absorbance and Surface Tension

3.7.1 UV-vis Spectrophotometer

The calibration solutions and adsorption samples were analysed with a Shimadzu UV-vis Spectrophotometer. The analyses were performed at a wavelength of 260 nm, corresponding to the light absorbed by SDBS. The sample solvent, brine, was used to create the spectrophotometric baseline in order to control background noise from the solvent during the analyses of calibration solutions. The adsorption samples were measured twice with different baselines—once where brine water was used, and once where the baseline was created with the supernatant of a blank adsorption sample. The analyses were conducted at 25°C.

3.7.2 Tensiometer

The density of the calibration solutions and adsorption samples were measured, and the surface tension was detected with a Sigma 70 Tensiometer. Settings for ring measurements and control options are presented in Table 4, and these settings were applied to all analyses conducted with the tensiometer.

Table 4. Ring measurement settings and control options for analyses of calibration solutions and samples.

Ring Measurements	**Control Options**
Speed up: 5 mm/min	Wait between: 10 sec
Speed down: 20 mm/min	Detect range: 2.0 mN/m
Dwell down: 100%	Start depth: 2.0 mm
Min. No. of points: 20	Go below start: 3.0 mm
Min. Meas. Time: 60 min	Return position: 5.0 mm
Temperature: 25°C	Reset speed: 40.0

4 Results and Discussion

4.1 Pretreatment of Kaolinite

The kaolinite was pretreated into a purified sodium state. The mass of Na-kaolinite product, in addition to conductivity and pH measurements related to the washing steps in the experimental method, are presented in Appendix B.

Pretreated and natural kaolinite were mixed with MilliQ water for 24 hours. The conductivity and surface tension in the bulk solution after mixing were measured and compared. The measurements were conducted at 25°C. The surface tension was measured to 71.22 ± 0.03 mN/m and 71.23 ± 0.04 mN/m for treated and untreated kaolinite, respectively. Thus, the pretreatment of kaolinite did not provide any observable change in the measured surface tension. The conductivity was measured to 9.57 ± 0.06 µS/cm and 9.77 ± 0.06 µS/cm for treated and untreated kaolinite, respectively. This indicated a small decrease in conductivity of the bulk solution after pretreatment of the clay, which might be an effect of fewer impurities and ions released from kaolinite. Thus, this result pointed towards a purer clay after the pretreatment.

4.2 Calibration Curves

SDBS calibration solutions with different salinities were analysed at 25°C with an UV-vis spectrophotometer at 260 nm and a Du Noüy ring tensiometer. The concentrations of SDBS are provided in Table 2, and the average absorbance, surface tension and density of the calibration solutions are provided in Appendix C. Tyler et al. (1978) stated that petroleum sulfonates are insoluble in water with salinity greater than 20,000 ppm, or 200-500 ppm when brine is based on divalent ions. Precipitation was also observed in this study when surfactant solutions with $CaCl_2$ at an ionic strength above 80.0 mM were prepared. Thus, no SDBS calibration curve was created with $CaCl_2$ in high salinity brine.

4.2.1 Absorbance Measurements

The calibration curves for SDBS in LS and LS w/Ca^{2+} are presented in Figures 17 and 18, respectively. An approximately linear relationship between absorbance and SDBS concentration was observed for both salinities, and the equations for the trend lines are provided in the same figures. The calibration curves were created from solutions prepared the same day. The figures also display measurements of the same solutions measured after one week of storage; these measurements were performed in order to investigate how ageing of surfactant solutions affected the absorbance. Regarding the calibration solutions for SDBS in LS, ageing did not influence the absorbance significantly, as shown in Figure 17. However, storing the solutions influenced the absorbance measurements of SDBS in LS w/Ca^{2+} significantly. In these measurements, the relationship between absorbance and SDBS concentration were not linear after ageing, but rather S-shaped. This is illustrated in Figure 18.

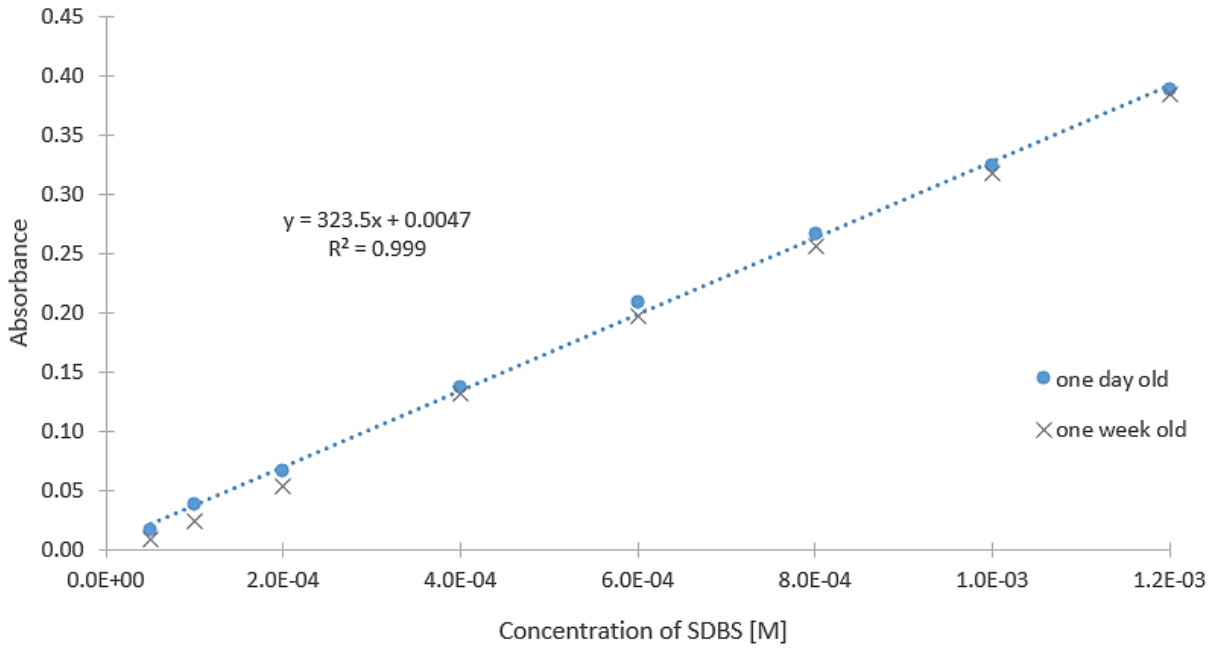

Figure 17. Calibration curve of SDBS in LS brine. Absorbance at 260 nm as a function of SDBS concentration in samples before and after ageing.

Cohen et al. (2013) studied the calcium ion tolerance of different anionic surfactant solutions and divided the surfactant phase into three zones depending on Ca^{2+} and surfactant

concentration. At a constant Ca^{2+} concentration, the behaviour of the solution progresses through zones 1-3 as the surfactant concentration increases. The zones may be described as follows. Zone 1: the solution is transparent, and the surfactants are present only as monomers. Zone 2: the solution shows a turbid appearance and there is equilibrium between monomers, micelles and precipitate. Zone 3: the solution is transparent and monomers and micelles are present. In the transition between zones 1 and 2, Ca^{2+} creates a bridge between two charged head groups of the surfactants and precipitate is formed. As the surfactant concentration increases further, the precipitate redissolves by the increased amount of micelles in solution. Cohen et al. (2013) observed an increase in turbidity and precipitate with sample ageing, and witnessed that precipitate in solution gives false and disperse values when measured by UV spectroscopy. The phase alteration observed by Cohen et al. (2013) seemed to describe the phenomenon observed in Figure 18 for samples after ageing.

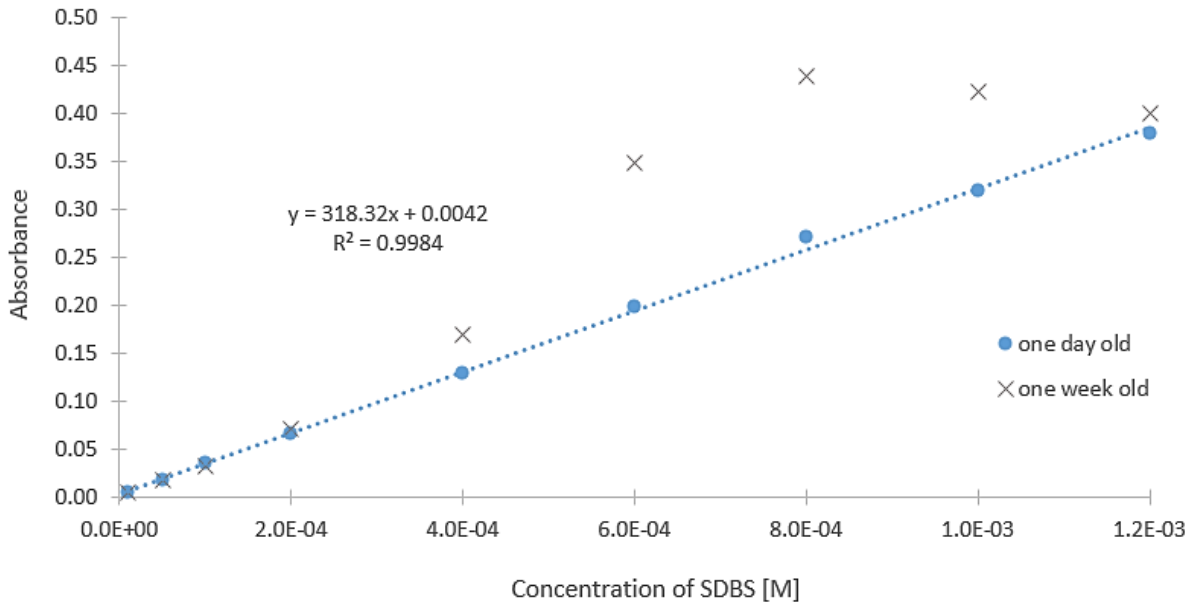

Figure 18. Calibration curve of SDBS in LS w/Ca^{2+} brine. Absorbance at 260 nm as a function of SDBS concentration in samples measured before and after ageing.

Calibration curves of SDBS in MS, MS w/Ca^{2+} and HS created from absorbance measurements are provided in Appendix C, and an absorption spectrum of SDBS calibration solutions in LS brine is provided in Figure D1, Appendix D.

4.2.2 Surface Tension Measurements

SDBS calibration curves for determination of the CMC were created from surface tension measurements. The concentrations of SDBS in the calibration solutions are given in Table 2. The calibration curve of SDBS in LS are presented in Figure 19, while calibration curves of SDBS in LS w/Ca^{2+}, MS, MS w/Ca^{2+} and HS for determination of the CMC are provided in Appendix C. Figure 19 exemplifies that the calibration curve has two distinct and approximately linear areas, which is also illustrated by the standard appearance of the correlation between surface tension and surfactant concentration presented in Figure 15, section 2.8.2. The point at which the two linear curves intersect correlates to the CMC; the CMC values for the five different surfactant systems are presented in Table 5.

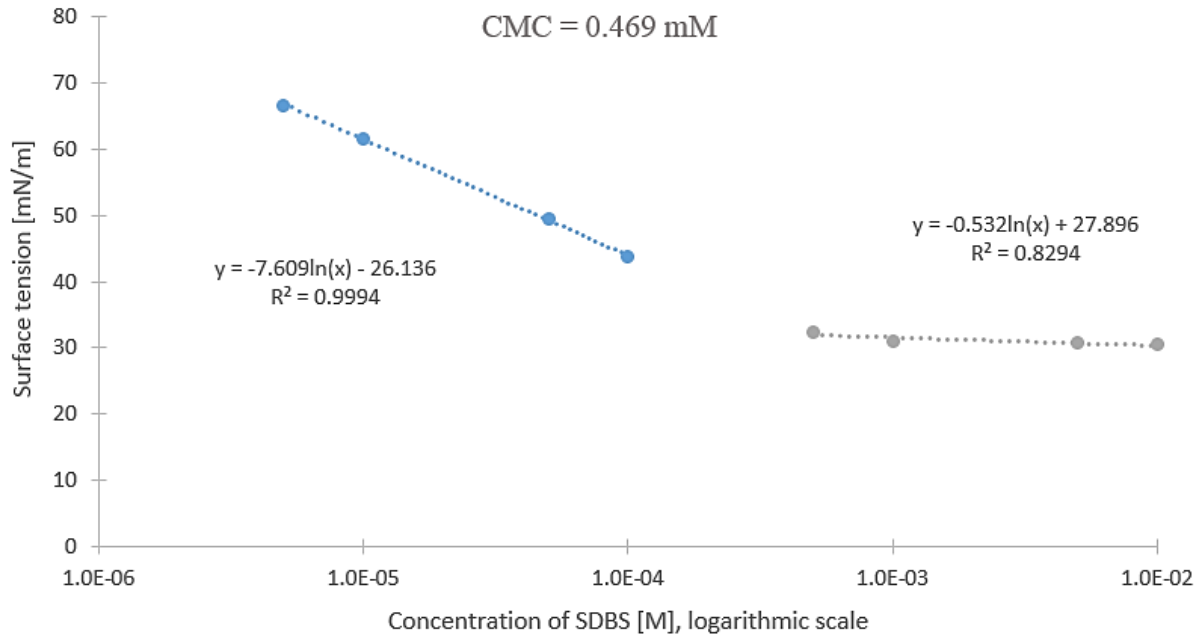

Figure 19. Calibration curve and determination of the CMC for SDBS in LS brine. Surface tension at 25°C as a function of SDBS concentration.

The calculated CMC values of SDBS decreased as the ionic strength of the calibration solutions increased. This result was expected because the addition of electrolytes reduces the repulsion between the charged head groups of SDBS, which promotes micelle formation. This is illustrated by Equation (3): the Debye length is inversely proportional to the square root of the

electrolyte concentration (c_i), and thus the screening length becomes shorter as the concentration increases. The CMC values of SDBS in solutions with $CaCl_2$ were lower than in solutions with only NaCl at the same ionic strength. Due to an equal ionic strength, these systems had a theoretically equal Debye length, which implied that Ca^{2+} had a greater ability to stabilize the repulsion between the ionic head groups of SDBS than what could be expected from simple electrostatics.

Torn et al. (2003) determined the CMC of SDBS in 10 mM NaCl solution to 0.70 mM, and Chou and Bae (1983) estimated the CMC to be between 0.20 and 0.30 mM in brine of 100 mM NaCl. The CMC values measured in this study, 0.469 mM in 20.0 mM NaCl (LS) and 0.125 mM in 200 mM NaCl (HS), were as expected between and below these two literature values, respectively. However, the CMC measured to 0.171 mM for SDBS in 80.0 mM NaCl (MS), was lower than expected.

Table 5. Calculated CMC of SDBS in brines with different composition and ionic strength

Brine standard	CMC of SDBS [mM]
LS	0.469
LS w/Ca^{2+}	0.257
MS	0.171
MS w/Ca^{2+}	0.132
HS	0.125

4.3 Test Experiments

SDBS in low salinity brine was adsorbed on kaolinite during mixing over 24 hours. The calibration equations in Figures 17 and 19 were used in the calculation of initial SDBS concentration (C_0) and equilibrium concentration of SDBS after adsorption on kaolinite (C_e), for absorbance and surface tension measurements, respectively. The amount of SDBS adsorbed on kaolinite was calculated by Equation (4), and the results and sample properties for all adsorption samples presented in this section are given in Appendix E. Table 3 provides a short description of each test experiment.

4.3.1 UV-vis Spectroscopy

Test experiment 1

In Test experiment 1, adsorption samples in LS brine were prepared by the general procedure described in section 3.5.1. The result is presented as an adsorption isotherm in Figure 20, where SDBS adsorption on kaolinite is plotted as a function of equilibrium concentration of SDBS.

The analyses performed by UV-vis spectroscopy resulted in negative calculated SDBS adsorption for all samples. Negative adsorption was not possible since there were no SDBS molecules adsorbed on the clay before the experiment was conducted. This result suggested the presence of impurities in the analytical samples. Because of the pretreatment of kaolinite, it was likely that these impurities were mainly fines of clay, and that the incident light was scattered by the fines during the spectroscopic analysis. Furthermore, it has been reported that Na-kaolinite generates as much as 0.1 mM Al^{3+} in 0.1 mM NaCl solutions at long contact times (Hanna and Somasundaran, 1979), and these impurities might also have influenced the analysis.

The particle size of two low salinity adsorption samples was measured before and after filtration with 0.20 µm filters in order to investigate the presence of particles and the necessity of filtration. The average particle diameter in the supernatant was determined to be 5579 nm before filtration and 1310 nm after filtration for blank adsorption sample, 0 M SDBS. Whereas for an adsorption sample with a SDBS concentration of $5.00 \cdot 10^{-3}$ M, the average particle diameter was determined to be 190.4 nm before filtration and 129.7 nm after filtration. This indicated that there were particles in the analytical samples, and that these were reduced by filtration.

Furthermore, the results pointed towards bigger particles in solutions with lower SDBS concentration, which was also observable.

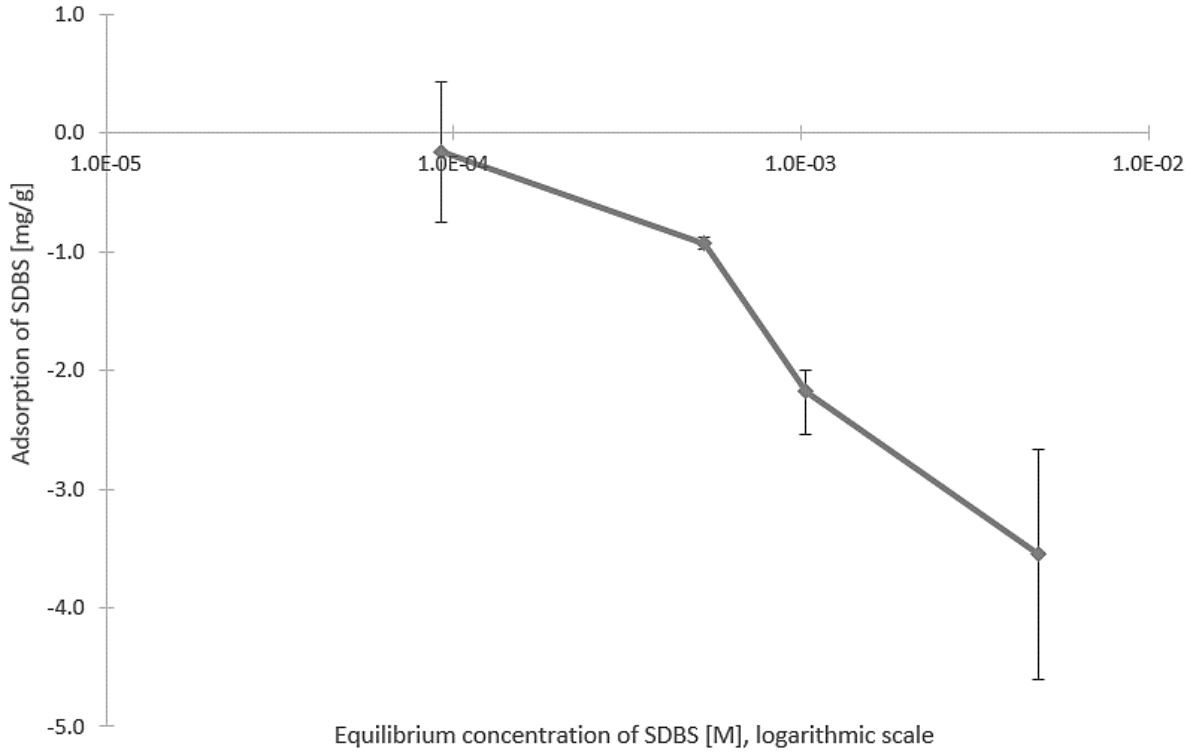

Figure 20. Results from Test experiment 1, where adsorption samples in LS were prepared by the general procedure. Adsorption of SDBS on kaolinite at 25°C as a function of equilibrium SDBS concentration based on analysis conducted with an UV-vis spectrophotometer at 260 nm.

Test experiment 2

In order to improve the general procedure described in section 3.5.1, the effect of filtration and additional centrifugation were investigated in Test experiment 2. Figure 21 illustrates the calculated amount of SDBS adsorbed on kaolinite for samples prepared by the general procedure, additional centrifugation and after filtration. It became evident that additional centrifugation or filtration led to a lower measured absorbance, and consequently a greater calculated SDBS adsorption. This result indicated that fines of clay in the solution influenced the absorption spectrum of SDBS, and that the removal of these fines was required to obtain a reliable result. The figure illustrates that additional centrifugation had a greater impact on the result compared to filtration.

Figure 21 also displays the SDBS adsorption calculated from measurements conducted after the adsorption samples had been stored for four days. The results from high SDBS concentration revealed a decrease in calculated SDBS adsorption after ageing. In other words, the measured absorbance increased when the samples were stored. This result had similarities to the trend discovered when creating the calibration curve from absorbance measurements of SDBS in brine with Ca^{2+}, as presented in Figure 18. This might have indicated the presence of polyvalent ions in the analytic samples even after the clay was pretreated. Another possibility was that fines in the analytic samples created a similar effect as the divalent ions with respect to measured absorbance.

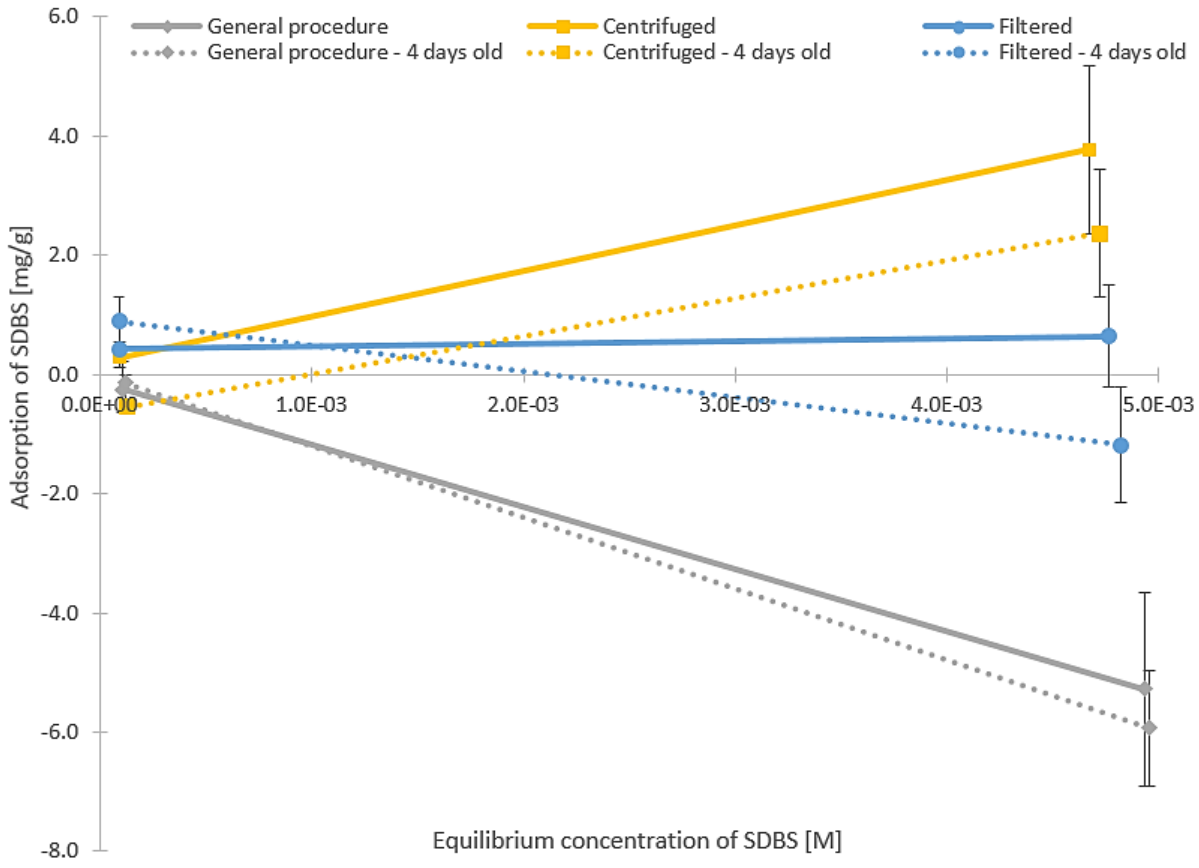

Figure 21. Results from Test experiment 2, where adsorption samples in LS were prepared by the general procedure, additional centrifugation, and filtration. Adsorption of SDBS on kaolinite at 25°C as a function of equilibrium SDBS concentration based on analysis conducted with an UV-vis spectrophotometer at 260 nm before and after ageing.

Test experiment 3

Because of the suspected alteration of the sample matrix during the adsorption experiments—addition of mineral fines and possibly ions, Test experiment 3 was conducted. In this experiment, the analytical samples were measured with two different spectrophotometric baselines. The SDBS adsorption isotherms are displayed in Figure 22, where the grey and yellow graph illustrates the isotherms derived from measurements with the baseline created from pure low salinity brine and a blank adsorption sample (a sample undergone the same preparation as the adsorption samples, but without SDBS in the solution), respectively. In this experiment, the adsorption samples were prepared by both additional centrifugation and filtration after the general procedure. The figure illustrates that the calculated adsorption of SDBS on kaolinite was greater when the baseline was created by the blank adsorption sample. This result confirmed that the composition of the sample matrix was altered during the adsorption experiment, and the experiments that followed were thus analysed with a spectrophotometric baseline from a blank adsorption sample.

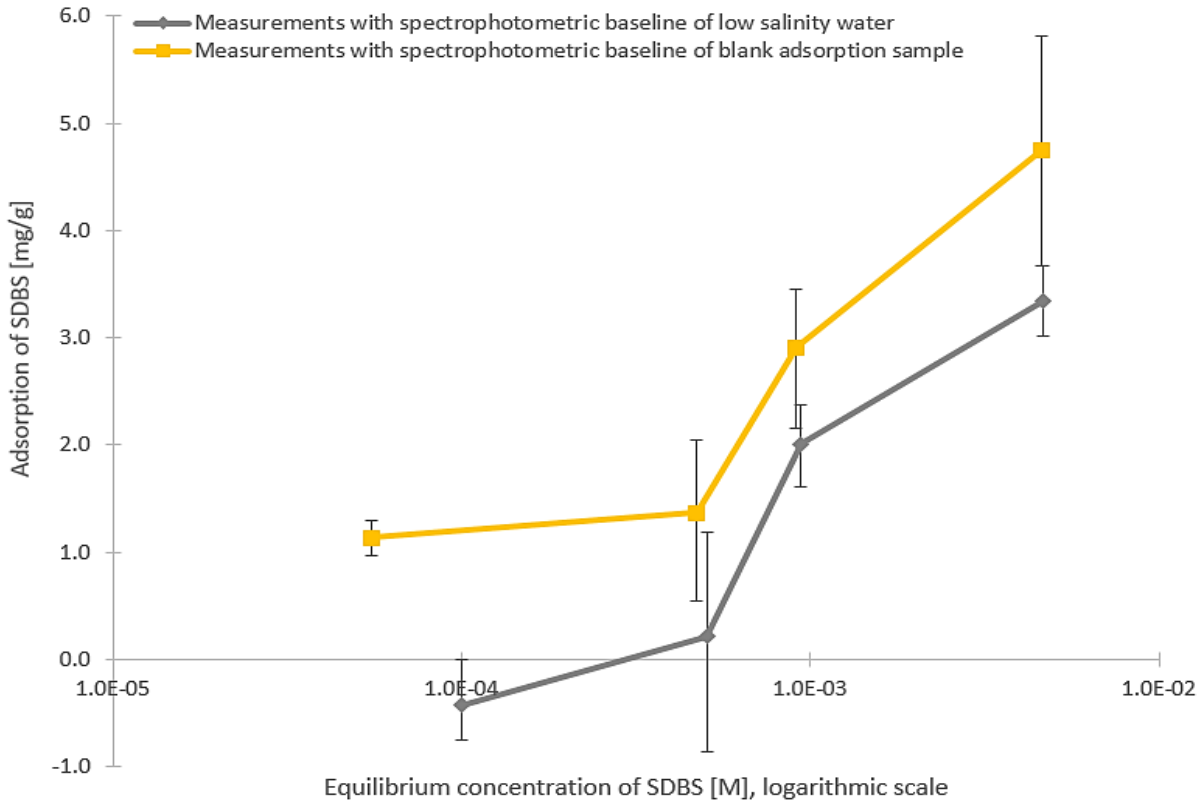

Figure 22. Results from Test experiment 3, where adsorption samples in LS were prepared by the general procedure with additional centrifugation and filtration. Adsorption of SDBS on kaolinite at 25°C as a function of equilibrium SDBS concentration based on analysis conducted with an UV-vis spectrophotometer at 260 nm with two different spectrophotometric baselines.

4.3.2 Surface Tension

Test experiment 4

The adsorption isotherm for samples analysed with tensiometer was constructed with four initial nominal SDBS concentrations below the CMC: $5.00 \cdot 10^{-6}$, $1.00 \cdot 10^{-5}$, $5.00 \cdot 10^{-5}$ and $1.00 \cdot 10^{-4}$ M. As described in the theory and observed in the corresponding calibration curve, the surface tension is approximately constant with surfactant concentrations above the CMC. Thus, the calibration curve was only valid below the CMC. Dilution of the samples was avoided because it would cause a substantial uncertainty in the measurements. Figure 23 displays two adsorption isotherms—grey isotherm represents the isotherm created from analyses of samples prepared by the general procedure (section 3.5.1), and yellow represents the isotherm created from analyses of samples that had undergone additional centrifugation. At low concentrations, the isotherms overlap largely, but at a nominal initial SDBS concentration of $1.00 \cdot 10^{-4}$ M, the isotherms were significantly different. At this concentration, additional centrifugation of the samples led to a higher measured surface tension, and consequently, a lower calculated adsorption of SDBS.

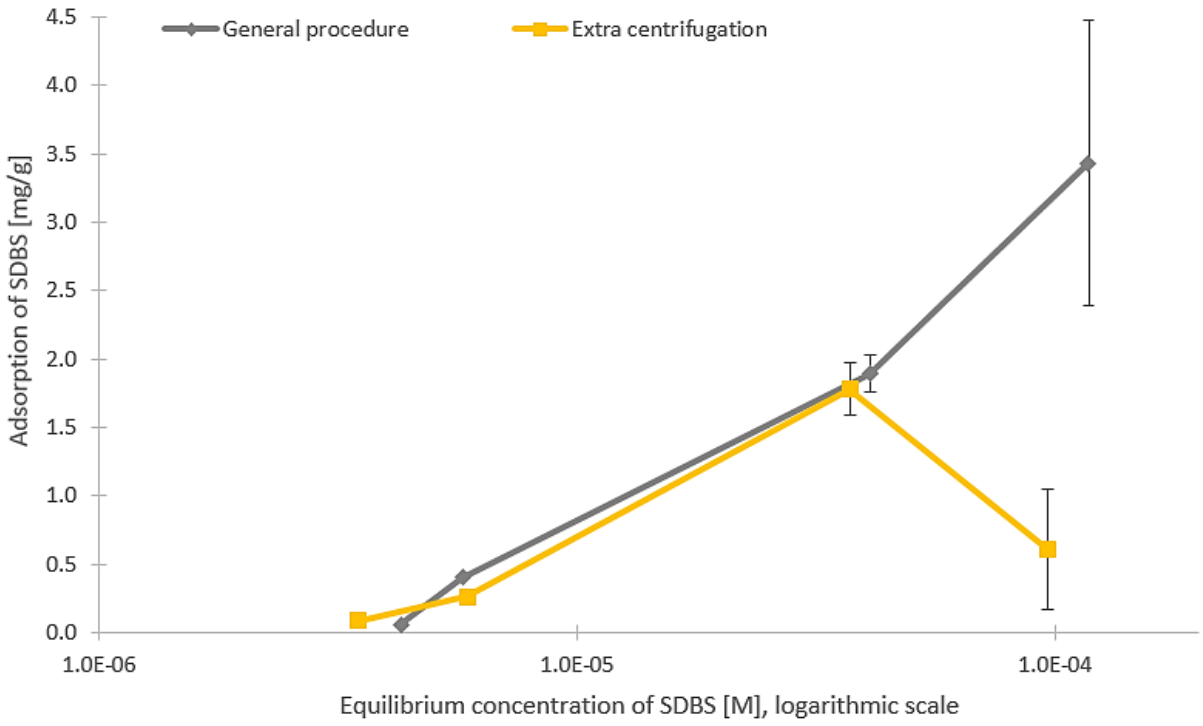

Figure 23. Results from Test experiment 4, where adsorption samples in LS were prepared by the general procedure and additional centrifugation. Adsorption of SDBS on kaolinite as a function of equilibrium SDBS concentration based on analysis conducted with a ring tensiometer at 25°C.

Wang (2013) observed that the presence of nanoparticles on a liquid-liquid interface reduces the interfacial tension. The interfacial tension decreases as the concentration of nanoparticles increases until a critical value is reached, at which point the nanoparticles form aggregates. This phenomenon might have occurred at the liquid-air interface in this experiment. The removal of particles during centrifugation and the resulting increase in surface tension would explain the deviation between the measured surface tension of samples with initial nominal concentration of $1.00 \cdot 10^{-4}$ M SDBS. A greater proportion of particles were observed in samples with low SDBS concentration compared to high, which was also confirmed by the particle size measurements. Thus, the insignificant difference between surface tension measurements of samples with and without further centrifugation at low SDBS concentrations could possibly be explained by a nanoparticle concentration above the critical value. If the additional centrifugation of the samples did not decrease the concentration of nanoparticles below the critical value, the surface tension would not be significantly influenced, and thus would explain the similar results.

The measurements conducted with Du Noüy ring tensiometer were time-consuming. Some of the samples did not stabilize, which consequently led to a measurement uncertainty. Because of the time consumption of this analysis method, further experiments were only measured by UV-vis spectroscopy.

4.4 Adsorption Studies of Surfactant on Kaolinite

SDBS in solutions with different salinities was adsorbed on kaolinite during mixing over 24 hours. UV-vis spectrophotometric measurements at 260 nm and the calibration curves presented in section 4.2 and Appendix C, were used in the calculations of initial SDBS concentration (C_0) and equilibrium concentration of SDBS after adsorption on kaolinite (C_e). Equation (4) was used in the calculation of the amount of SDBS adsorbed on kaolinite. The sample properties and the measured absorbance of all adsorption samples presented in this section are given in Appendix F, while the calculated results utilized to produce adsorption isotherms, are provided in Appendix G. Appendix H provides all the SDBS adsorption isotherms presented in this section as independent plots.

4.4.1 Adsorption Studies of SDBS in Brine with Monovalent Ions

It was difficult to predict whether filtration of the adsorption samples would contribute to increased accuracy of the results. The risk of filtration was that some of the SDBS molecules in the solution might have adsorbed on the filter membrane, and consequently led to loss of analyte. On the other hand, the test experiments pointed towards impurities in the analytical samples that led to a positive error in the absorbance measurements. Particle size measurements showed that filtration of the samples removed some of these impurities. Because of this uncertainty, adsorption studies of SDBS in LS and MS were conducted both with and without filtration. Adsorption experiments with the other brine compositions were only conducted without filtration due to high filter prices. An absorption spectrum of SDBS in filtered LS samples is provided in Figure D2, Appendix D.

Figure 24 presents the adsorption isotherms from adsorption studies of LS and MS where the adsorption samples were filtered before the spectrophotometric analysis. The calculated CMC values are marked with red dots in the curves. The SDBS adsorption isotherms of LS and MS have noticeable similarities, and both isotherms have two adsorption maxima. The first adsorption maximum was reached at a SDBS concentration close to the CMC. Consequently, the maximum was at a lower SDBS concentration in MS than LS. The shape of the adsorption isotherms was not as expected in that the isotherms had no similarities to the theoretical four-region isotherm described in section 2.6.4.

Scamehorn et al. (1982a) used isomerically pure SDBS in adsorption studies on kaolinite, and suggested that maxima and minima observed in other studies might be due to complex surfactant intercomponent interactions. In a second publication (Scamehorn et al., 1982b), this phenomenon was further studied and explained. Two SDBS isomers at a constant feed composition, with mole fractions of 0.9 and 0.1, in brine of 0.171 M NaCl were used for this purpose. The results indicate that in systems with high L/S ratios, the total monomer concentration increases further after the CMC is reached. However, at the same time the mole fraction of the lesser adsorbing isomer increases in the bulk solution, which will tend to decrease adsorption. As the total concentration increases further, the large amount of monomers reverses this trend, resulting in both a maximum and a minimum in the adsorption isotherm. Scamehorn et al. (1982b) explain this phenomenon in more detail.

In this study, a technical-grade SDBS was used. The product specification from Sigma Aldrich (2014) specifies that the material may contain positional isomers and branched isomers. The

similarities between this study and the work reported by Scamehorn et al. (1982b) (SDBS adsorption on kaolinite, high L/S ratio, decrease in adsorption close to CMC etc.), might indicate that isomeric impurities in the SDBS chemical contributed to the observed maxima and minima in Figure 24. Adsorption maxima and minima due to surface-active impurities were also suggested by Giles et al. (1974) and Paria and Khilar (2004).

Figure 24 illustrates that the adsorption of SDBS on kaolinite was higher in MS brine compared to LS brine. These results are supported by studies performed by Glover et al. (1979) on surfactant retention in Berea cores, which imply a linear increase of surfactant adsorption with increased salinity. According to Equation (3), the extension of the electrical double layer decreases with increasing electrolyte concentration (c_i). As described in the theory, this will make it easier for the surfactants to approach the surface, which might have contributed to increased adsorption. Furthermore, the electrostatic repulsion between the surfactants' head groups is also reduced, permitting the head groups to move closer together; this enables a higher packing density on the clay surface as it reduces the effective head group area.

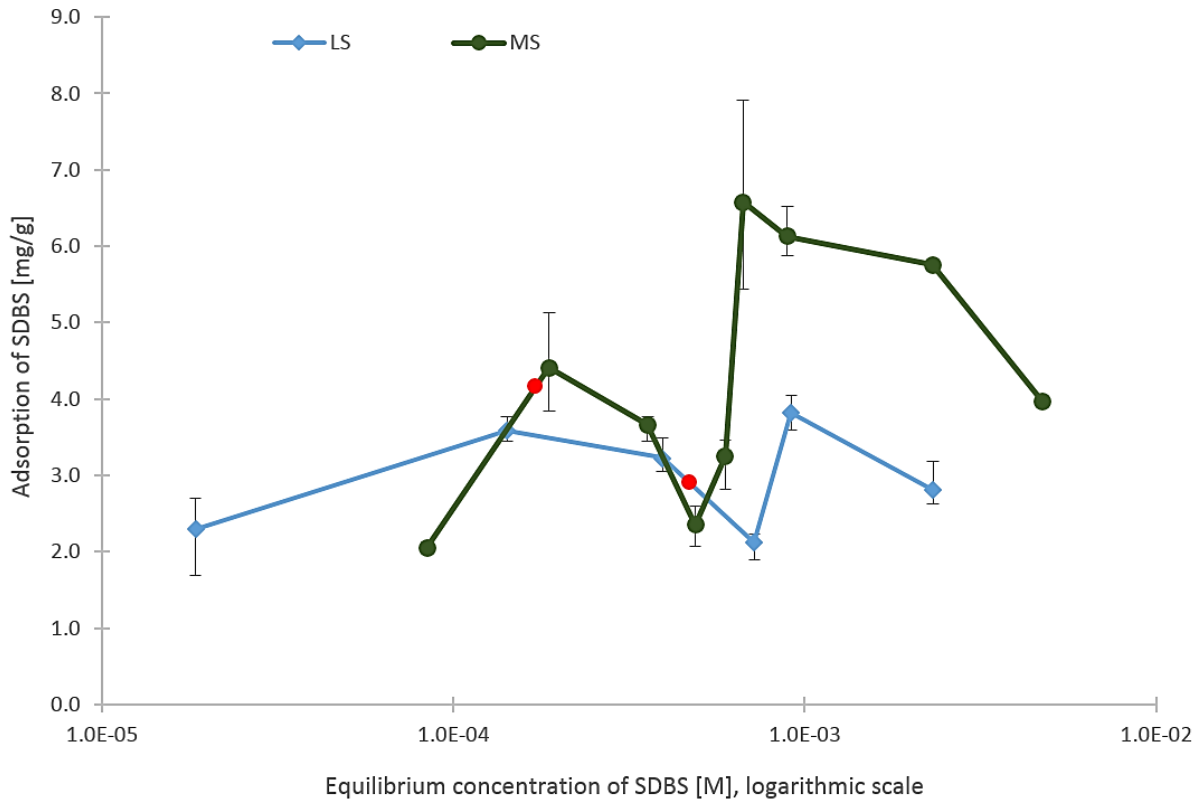

Figure 24. Adsorption isotherm of SDBS in filtered LS and MS samples. Red marks indicate the CMC. Calculated SDBS adsorption on kaolinite at 25°C as a function of equilibrium SDBS concentration, based on analysis conducted with an UV-vis spectrophotometer at 260 nm.

Figure 25 displays the adsorption isotherms developed from adsorption studies of SDBS in LS, MS and HS without filtration of the adsorption samples. The calculated SDBS adsorption was, as expected, lower than for the experiments with filtration, but whether this was due to the removal of impurities or loss of surfactants on the filter membrane during filtration was not evident.

The isotherms created from samples without filtration did not have shapes as distinct as the isotherms from filtered samples. However, maxima and minima were observed, and a comparison of the isotherms derived from SDBS in MS and HS indicated a similar trend to what was discussed above, with adsorption maxima at lower SDBS equilibrium concentration with increased salinity. However, the isotherms of SDBS in LS and MS showed an adsorption minimum before the CMC was reached. This result was difficult to explain; based on adsorption theory, it was expected that the adsorption would increase linearly and obey Henry's Law at low SDBS concentrations.

It was difficult to conclude a specific difference between amount of SDBS adsorbed on kaolinite in LS and MS brine. However, the adsorption of SDBS in HS was significantly higher as compared to SDBS in MS and LS. This confirmed the increased SDBS adsorption with salinity, as discussed above. Lv et al. (2011) determined the plateau adsorption of SDBS on untreated kaolinite in 0.17 M NaCl to be 2.3848 mg/g. This was a lower value than the maximum adsorption measured in this study of 3.6 ± 0.4 mg/g in HS brine (0.20 M NaCl). Hanna and Somasundaran (1979) investigated the effect of pretreatment of kaolinite on sulfonate adsorption, and those results show that the adsorption capacity of purified Na-kaolinite is higher than the untreated kaolinite. The difference between the two plateau adsorptions might be attributed to the small difference in ionic strength and the different equilibrium states of the kaolinite.

The pH in the adsorption samples were measured after the adsorption experiments to be 5.08-6.98, 4.73-6.90 and 4.66-6.53, in LS, MS and HS samples, respectively, and the exact pH of each sample is given in Appendix F. The general trend was an increase in pH as the SDBS concentration increased and as the ionic strength decreased; these observations may be explained by ion exchange. When NaCl is added to the system, H^+ at the kaolinite surface can exchange with Na^+ in the solution leading to a decrease in the pH. The addition of SDBS creates more possibilities for ion exchange. The sulfonate ions can exchange with hydroxide ions at the kaolinite surface, and thus establish a more alkaline environment (Hanna and Somasundaran, 1979). In the measured pH intervals, kaolinite was expected to have a net negative surface

charge. However, as stated in the theory, the edges of kaolinite usually have positive adsorption sites. It can be assumed that SDBS was adsorbed by electrostatic attraction between the anionic head groups of SDBS and the positively charged sites. Formation of surface aggregates has been reported by several researchers (Lv et al., 2011; Scamehorn et al., 1982a), but the adsorption isotherms presented in Figure 25 were too inconclusive to permit such conclusions.

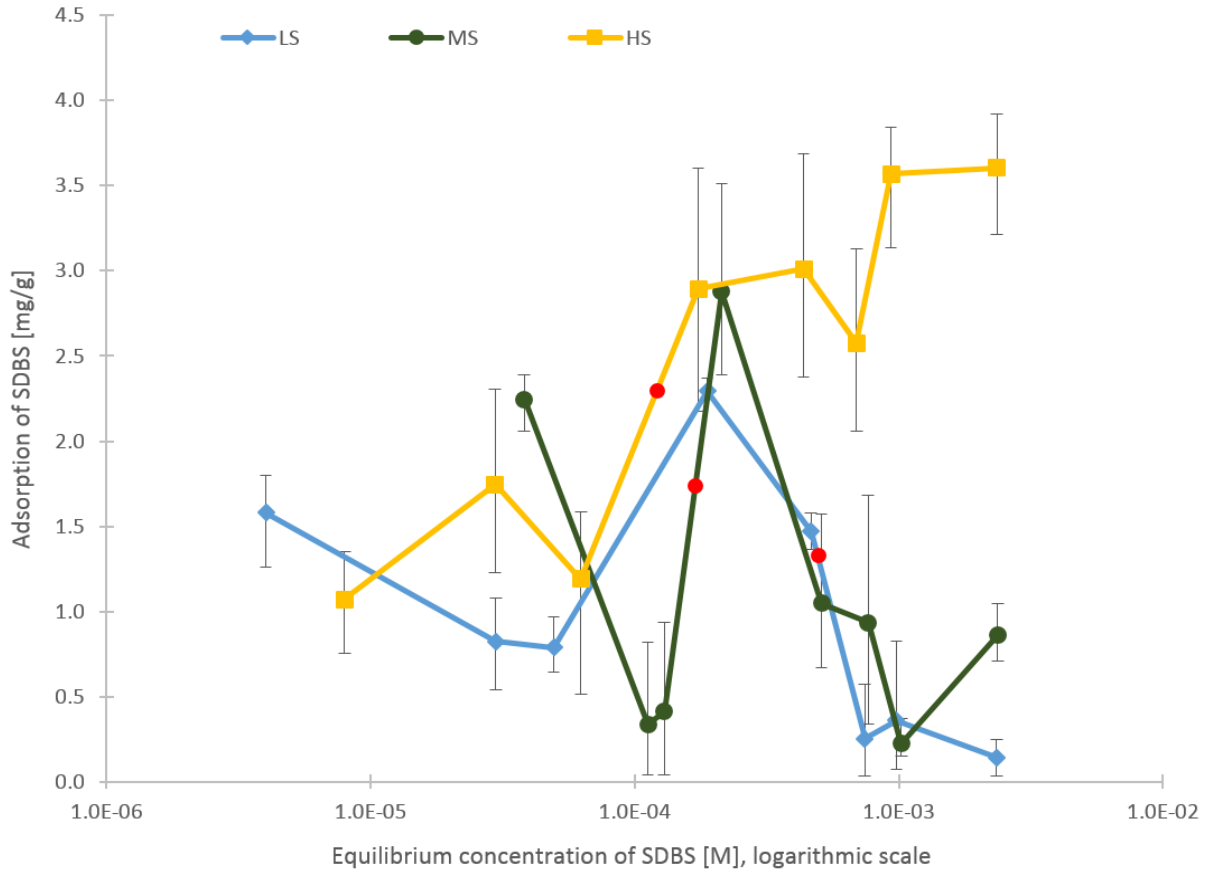

Figure 25. Adsorption isotherm of SDBS in LS, MS and HS brine. Red marks indicate the CMC. Calculated SDBS adsorption on kaolinite at 25°C as a function of equilibrium SDBS concentration, based on analysis conducted with an UV-vis spectrophotometer at 260 nm.

4.4.2 Adsorption Studies of SDBS in Brine with Divalent Ions

The calibration curve of SDBS in LS w/Ca^{2+} presented in Figure 18 illustrates how ageing influenced the absorbance measurements, and it was speculated that this phenomenon was due to phase alteration of the surfactant solutions. This speculated phase alteration had a significant impact on the results related to the adsorption studies of SDBS in LS w/Ca^{2+} and MS w/Ca^{2+}.

The adsorption of SDBS on kaolinite was calculated from the difference between the initial concentration (C_0), and the equilibrium concentration at the end of the adsorption experiment (C_e), as illustrated by Equation (4). The initial concentration, which corresponded to the concentration of the diluted stock solutions used in the preparation of the adsorption samples, was measured at the beginning (C_0) and end (C_0') of the adsorption experiments. These measurements, at t = 0 h and t = 24 h, gave different results because storing the diluted stock solutions during the 24 hours of the experiment altered the solutions. It was expected that the speculated phase alteration that influenced the absorbance measurements of the diluted stock solutions also took place in the bulk phase of the adsorption samples during mixing. Thus, it was difficult to decide if C_0 or C_0' would provide the best foundation to calculate the amount of SDBS adsorbed on kaolinite. Figure 26 presents the adsorption isotherms developed from adsorption studies of SDBS in LS w/Ca^{2+} and MS w/Ca^{2+}. The dotted and solid lines represent the isotherms calculated on the basis of C_0 and C_0', respectively. It was expected that the actual amount of SDBS adsorbed on kaolinite would be in the range between these values, and from the extensive amount of calculated adsorbed SDBS, it was evident that the solid isotherms were overestimated.

The isotherms show an S-shape, which is a typical characteristic for adsorption of negatively charged surfactants on kaolinite. According to adsorption theory, the adsorption at low surfactant concentrations is due to electrostatic interactions between the charged surface and the surfactant head groups. As the concentration increases, surface aggregates are formed due to lateral interactions between the hydrophobic tails of the surfactants. The isotherms in Figure 26 show an adsorption maximum in the last region. Lv et al. (2011) explained the maximum adsorption by precipitation of surfactant molecules due to interactions with multivalent cations, and the subsequent redissolution of the precipitate by micelles. This is similar to the suggested phase alteration theory. Precipitation of surfactants would affect the results differently according to the experimental techniques and analysis methods. The adsorption maximum may arise if the precipitation is not detected; thus, the measured equilibrium concentration is lower than the actual, and subsequently the calculated adsorption gets a positive error, creating a maximum. In this study, the increased turbidity from precipitate in the solutions created an opposite effect, and the measured absorbance was greater. The overestimated SDBS adsorption probably arose from a greater error in measurements of the initial concentration compared to the measurements of the equilibrium concentration, and resulted in a positive error of the calculated adsorption according to Equation (4).

The isotherms show an increase in the slope towards maximum adsorption close to the calculated CMC, illustrated by red marks in Figure 26. As described in the theory, only monomers are known to adsorb on the kaolinite surface, and thus adsorption of micelles would not explain this result. However, Figure 18 illustrates that the suspected phase alteration starts close to the CMC, which possibly contributed to this phenomenon.

Because of the turbidity of the solutions, the calculated quantity of adsorbed SDBS above CMC was untrustworthy. However, the trend of the results pointed towards a greater SDBS adsorption on kaolinite in MS w/Ca^{2+} than LS w/Ca^{2+}, which confirmed an increased adsorption with ionic strength as observed in monovalent brine.

The pH in the adsorption samples were measured after the adsorption experiments to 4.80-7.00 and 4.59-6.64, in LS w/Ca^{2+} and MS w/Ca^{2+} samples, respectively. As observed in samples with only monovalent ions, the general trend was an increase in pH with increased SDBS concentration and decreased ionic strength. The exact pH in each sample is given in Appendix F.

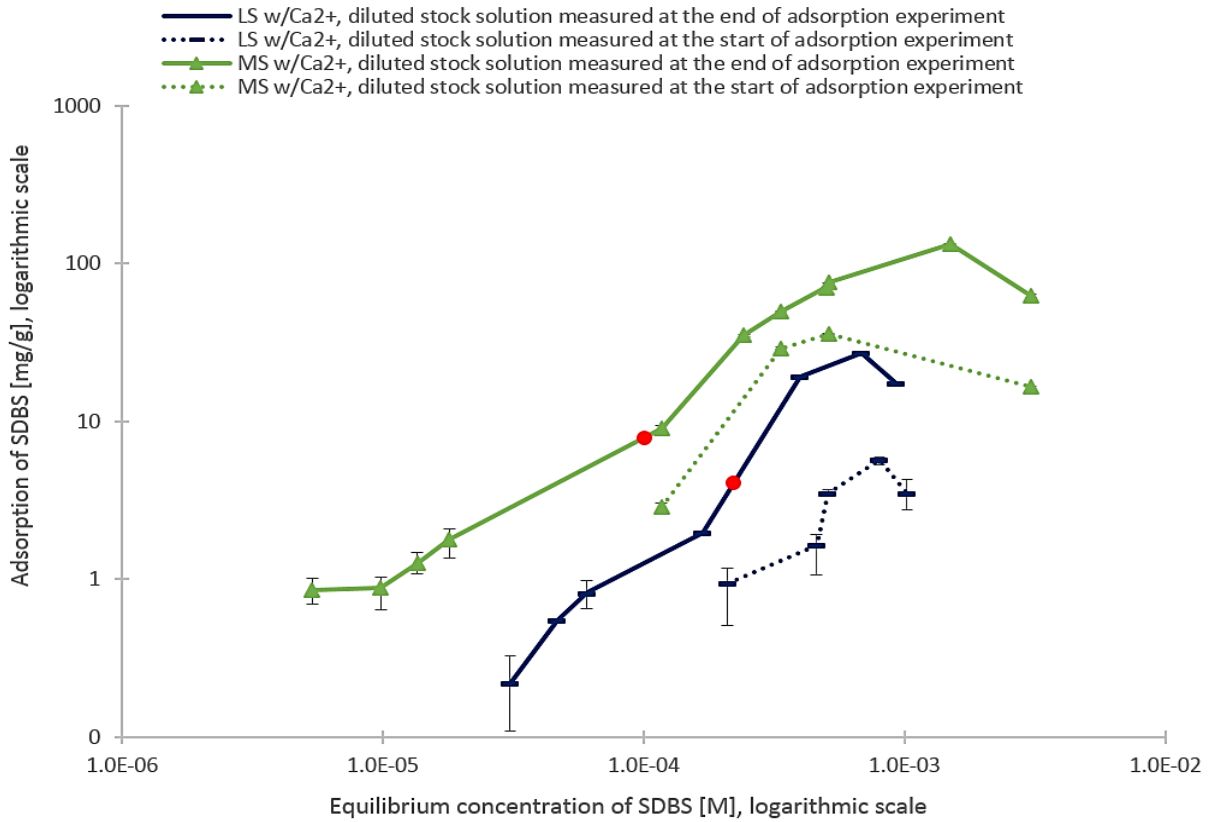

Figure 26. Adsorption isotherm of SDBS in LS w/Ca^{2+} and MS w/Ca^{2+} brine. Red marks indicate the CMC. Calculated SDBS adsorption on kaolinite at 25°C as a function of equilibrium SDBS concentration, based on analysis conducted with an UV-vis spectrophotometer at 260 nm. Both scales are logarithmic.

4.4.3 Influence of Divalent Ions on the Adsorption of SDBS on Kaolinite

In order to investigate the effect of divalent ions on the adsorption of SDBS on kaolinite, the previously presented adsorption isotherms are displayed according to ionic strength. To have a basis for comparison, only the results from the experiments without filtration were chosen for further analysing. Figure 27 presents the adsorption isotherms of SDBS in LS and LS w/Ca^{2+}; the results indicated that the presence of divalent ions led to an increased adsorption at high SDBS concentrations. However, below the CMC, the results implied a small decrease in adsorption of SDBS on kaolinite in LS w/Ca^{2+} as compared to LS. Figure 28 presents the adsorption isotherms of SDBS in MS and MS w/Ca^{2+}. The results indicated that the presence of divalent ions led to an increased SDBS adsorption at all measured concentrations.

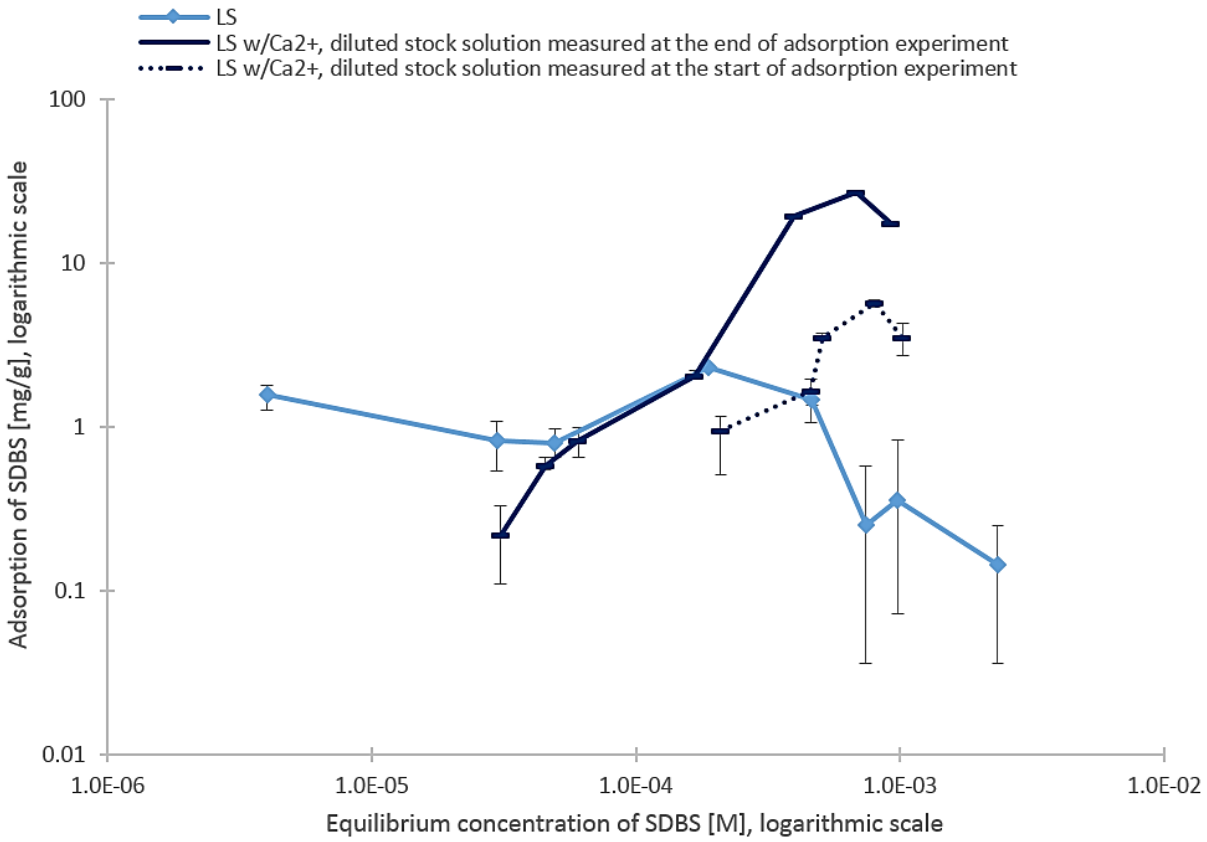

Figure 27. Adsorption isotherm of SDBS in LS and LS w/Ca^{2+} brine with an ionic strength of 20.0 mM. Calculated SDBS adsorption on kaolinite at 25°C as a function of equilibrium SDBS concentration, based on analysis conducted with an UV-vis spectrophotometer at 260 nm. Both scales are logarithmic.

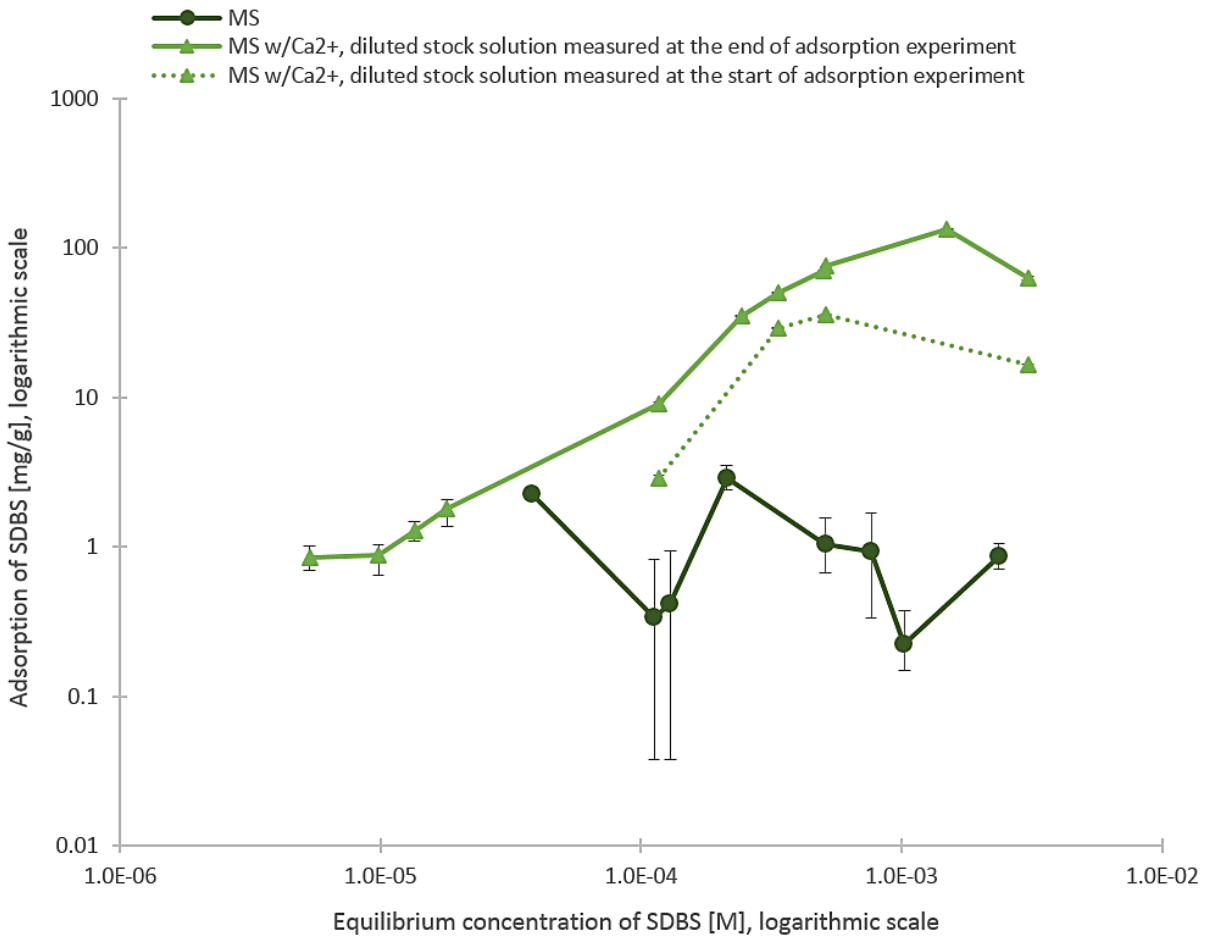

Figure 28. Adsorption isotherm of SDBS in MS and MS w/Ca^{2+} brine with an ionic strength of 80.0 mM. Calculated SDBS adsorption on kaolinite at 25°C as a function of equilibrium SDBS concentration, based on analysis conducted with an UV-vis spectrophotometer at 260 nm. Both scales are logarithmic.

Possible explanations of the increased SDBS adsorption when adding divalent ions are the alteration of electrostatic interaction between surfactant-surfactant, and between surfactant-kaolinite. Ca^{2+} affects the double layer force in two ways: 1) by adsorption that changes the surface potential and thus the overall magnitude of the force, 2) in solution by screening the electrostatic repulsion between head groups and compressing the double layer.

In the first case, a reduction of the negative surface charge on kaolinite would decrease the repulsion between equal charges. As mentioned in the theory, compared to Na^{+}, Ca^{2+} is known to have greater affinity towards kaolinite. Wanless and Ducker (1997) studied how a negative surface was altered by increasing the concentration of divalent cations, and the results indicate that as the concentration of divalent ions increases, the negative surface charge decreases, and at high electrolyte concentrations charge reversal of the surface occurs. These discoveries

support the results from this study. It was also likely that organo-metallic complexes might have been formed, where Ca^{2+} act as a bridge between the negative charged surfactant and a negative site on the clay surface. These complexes were proposed by Figdore (1982), and would explain increased adsorption with divalent cations.

In the second case, a decrease in the extension of the electrical double layer permits ionic head groups to move closer together. However, in this study, surfactant systems with and without divalent ions were compared at the same ionic strength, and thus had an equal Debye length as quantified in the next section. Nevertheless, the CMC measurements implied that compared to Na^{+}, Ca^{2+} had a greater ability to stabilize the repulsion between the ionic head groups of SDBS. Thus, the surfactants might have been adsorbed closer together at the kaolinite surface in the presence of Ca^{2+}, resulting in an increased adsorption. Force measurement performed by Wanless and Ducker (1997) supports this theory, as it suggests that there is a transition from a thin layer to a thicker layer of surfactants on the solid surface as divalent ions are added.

4.4.4 Extension of the Electrical Double Layer

The Debye length, expressed by Equation (3), was calculated for the five different brine-clay systems at 25°C and are provided in Table 6. The calculated Debye lengths quantified the principle of decreased extension of the electrical double layer with increased ionic strength, as discussed in previous sections. The calculations are based on the brine-clay systems without SDBS. Since SDBS is an ionic compound, the Debye length was expected to decrease with increasing equilibrium concentration of SDBS.

Table 6. Calculated Debye length (κ^{-1}) at 25°C of charged kaolinite particles in brine solutions with different composition and ionic strength.

Brine standard	**κ^{-1} [nm]**
LS	2.16
LS w/Ca^{2+}	2.16
MS	1.08
MS w/Ca^{2+}	1.08
HS	0.682

4.5 Langmuir and Freundlich Isotherm Models

The results from the adsorption studies of SDBS were analysed by the Langmuir and Freundlich models by creating linear regression curves from Equation (6) and (8), respectively.

4.5.1 Brine with Monovalent Ions

Figures 29, 30 and 31, display the Langmuir and Freundlich plots for the adsorption of SDBS on kaolinite in LS, MS and HS brine, respectively.

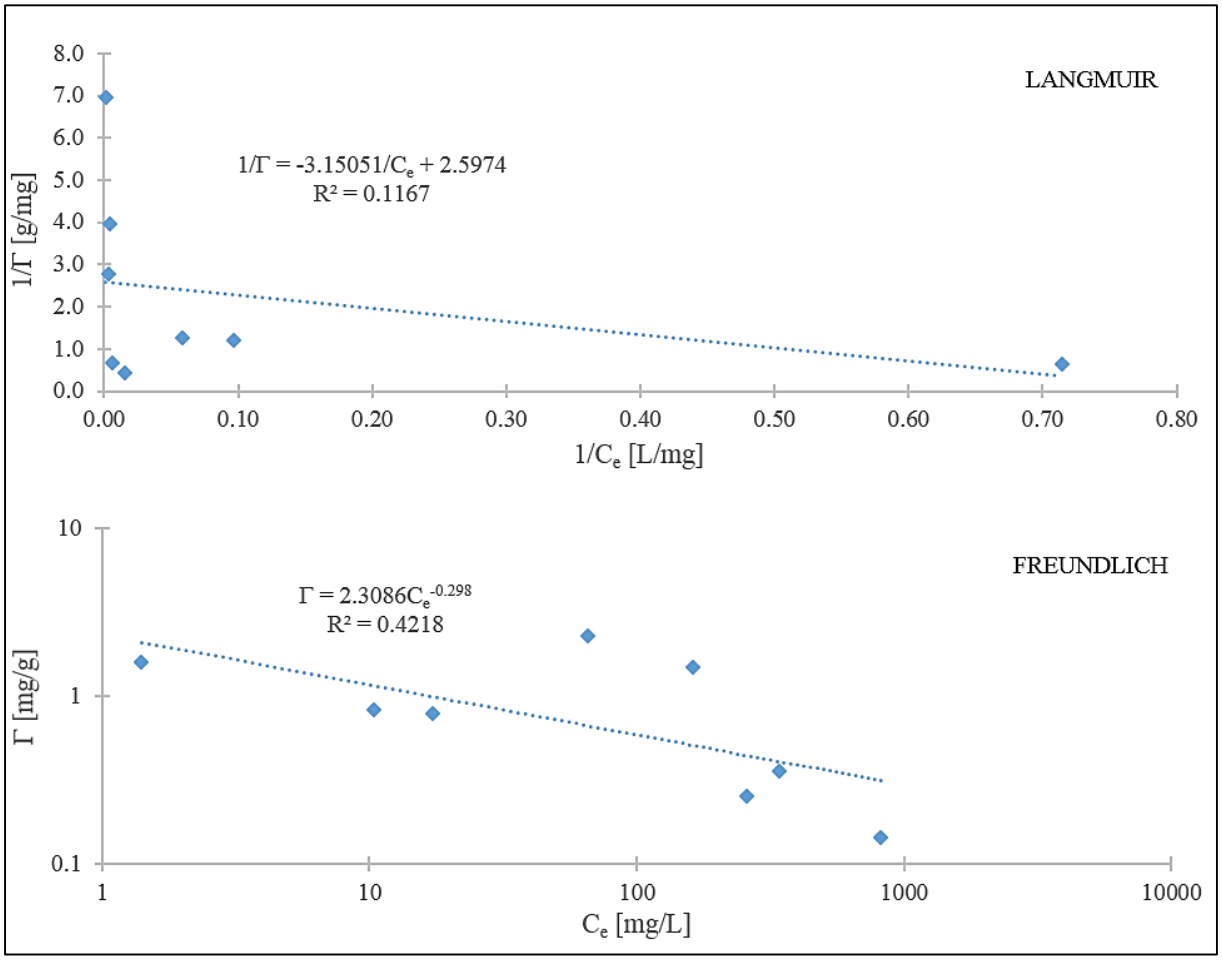

Figure 29. Application of Langmuir and Freundlich equations to the experimental data determined for the adsorption of SDBS on kaolinite in LS brine.

The equation of the trend line and the correlation coefficient, R^2, are presented in each figure. Based on the R^2 values, neither the Langmuir nor the Freundlich model applied for adsorption of SDBS in LS and MS brine.

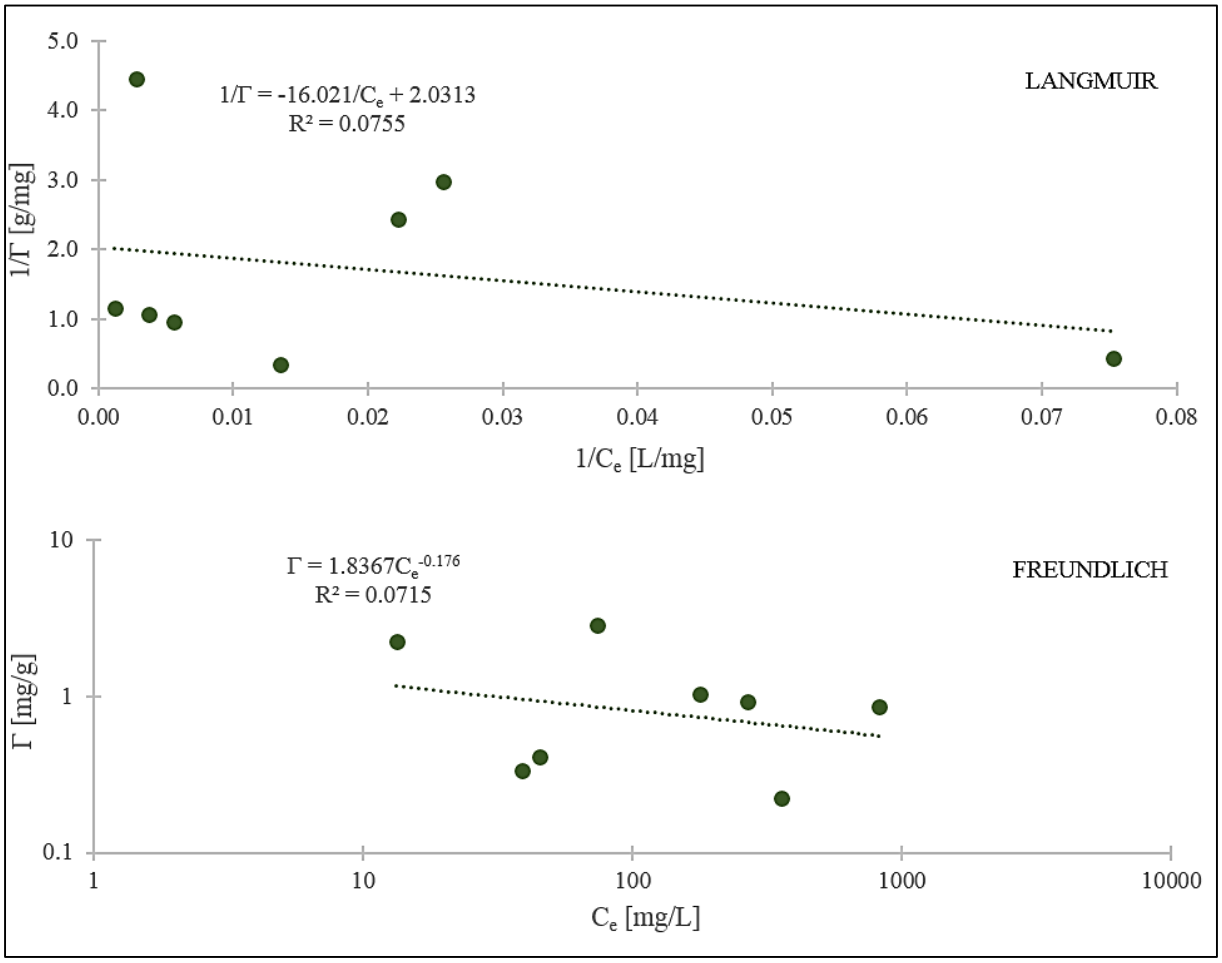

Figure 30. Application of Langmuir and Freundlich equations to the experimental data determined for the adsorption of SDBS on kaolinite in MS brine.

Figure 31 presents the Langmuir and Freundlich plots for the adsorption of SDBS in HS brine. The experimental values matched the models better than for the systems with lower salinities, and the SDBS adsorption in HS brine was considered as the only system with monovalent ions that were applicable to either of the isotherm models. The Freundlich model, with an R^2 value of 0.8113, had the best fit to the system. The Freundlich constants k_f and n were calculated to be 15.4 L/g and 4.44, respectively.

By comparing the typical shape of the Langmuir and Freundlich isotherms (Figure 11) with the shape of the SDBS adsorption isotherms in systems with monovalent ions (Figure 25), the

results presented in this section were confirmed. There were no similarities between the shape of the experimental isotherms and the Langmuir model. Since none of the assumptions that form the basis of this model applied the surfactant systems, it was not expected that the Langmuir model would be a perfect fit for the experimental data. However, it was expected that the experimental isotherms would have more similarities to the four-region adsorption isotherm and subsequently a somewhat better fit to the Langmuir model than observed. The unexpected shapes of the isotherms created for SDBS in LS and MS brine resulted in a bad fit for the Freundlich isotherm as well.

Even though the adsorption isotherm of SDBS in HS brine showed maxima and minima, the general trend was a gradual increased adsorption as the SDBS concentration increased. The Freundlich isotherm model mathematically approaches infinite surface coverage, which might have contributed to the match between the experimental results and the theoretical model.

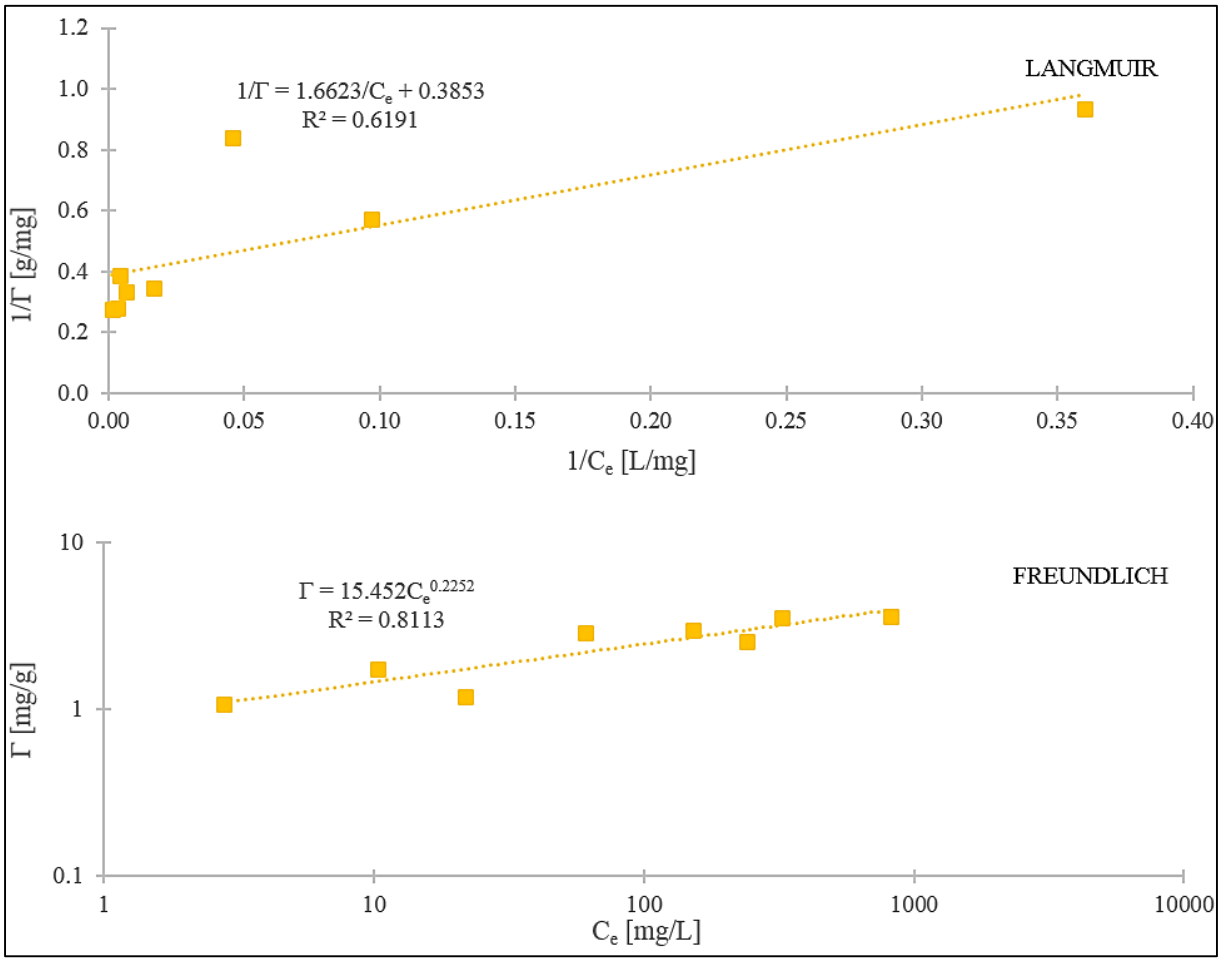

Figure 31. Application of Langmuir and Freundlich equations to the experimental data determined for the adsorption of SDBS on kaolinite in HS brine.

4.5.2 Brine with Divalent Ions

The Langmuir and Freundlich isotherm plots for the adsorption of SDBS on kaolinite in LS w/Ca^{2+} and MS w/Ca^{2+} brine, are presented in Figures 32 and 33, respectively. The equation of the trend line and the R^2 value are presented in both figures. Examination of the plots suggested that both models had good fits for the adsorption of SDBS in brine with divalent ions. Based on the R^2 values, the Freundlich model gave a somewhat better match than the Langmuir model for both salinities. When comparing the typical shape of the Langmuir and Freundlich isotherms (Figure 11) and the shape of the solid SDBS adsorption isotherms in systems with divalent ions (Figure 26), the similarities are greater compared to the observations for the monovalent systems.

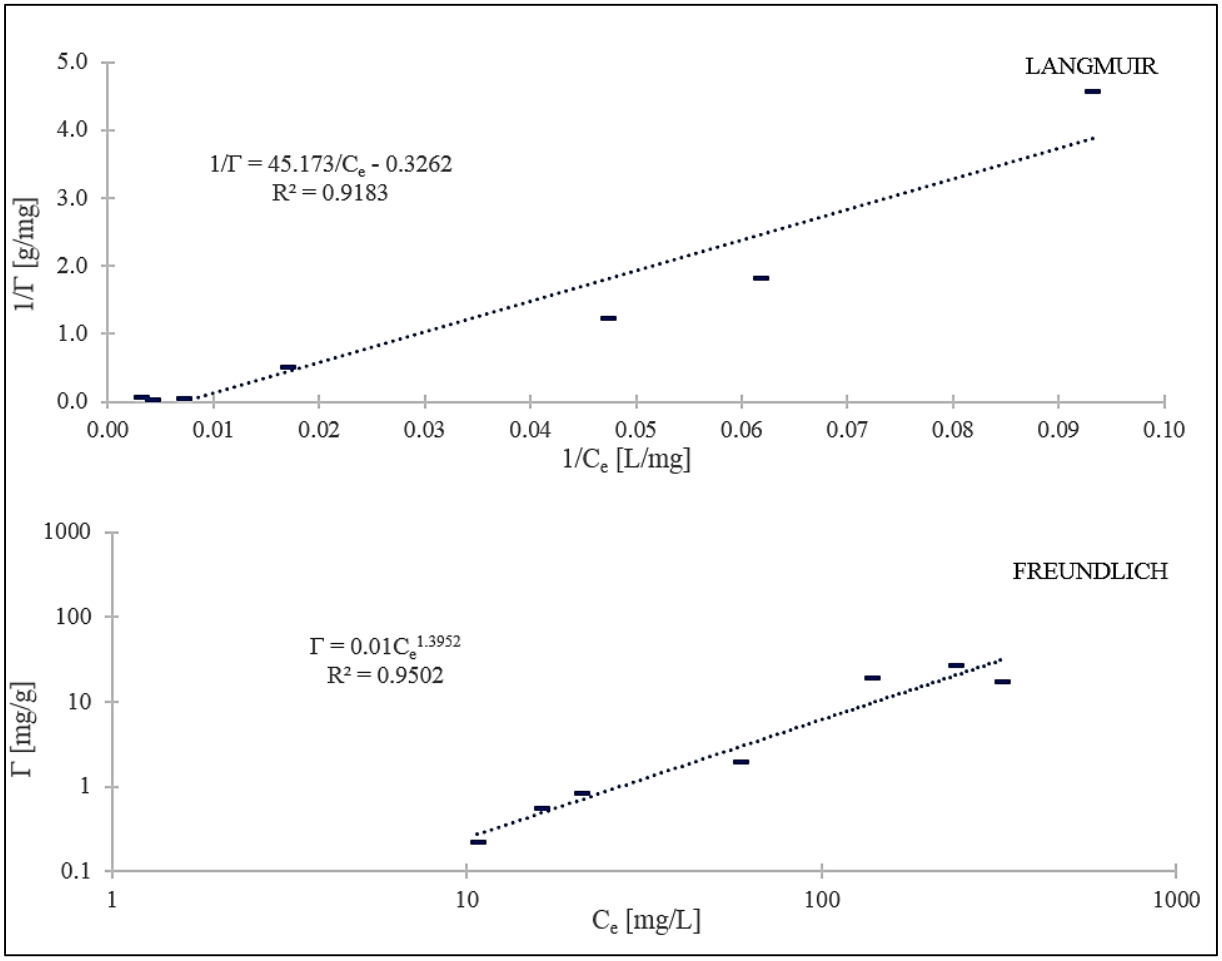

Figure 32. Application of Langmuir and Freundlich equations to the experimental data determined for the adsorption of SDBS on kaolinite in LS w/Ca^{2+} brine.

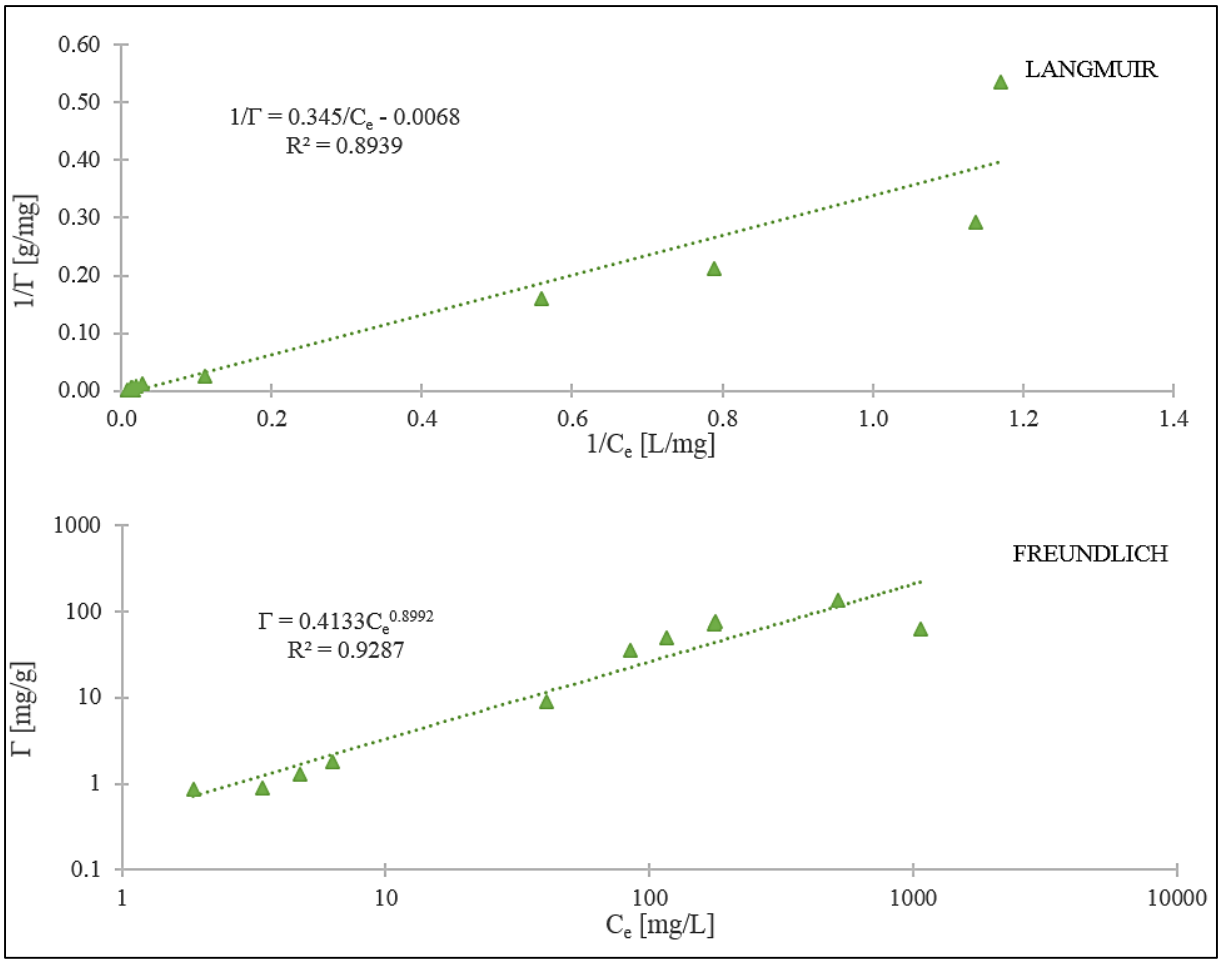

Figure 33. Application of Langmuir and Freundlich equations to the experimental data determined for the adsorption of SDBS on kaolinite in MS w/Ca^{2+} brine.

The linearized Langmuir plots had a negative intercept for both divalent surfactant systems. Thus, the Langmuir constants were negative and could not be assigned a physical significance. The Freundlich constants, k_f and n, were determined to be 0.010 L/g and 0.717, and 0.413 L/g and 1.11 in LS w/Ca^{2+} and MS w/Ca^{2+}, respectively. The Freundlich constant n, as described in the theory, usually has a value in the range of 2-10. The determined constant for these systems were unusually low, and indicated cooperative adsorption and a heterogeneous surface. Furthermore, a low value of n suggests a poor adsorption at low concentrations, but good adsorption in high concentrations (Muherei and Junin, 2009). The Freundlich constant k_f, indicated that the extent of adsorption was lower for the LS w/Ca^{2+} system compared to MS w/Ca^{2+}. These indications corresponded well with the observed results.

5 Conclusion

The equilibrium adsorption of SDBS on kaolinite was studied by static methods, and several test experiments were conducted in order to establish a good experimental procedure. The analyses were conducted using both an UV-vis spectrophotometer and a ring tensiometer. The presence of mineral fines in the analytical samples influenced the measurements performed by both techniques, and the removal of these fines was required to obtain a reliable result. The measurements of surface tension were time-consuming, and the uncertainty associated with these measurements was considered greater as compared to the absorbance measurements. Thus, the spectroscopic method was considered as the best approach for this study

The adsorption of SDBS on kaolinite in brines with different composition and ionic strength was investigated. The results indicated increasing SDBS adsorption with ionic strength, which implied promising results in term of reduced surfactant adsorption when combining the EOR techniques surfactant flooding and low salinity waterflooding. However, this study comprised only lab scale experiments conducted with parameters dissimilar to reservoir conditions, and consequently, field application may give different results. Furthermore, the results indicated that the presence of divalent ions led to an increased SDBS adsorption. However, in brine with divalent ions, turbidity affected the UV-vis spectrophotometric analysis for surfactant solutions above the CMC, and accordingly added a significant uncertainty to the results.

The adsorption isotherms for SDBS in monovalent brine had unexpected shapes. Both maxima and minima were observed, there was not an adsorption plateau, but continued adsorption after the CMC. Adsorption isotherms with a characteristic S-shape were obtained for studies in divalent brine, and it was suspected that the adsorption maximum in these isotherms was due to the formation of precipitate when SDBS interacted with divalent ions.

The SDBS adsorption isotherms were analysed by the Langmuir and Freundlich adsorption models. The Freundlich model described the experimental data best, and SDBS systems with high salinity or divalent ions had the best fit to the theoretical model.

6 Further Work

Further work should be considered to improve the experimental method. During this study, samples often had to be remade, either because of impurities in the sample or because of sample alteration by ageing. A comparison of results from experiments performed with and without filtration of samples indicated a higher repeatability when the samples were filtered. Thus, a more effective removal of fines should be incorporated to the experimental method. Furthermore, it was difficult to detect SDBS by UV-vis spectroscopy at low SDBS concentrations, especially in high salinity brine. Several studies with spectrophotometric determination of anionic surfactants are based on the formation of ion associates and their subsequent extraction into organic solvents (Ghiasvand et al., 2009; Adak et al., 2005; Motomizu et al., 1982). Various cationic dyes have been reportedly utilized for this purpose, hence they could be considered for further studies in order to enable detection at lower surfactant concentrations. An alternative to filtration and extraction is reverse-phase ion-pair chromatography, which is a well-documented technique to separate anionic surfactants, and this technique will avoid light scattering from mineral fines in the solution (Austad et al., 1991a).

It would have been interesting to study the alteration of the clay surface in terms of surface potential and wettability. Measurements of the zeta potential would provide a better foundation for understanding the adsorption mechanisms. Contact angle measurements would provide insight into the hydrophobicity of the surface and would offer a validation of the adsorption isotherms as it is expected that the contact angle would increase with adsorbed surfactant.

Zhu and Gu (1989) proposed a general isotherm equation based on the two-step adsorption mechanism of surfactants at the solid/liquid interface. The first step refers to adsorption by surface-surfactant interactions, and the second step refers to adsorption by hydrophobic interactions between surfactant-surfactant. Since this isotherm allows for the expression of several adsorption phenomenon of surfactant adsorption, it is utilized by a number of researchers (Milne et al., 2011; Shin et al., 2011). The application of this isotherm equation could be considered for further studies.

References

Adak, A., Pal, A., Bandyopadhyay, M. (2005), Spectrophotometric determination of anionic surfactants in wastewater using acridine orange, *Journal of Chemical Technology*, **12**, 145-148.

Alagic, E., Spildo, K., Skauge, A., Solbakken, J. (2011), Effect of crude oil ageing on low salinity and low salinity surfactant flooding, *Journal of Petroleum Science and Engineering*, **78**, 220-227.

Alagic, E. (2010), *Combination of low salinity water flooding with surfactant injection – A new hybrid EOR process.* Ph.D. thesis, University of Bergen, Norway.

Alagic, E., Skauge, A., Spildo, K. (2010), Effect of surfactant concentration and slug size efficiency of low salinity surfactant injections, unpublished[*].

Alagic, E., Skauge, A. (2010), Combined Low Salinity Brine Injection and Surfactant Flooding in Mixed – Wet Sandstone Cores, *Energy & Fuels*, **24**, 3551-3559.

Alvarado, V., Manrique, E. (2010), *Enhanced Oil Recovery*, Gulf Professional Publishing, Burlington USA.

Austad, T., RezaeiDoust, A., Puntervold, T. (2010), Chemical Mechanism of Low Salinity Water Flooding in Sandstone Reservoirs. **SPE 129767**: Presented at the 2010 SPE Improved Oil Recovery Symposium, Tulsa, Oklahoma, USA, 24-28 April 2010.

Austad, T., Løvereide, T., Olsvik, K., Rolvsvåg, T.A., Staurland, G. (1991a), Adsorption I. Competitive static adsorption of mixtures of ethoxylated surfactants onto kaolinite and quarts, *Journal of Petroleum Science and Engineering*, **6**, 107-124.

Austad, T., Bjørkum, P.A., Rolvsvåg, T.A., Øysæd, K.B. (1991b), Adsorption III. Nonequlibrium adsorption of surfactants onto reservoir cores from the North Sea. The effect of oil and clay minerals, *Journal of Petroleum Science and Engineering*, **6**, 137-148.

Beaufort, D., Cassagnabere, A., Petit, S., Lanson, B., Berger, G., Lacharpagne, J.C., Johansen, H. (1998), Kaolinite-to-dickite reaction in sandstone reservoirs, *Clay Minerals*, **33**, 297-316.

Biolin Scientific, 2011a. *Surface tension*. Available from: http://www.attension.com/applications/measurements/surface-tension [Viewed: 12.11.2013].

[*] Part of Alagic, E. (2010). *Combination of low salinity water flooding with surfactant injection – A new hybrid EOR process*. Ph.D. thesis, University of Bergen, Norway.

Biolin Scientific, 2011b. *Critical micelle concentration*. Available from: http://www.attension.com/applications/measurements/critical-micelle-concentration [Viewed: 12.11.2013].

Byham, D.E. (1985), Tertiary oil recovery, *U.S. Pat*. **No. 4502540 A.**

Chou, S.I., Bae, J.H. (1983), Surfactant Precipitation and Redissolution in Brine, *Journal of Colloid and Interface Science*, **96**(1), 192-203.

Cohen, L., Sánchez, J.A., Soto, F., Sánchez, E. (2013), Comparative studies of Calcium ion tolerance of different anionic surfactant solutions: An Integrated methodology, *H&PC Today Surfactants*, **8**(3), 7-12.

CSC Scientific Company, 2013. *Surface Tension, Precision and Interfacial DuNouy Tensiometer*. Available from: http://www.cscscientific.com/surface-tension/tensiometer/ [Viewed: 10.11.13].

Dick, S.G., Fuerstenau, D.W., Healy, T.W. (1971), Adsorption of Alkylbenzene Sulfonate (A.B.S) Surfactants at the Alumina-Water Interface, *Journal of Colloid and Interface Science*, **37**(3), 595-602.

Figdore, P.E. (1982), Adsorption of Surfactants on Kaolinite: NaCl versus $CaCl_2$ Salt Effects, *Journal of Colloid and Interface Science*, **87**(2), 500-517.

Ghiasvand, A.R., Taherimaslak, Z., Allahyari, M. (2009), Sensitive and Selective Spectrophotometric and a new Adsorptive Striping Voltammetric Determination of Sodium Dodecyl Sulfate in Nonaqueous Solution after its Extraction Using Toluidine Blue, *International Journal of Electrochemical Science*, **4**, 320-335.

Giles, C.H., Smith, D., Huitson, A. (1974), A General Treatment and Classification of the Solute Adsorption Isotherm. I. Theoretical, *Journal of Colloid and Interface Science*, **47**(3), 755-765.

Glover, C.J., Puerto, M.C., Maerker, J.M., Sandvik, E.L. (1979), Surfactant Phase Behavior and Retention in Porous Media, *Society of Petroleum Engineers*, **19**(3), 183-193.

Green, D.W., Willhite, G.P. (1998), *Enhanced Oil Recovery*, Society of Petroleum Engineers INC, Texas USA.

Hancock, N.J., Tayler, A.M. (1978), Clay mineral diagenesis and oil migration in the Middle Jurassic Brent Sand Formation, *Journal of the Geological Society*, **135**, 69-72.

Hanna, H.S., Somasundaran, P. (1979), Equilibration of Kaolinite in Aqueous Inorganic and Surfactant Solutions, *Journal of Colloid and Interface Science*, **70**, 181-191.

Healy, T.W., Somasundaran, P., Fuerstenau, D.W. (2003), The adsorption of alkyl and alkylbenzene sulfonates at mineral oxide-water interfaces, *Int. Miner. Process*, **72**, 3-10.

Hiemenz, P.C., Rajagopalan, R. (1997), *Principles of Colloid and Surface Chemistry*, 3rd edition, CRC Press, Florida USA.

Ho, Y.S., Porter, J.F., McKay, G. (2002), Equilibrium isotherm studies for the sorption of divalent metal ions onto peat: copper, nickel and lead single component systems, *Water, Air, and Soil Pollution*, **141**, 1-33.

Holmberg, K., Jönsson, B., Kronberg, B, Lindman, B. (2002), *Surfactants and Polymers in Aqueous Solutions*, John Wiley and Sons Ltd, Chichester England.

Jadhunandan, P.P., Morrow, N.R. (1991), Spontaneous imbibition of water by crude oil/brine/rock systems, *In Situ*, **15**(4), 319–345.

Jadhunandan, P.P., Morrow, N. R. (1995), Effect of wettability on waterflood recovery for crude oil/brine/rock systems, *Society of Petroleum Engineers*, **10**(1), 40–46.

Kosswig, K. (2012), Surfactants, *Ullmann's Encyclopedia of Industrial Chemistry*, **35**, 431-505.

Kuila, U., Prasad, M. (2013), Specific surface area and pore-size distribution in clays and shales, *Geophysical Prospecting*, **61**, 341-362.

Lager, A., Webb, K.J., Black, C.J.J., Singleton, M., Sorbie, K.S. (2008), Low salinity oil recovery - an experimental investigation, *Petrophysics*, **49**(1), 28-35.

Langmuir, I. (1916), The adsorption of gases on plane surfaces of glass, mica and platinum, *Journal of the American Chemical Society*, **40**, 1361-1368.

Lv, W., Bazin, B., Ma, D., Liu, Q., Han, D., Wu, K. (2011), Static and dynamic adsorption of anionic and amphoteric surfactants with and without the presence of alkali, *Journal of Petroleum Science and Engineering*, **77**, 209-218.

McGuire, P.L., Chatham, J.R., Paskvan, F.K., Sommer, D.M., Carini, F.H. (2005), Low salinity oil recovery: An exciting new EOR opportunity for Alaska's North Slope. **SPE 154247:** Presented at the 2005 SPE Western Regional Meeting, Irvine, CA, USA, 30. March – 1. April 2005.

Milne, A.J.B., Elliott, J.A.W., Zabeti, P., Zhou, J., Amirfazli, A. (2011), Model and experimental studies for contact angles of surfactant solutions on rough and smooth hydrophobic surfaces, *Physical Chemistry Chemical Physics*, **13**, 16208–16219.

Motomizu, S., Fujiwara, S., Fujiwara, A., Tôei, K. (1982), Anionic Surfactants with Ethyl Violet, *Analytical Chemistry*, **54**(3), 392–397.

Moulijn, J.A., Makkee, M., van Diepen, A. (2002), *Chemical Process Technology*, John Wiley and sons Ltd, Chichester England.

Muherei, M.A., Junin, R. (2009), Equilibrium Adsorption Isotherms of Anionic, Nonionic Surfactants and Their Mixtures to Shale and Sandstone, *Modern Applied Science*, **3**(2), 158-167.

Mørk, P.C. (2004), *Overflate og kolloidkjemi, grunnleggende prinsipper og teorier*. 8th edition, NTNU, Department of Chemical Engineering, Trondheim Norway.

Okeola, F.O., Odebunmi, E.O. (2010), Comparison of Freundlich and Langmuir Isotherms for Adsorption of Methylene Blue by Agrowaste Derived Activated Carbon, *Advances in Environmental Biology*, **4**(3), 329-335.

Paria, S., Khilar, K.C. (2004), A review on experimental studies of surfactant adsorption at the hydrophilic solid – water interface, *Advances in Colloid and Interface Science*, **110**, 75-95.

Paul, G.W., Froning, H.R. (1973), Salinity Effects of Micellar Flooding, *Journal of Petroleum Technology*, **25**(8), 957-958.

Regnier, E. (2007), Oil and energy price volatility, *Energy Economics*, **29**(3), 405-427.

RezaeiDoust, A., Puntervold, T., Strand, S., Austad, T. (2009), Smart Water as Wettability Modifier in Carbonate and Sandstone: A Discussion of Similarities/Differences in the Chemical Mechanisms, *Energy & Fuels*, **23**(9), 4479-4485.

Sastry, N.V., Séquaris, J.-M., Schwuger, M.J. (1995), Adsorption of Polyacrylic Acid and Sodium Dodecylbenzenesulfonate on Kaolinite, *Journal of Colloid and Interface Science*, **171**, 224-233.

Sayavedra, L., Mogollon, J.L., Boothe, M., Lokhandwala, T., Hull, R. (2013), A Discussion of the Different Approaches for Managing the Timing of EOR Projects. **SPE 165304:** Presented at the 2013 SPE Enhanced Oil Recovery Conference, Kuala Lumpur, Malaysia, 2-4 July 2013.

Scamehorn, J.F., Schechter, R.S., Wade, W.H. (1982a), Adsorption of Surfactants on Mineral Oxide Surfaces from Aqueous Solutions. I: Isomerically Pure Anionic Surfactants, *Journal of Colloid and Interface Science*, **85**(2), 463-468.

Scamehorn, J.F., Schechter, R.S., Wade, W.H. (1982b), Adsorption of Surfactants on Mineral Oxide Surfaces from Aqueous Solutions. II: Binary Mixtures of Anionic Surfactants, *Journal of Colloid and Interface Science*, **85**(2), 479-493.

Schramm, L.L. (2000), *Surfactants, Fundamentals and Applications in the Petroleum Industry*. Cambridge University Press, Cambridge England.

Scott, D[†]. (1999), Reservoir Engineering: Augmented Recovery, *Journal of Petroleum Technology*, **12**, 18-41.

Sharma, M.K., Shah, D.O. (1989), Chapter 10 Use of Surfactants in Oil Recovery. *Developments in Petroleum Science*, **17B**, p. 255–315.

Shelton, J.W. (1964), Authigenic kaolinite in sandstone, *Journal of Sedimentary Petrology*, **34**, 102-111.

Sheng, J.J. (2011), *Modern Chemical Enhanced Oil Recovery Theory and Practice*. Elsevier Inc, Burlingon, USA.

Shin, T.G., Müter, D., Meissner, J., Paris, O., Findenegg, G.H. (2011), Structural Characterization of Surfactant Aggregates Adsorbed in Cylindrical Silica Nanopores, *Langmuir*, **27**, 5252-5263.

Shiran, B.S., Skauge, A. (2013), Enhanced Oil Recovery (EOR) by Combined Low Salinity Water/Polymer Flooding, *Energy & Fuels*, **27**, 1223-1235.

Siffert, B., Jada, A., Wersinger, E. (1992), Anionic surfactant adsorption on asphalt-covered clays, *Colloid and Surfaces*, **69**, 45-41.

Sigma Aldrich, 2014. *Product Specification*. Downloaded from: http://www.sigmaaldrich.com/Graphics/COfAInfo/SigmaSAPQM/SPEC/28/289957/289957-BULK_____ALDRICH__.pdf [Viewed: 22.05.2014].

Sim Science, n.d. *Microemulsions*. Available from: http://simscience.org/membranes/advanced/essay/surfactants-microemulsions.html [Viewed: 22.11.2013].

[†] Dillon Scott is the editor of Journal of Petroleum Technology December issue 1999. The author of the specific article is not mentioned.

Sigma Aldrich, 2013. *Sodium dedecylbenzenesulfonate*. Available from: http://www.sigmaaldrich.com/catalog/product/aldrich/289957?lang=en&region=NO [Viewed: 17.11.2013].

Skoog, D.A., West, D.M., Holler, F.J., Crouch, S.R. (2004), *Fundamentals of Analytical Chemistry*. 8th edition, Brooks/Cole, Belmont USA.

Somasundaran, P., Krishnakumar, S. (1997), Adsorption of surfactants and polymers at the solid-liquid interface, *Colloid and Surfaces*, **123-124**, 491-513.

Somasundaran, P., Fuerstenau, D.W. (1966), Mechanisms of Alkyl Sulfonate Adsorption at the Alumina-Water Interface', *The Journal of Physical Chemistry*, **70**, 90-96.

Somasundaran, P., Healy, T.W., Fuerstenau, D.W. (1964), Surfactant Adsorption at the Solid-Liquid Interface-Dependence of Mechanism on Chain Length, *The Journal of Physical Chemistry*, **68**, 3562-3566.

Sun, L., Spildo, K., Djurhuus, K., Skauge, A. (2014), Salinity Selection for a Low Salinity Water-Low Salinity Surfactant Process, *Journal of Dispersion Science and Technology*, **35**(4) 551-555.

Tang, G.-Q., Morrow, N. R. (1999), Influence of brine composition and fines migration on crude oil brine rock interactions and oil recovery, *Journal of Petroleum Science & Engineering*, **24**, 99–111.

Thermo Spectronic, n.d. *Basic UV-Vis Theory, Concepts and Applications.* Downloaded from: http://www.molecularinfo.com/MTM/UV.pdf [Viewed 10.11.13].

Tichelkamp, T., Vu, Y., Nourani, M., Øye, G. (2014), Interfacial Tension between Low Salinity Solutions of Sulfonate Surfactants and Crude and Model Oils, *Energy & Fuels*, **28**, 2408-2414.

Torn, L.H., de Keizer, A., Koopal, L.K., Lyklema, J. (2003), Mixed adsorption of poly(vinylpyrrolidone) and sodium dodecylbenzenesulfonate on kaolinite, *Journal of Colloid and Interface Science*, **260**, 1-8.

Tyler, T.N., Mills, M.E., Wells, J.A., Carlin, J.T. (1978), Salinity tolerant surfactant oil recovery process, *U.S. Pat*. **No. 4110228.**

U.S Department of Energy, Office of Fossil Energy, n.d. *Enhanced oil Recovery*. Available from: http://energy.gov/fe/science-innovation/oil-gas/enhanced-oil-recovery [Viewed: 12.09.2013].

Wang, R. (2013), Nanoparticles influence droplet formation in a T-shaped microfluidic, *Journal of Nanoparticle Research*, **15:2128**, 1-9.

Wanless, E.J., Ducker, W.A. (1997), Weak Influence of Divalent Ions on Anionic Surfactant Surface-Aggregation, *Langmuir*, **13**, 1463-1474.

Weckhuysen, B.M. (2004), *In-situ Spectroscopy of Catalysts.* American Scientific Publishers, Utrecht the Netherlands.

Wilson, D., Pittman, E.D. (1977), Authigenic clays in sandstones: Recognition and influence on reservoir properties and paleoenvironmental analysis, *The Society of Economic Paleontologists and Mineralogists*, **47**(1), 3-31.

Yildiz, H.O., Morrow, N.R. (1996), Effect of brine composition on recovery waterflooding of Moutray crude oil by waterflooding, *Petroleum Science & Engineering*, **14**(4), 159–168.

Zhu, B.Y., Gu, T. (1989), General Isotherm Equation for Adsorption of Surfactants at Solid/Liquid Interfaces. Part 1. *Theoretical, Journal of the Chemical Society, Faraday Transactions 1: Physical Chemistry in Condensed Phases*, **85**(11), 3813-3817.

List of Appendices

NTNU / HSE	Hazardous activity identification process	Prepared by	Number	Date
		HSE section	HMSRV2601	22/03/2011
		Approved by	Page	Replaces
		The Rector		01/12/2006

Unit: *(Institute)* **IKP** **Date:** 01/03/2014

Line manager: **Edd Blekkan**

Participants in the identification process (incl. function): Gisle Øye, Trine Johansen, Meysam Nourani
(supervisor, student, co-supervisor, others)

Short description of the main activity/main process: Master Thesis, investigation of loss of surfactants

Is the project work purely theoretical? (YES/NO) NO

Answer "YES" implies that ***supervisor is assured that no activities requiring risk assessment are involved in the work*** *. If YES, skip rest of the form.*

Signatures: *Responsible supervisor:* _____ *Student:* _____

ID nr.	Activity/process	Responsible person	Existing documentation	Existing safety measures	Laws, regulations etc.	Comment
1	Preparing solutions with SDBS	Trine Johansen	HSE-datasheet	Gloves, safety glasses, fumehood	Arbeidsmiljøloven, Kjemikalieforskrifter og Laboratorie- og verkstedhåndbok for NTNU	
2	Preparing solutions with kaolinite	Trine Johansen	HSE-datasheet	Safety glasses	Arbeidsmiljøloven, Kjemikalieforskrifter og Laboratorie- og verkstedhåndbok for NTNU	
3	Preparing solutions with NaCl	Trine Johansen	HSE-datasheet	Safety glasses	Arbeidsmiljøloven, Kjemikalieforskrifter og Laboratorie- og verkstedhåndbok for NTNU	
4	Preparing solutions with $CaCl_2$	Trine Johansen	HSE-datasheet	Safety glasses	Arbeidsmiljøloven, Kjemikalieforskrifter og Laboratorie- og verkstedhåndbok for NTNU	
5	Treatment of clay with HCl	Trine Johansen	HSE-datasheet	Gloves, safety glasses, fumehood	Arbeidsmiljøloven, Kjemikalieforskrifter og Laboratorie- og verkstedhåndbok for NTNU	
6	Cleaning of equipment with acetone	Trine Johansen	HSE-datasheet	Gloves, safety glasses, fumehood	Arbeidsmiljøloven, Kjemikalieforskrifter og Laboratorie- og verkstedhåndbok for NTNU	
7	Cleaning of equipment with toluene	Trine Johansen	HSE-datasheet	Gloves, safety glasses, fumehood	Arbeidsmiljøloven, Kjemikalieforskrifter og Laboratorie- og verkstedhåndbok for NTNU	Need to be cleaned with open fire after each sample. Extra care must be taken.
8	Use of UV-spectrophotmeter	Trine Johansen	Instrument card / User manual	Gloves, safety glasses, fumehood	Arbeidsmiljøloven, Kjemikalieforskrifter og Laboratorie- og verkstedhåndbok for NTNU	
9	Use of tensiometer	Trine Johansen	Instrument card / User manual	Gloves, safety glasses, fumehood, lab coat	Arbeidsmiljøloven, Kjemikalieforskrifter og Laboratorie- og verkstedhåndbok for NTNU	
10	Use of zetasizer	Trine Johansen	Instrument card / User manual	Gloves and safety glasses	Arbeidsmiljøloven, Kjemikalieforskrifter og Laboratorie- og verkstedhåndbok for NTNU	

NTNU	Risk assessment	Prepared by	Nummer	Date
HMS/KS		HSE section	HMSRV2603	04/02/2011
		Approved by	Page	Replaces
		The Rector		09/02/2010

Unit: *(Institute)* *IKP* **Date:** 01/03/2014

Line manager: *Edd Blekkan*

Participants in the identification process (incl. function): *Gisle Øye, Trine Johansen, Meysam Nourani*
(supervisor, student, co-supervisor, others)

Risk assessment of: Master Thesis, investigation of loss of surfactants

Signatures: *Responsible supervisor:* *Student:*

ID nr.	Activity from the identification process form	Potential undesirable incident/strain	Likelihood:	Consequence:			Risk value (human)	Comments/status Suggested measures
			(1-5)	Human (A-E)	Enviroment (A-E)	Economy/ material (A-E)		
1	Preparing solutions with SDBS	Spill may irritate skin, cause eye injury. Inhalation may cause intoxication.	2	A	-	-	A2	
2	Preparing solutions with kaolinite	No potential risk	1	A	-	-	A1	
3	Preparing solutions with NaCl	No potential risk	1	A	-	-	A1	
4	Preparing solutions with $CaCl_2$	No potential risk	1	A	-	-	A1	
5	Treatment of clay with HCl	Spill may irritate skin, cause eye injury. Inhalation may cause intoxication.	1	B	-	-	B1	
6	Cleaning of equipment with acetone	Spill may irritate skin, cause eye injury. Inhalation may cause intoxication.	2	A	-	-	A2	
7	Cleaning of equipment with toluene	Spill may irritate skin, cause eye injury. Inhalation may cause intoxication.	2	B	-	-	B2	
8	Use of tensiometer	Cleaning of ring with open fire may cause skin burn, spill when transferring sample to beaker	2	B	-	-	B2	
9	Use of UV-spectrophotmeter	No potential risk	1	A	-	-	A1	
10	Use of zetasizer	No potential risk	1	A	-	-	A1	

Risk value = Likelihood (1, 2 ...) x consequence (A, B ...). Risk value A1 means very low risk. Risk value E5 means very large and serious risk

Likelihood		Consequence					
Value	**Criteria**	**Grading**		**Human**	**Environment**	**Economy/material**	
1	**Minimal**: Once every 50 year or less	**E**	**Very critical**	May produce fatality/ies	Very prolonged, non-reversible damage	Shutdown of work >1 year.	
2	**Low**: Once every 10 years or less	**D**	**Critical**	Permanent injury, may produce serious health damage/sickness	Prolonged damage. Long recovery time.	Shutdown of work 0.5-1 year.	
3	**Medium**: Once a year or less	**C**	**Dangerous**	Serious personal injury	Minor damage. Long recovery time	Shutdown of work < 1 month	
4	**High**: Once a month or less	**B**	**Relatively safe**	Injury that requires medical treatment	Minor damage. Short recovery time	Shutdown of work < 1week	
5	**Very high**: Once a week	**A**	**Safe**	Injury that requires first aid	Insignificant damage. Short recovery time	Shutdown of work < 1day	

MATRIX FOR RISK ASSESSMENT

CONSEQUENCE	**Very critical**	**E1**	**E2**	**E3**	**E4**	**E5**
	Critical	**D1**	**D2**	**D3**	**D4**	**D5**
	Dangerous	**C1**	**C2**	**C3**	**C4**	**C5**
	Relatively safe	**B1**	**B2**	**B3**	**B4**	**B5**
	Safe	**A1**	**A2**	**A3**	**A4**	**A5**
		Minimal	**Low**	**Medium**	**High**	**Very high**
		LIKELIHOOD				

Explanation of the colors used in the risk matrix.

Color	Description
Red	Unacceptable risk. Safety measures must be implemented.
Yellow	Measures to reduce risk shall be considered.
Green	Acceptabel risk.

Appendix B. Pretreatment of Clay

Table B 1. Mass of natural kaolinite, produced mass of purified Na-kaolinite and yield of the kaolinite pretreatment in five batches.

	Batch 1	**Batch 2**	**Batch 3**	**Batch 4**	**Batch 5**
Mass of natural kaolinite [g]	24.9992	24.9999	24.9993	24.9977	24.9940
Mass of produced Na-kaolinite [g]	21.8250	22.1873	22.9492	22.3892	19.6231
Yield [%]	99.87	99.89	99.92	99.90	99.79

Table B 2. Measured conductivity (25°C) and pH after each washing step. The washing steps are numbered according to the steps in the experimental procedure.

Washing step	Batch 1 Conductivity [µs/cm]	pH	Batch 2 Conductivity [µs/cm]	pH	Batch 3 Conductivity [µs/cm]	pH
1) MilliQ. 1.	26.2	7.51	29.9	6.51	28.8	7.12
1) MilliQ. 2.	10.5	7.47	13.8	6.61	13.7	7.02
1) MilliQ. 3.	6.4	7.37	10.3	6.75	11.5	7.07
1) MilliQ. 4.	5.2	7.50	8.8	6.75	8.8	6.98
2) 0.2 M NaCl. 1.	12560	7.01	18420	6.07	18520	6.54
2) 0.2 M NaCl. 2.	20600	6.83	20300	6.28	20300	6.54
2) 0.2 M NaCl. 3.	20800	6.94	20500	6.38	17790	6.55
3) 1.0 M NaCl. 1.	12580	3.23	12100	4.42	11950	3.96
3) 1.0 M NaCl. 2.	11120	3.90	11060	4.20	11250	4.11
3) 1.0 M NaCl. 3.	11580	3.92	11000	3.52	11210	3.83
4) 0.01 M NaCl 1.	2670	6.70	2860	4.83	3070	5.47
4) 0.01 M NaCl 2.	1444	6.90	1468	6.04	1601	6.44
4) 0.01 M NaCl 3.	1237	6.90	1240	6.19	1282	6.50

Washing step	Batch 4 Conductivity [µs/cm]	pH	Batch 5 Conductivity [µs/cm]	pH
1) MilliQ. 1.	34.7	7.24	33.9	7.16
1) MilliQ. 2.	15.6	7.23	14.4	7.13
1) MilliQ. 3.	12.9	7.08	11.1	7.02
1) MilliQ. 4.	9.8	7.12	9.0	7.44
2) 0.2 M NaCl. 1.	18450	6.60	18390	6.76
2) 0.2 M NaCl. 2.	20200	6.53	20000	6.50
2) 0.2 M NaCl. 3.	20400	7.64	20400	6.88
3) 1.0 M NaCl. 1.	12540	4.47	12370	4.30
3) 1.0 M NaCl. 2.	11150	3.87	11060	3.86
3) 1.0 M NaCl. 3.	10780	3.99	10820	4.05
4) 0.01 M NaCl 1.	2540	6.41	2730	5.83
4) 0.01 M NaCl 2.	1438	6.57	1482	6.42
4) 0.01 M NaCl 3.	1243	6.65	1247	6.65

Appendix C. Calibration Curves

Low Salinity

Table C1 presents SDBS absorbance measured before and after ageing, and measured surface tension and density at 25°C of calibration solutions in LS brine.

Table C 1. SDBS concentration, absorbance at 260 nm, surface tension and density at 25°C of low salinity calibration solutions analysed with UV-vis spectrophotometer and ring tensiometer.

SDBS concentration [M]	Absorbance One day old	Absorbance One week old	Surface tension [mN/m]	Density [kg/L]
$5.00 \cdot 10^{-6}$	-	-	66.6	0.997844
$1.00 \cdot 10^{-5}$	0.001	-0.001	61.6	0.997835
$5.00 \cdot 10^{-5}$	0.017	0.008	49.5	0.997836
$1.00 \cdot 10^{-4}$	0.037	0.023	43.7	0.997845
$2.00 \cdot 10^{-4}$	0.067	0.054	-	-
$4.00 \cdot 10^{-4}$	0.137	0.131	-	-
$5.00 \cdot 10^{-4}$	-	-	32.3	0.997885
$6.00 \cdot 10^{-4}$	0.208	0.197	-	-
$8.00 \cdot 10^{-4}$	0.266	0.257	-	-
$1.00 \cdot 10^{-3}$	0.325	0.318	31.1	0.997930
$1.20 \cdot 10^{-3}$	0.390	0.384	-	-
$5.00 \cdot 10^{-3}$	1.52	-	30.7	0.998332
$1.00 \cdot 10^{-2}$	-	-	30.5	0.998788

Low Salinity with $CaCl_2$

Table C2 presents SDBS absorbance measured before and after ageing, and measured surface tension and density at 25 °C of calibration solutions in LS w/Ca^{2+} brine. Figure C1 displays the calibration curve of SDBS in LS w/Ca^{2+} brine for determination of CMC.

Table C 2. SDBS concentration, absorbance at 260 nm, surface tension and density at 25°C of low salinity with $CaCl_2$ calibration solutions analysed with UV-vis spectrophotometer and ring tensiometer.

SDBS concentration [M]	Absorbance One day old	Absorbance One week old	Surface tension [mN/m]	Density [kg/L]
$5.00 \cdot 10^{-6}$	-	-	63.2	0.998535
$1.00 \cdot 10^{-5}$	0.006	0.006	56.9	0.998561
$5.00 \cdot 10^{-5}$	0.018	0.019	41.4	0.998563
$1.00 \cdot 10^{-4}$	0.036	0.032	35.7	0.998559
$2.00 \cdot 10^{-4}$	0.068	0.072	-	-
$4.00 \cdot 10^{-4}$	0.129	0.170	-	-
$5.00 \cdot 10^{-4}$	-	-	27.5	0.998606
$6.00 \cdot 10^{-4}$	0.198	0.349	-	-
$8.00 \cdot 10^{-4}$	0.272	0.439	-	-
$1.00 \cdot 10^{-3}$	0.319	0.423	27.3	0.998653
$1.20 \cdot 10^{-3}$	0.380	0.400	-	-
$5.00 \cdot 10^{-3}$	-	-	29.1	0.999033
$1.00 \cdot 10^{-2}$	-	-	29.7	0.999516

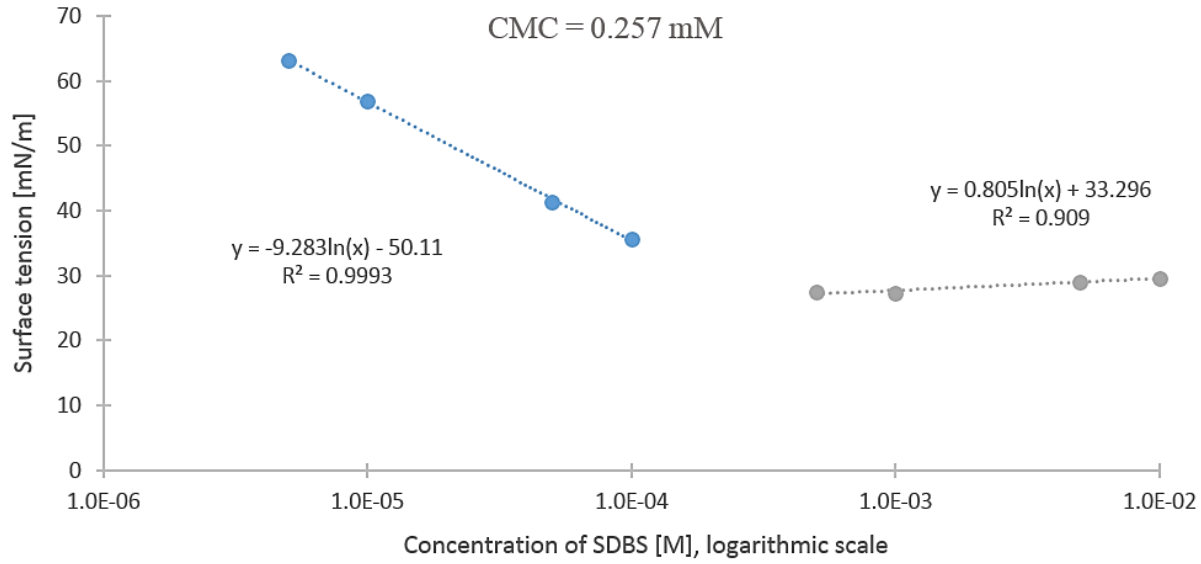

Figure C 1. Calibration curve and determination of CMC of SDBS in LS w/Ca^{2+} brine. Surface tension at 25°C as a function of SDBS concentration.

Medium Salinity

Measured absorbance, surface tension and density of SDBS calibration solutions in MS brine are presented in Table C3. Figures C2 and C3 display the calibration curves of SDBS in MS brine for measurements of absorbance at 260 nm and surface tension at 25°C, respectively.

Table C 3. SDBS concentration, absorbance at 260 nm, surface tension and density at 25°C of medium salinity calibration solutions analysed with UV-vis spectrophotometer and ring tensiometer.

SDBS concentration [M]	Absorbance	Surface tension [mN/m]	Density [kg/L]
$1.00 \cdot 10^{-6}$	-	71.2	1.001026
$5.00 \cdot 10^{-6}$	-	60.7	1.001021
$1.00 \cdot 10^{-5}$	-0.009	54.0	1.001020
$5.00 \cdot 10^{-5}$	-0.004	40.2	1.001018
$1.00 \cdot 10^{-4}$	0.020	34.7	1.001017
$2.00 \cdot 10^{-4}$	0.050	-	-
$4.00 \cdot 10^{-4}$	0.113	-	-
$5.00 \cdot 10^{-4}$	-	29.7	1.001049
$6.00 \cdot 10^{-4}$	0.174	-	-
$8.00 \cdot 10^{-4}$	0.231	-	-
$1.00 \cdot 10^{-3}$	0.311	28.8	1.001103
$1.20 \cdot 10^{-3}$	0.355	-	-
$5.00 \cdot 10^{-3}$	-	28.6	1.001463
$1.00 \cdot 10^{-2}$	-	28.5	1.001943

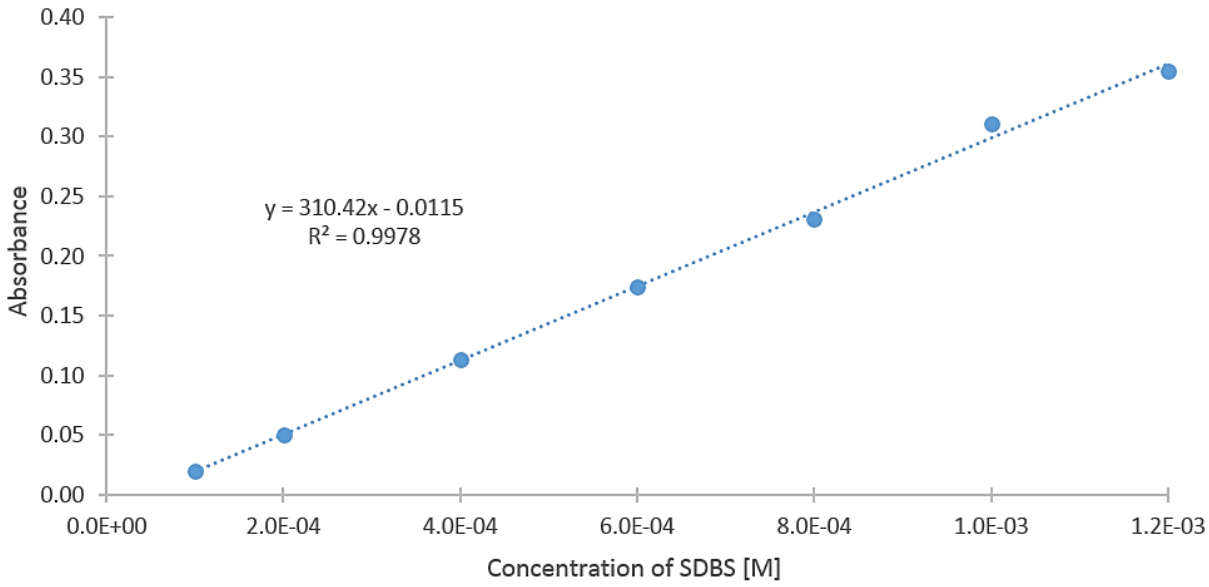

Figure C 2. Calibration curve of SDBS in MS brine. Absorbance at 260 nm as a function of SDBS concentration.

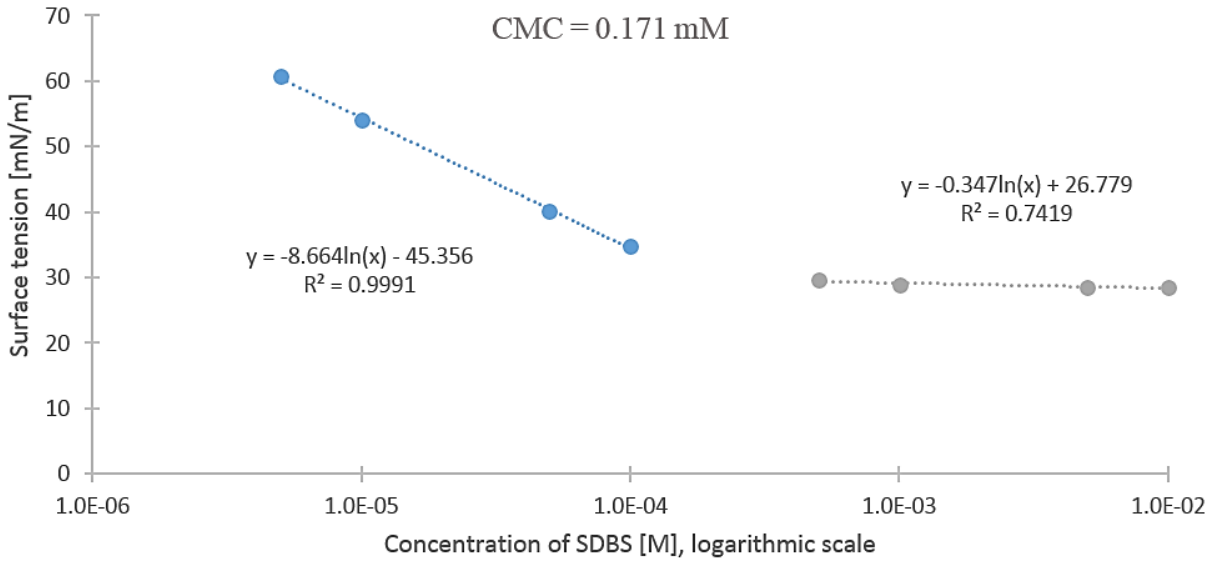

Figure C 3. Calibration curve and determination of CMC of SDBS in MS brine. Surface tension at 25°C as a function of SDBS concentration.

Medium Salinity with $CaCl_2$

Measured absorbance, surface tension and density of calibration solutions in MS w/Ca^{2+} brine are presented in Table C4. Figures C4 and C5 display the calibration curves of SDBS in MS w/Ca^{2+} for measurements of absorbance at 260 nm and surface tension at 25°C, respectively.

Table C 4. SDBS concentration, absorbance at 260 nm, surface tension and density at 25°C of medium salinity with $CaCl_2$ calibration solutions analysed with UV-vis spectrophotometer and ring tensiometer.

SDBS concentration [M]	Absorbance	Surface tension [mN/m]	Density [kg/L]
$1.00 \cdot 10^{-6}$	-	63.2	1.006146
$5.00 \cdot 10^{-6}$	-	58.5	1.006201
$1.00 \cdot 10^{-5}$	0.001	52.5	0.006122
$5.00 \cdot 10^{-5}$	0.019	37.0	1.006221
$1.00 \cdot 10^{-4}$	0.034	29.9	1.006036
$2.00 \cdot 10^{-4}$	0.071	-	-
$4.00 \cdot 10^{-4}$	0.188	-	-
$5.00 \cdot 10^{-4}$	-	27.5	1.006324
$6.00 \cdot 10^{-4}$	0.297	-	-
$8.00 \cdot 10^{-4}$	0.395	-	-
$1.00 \cdot 10^{-3}$	0.470	27.5	1.006258
$1.20 \cdot 10^{-3}$	0.485	-	-
$5.00 \cdot 10^{-3}$	-	27.1	1.006611
$1.00 \cdot 10^{-2}$	-	27.5	1.006999

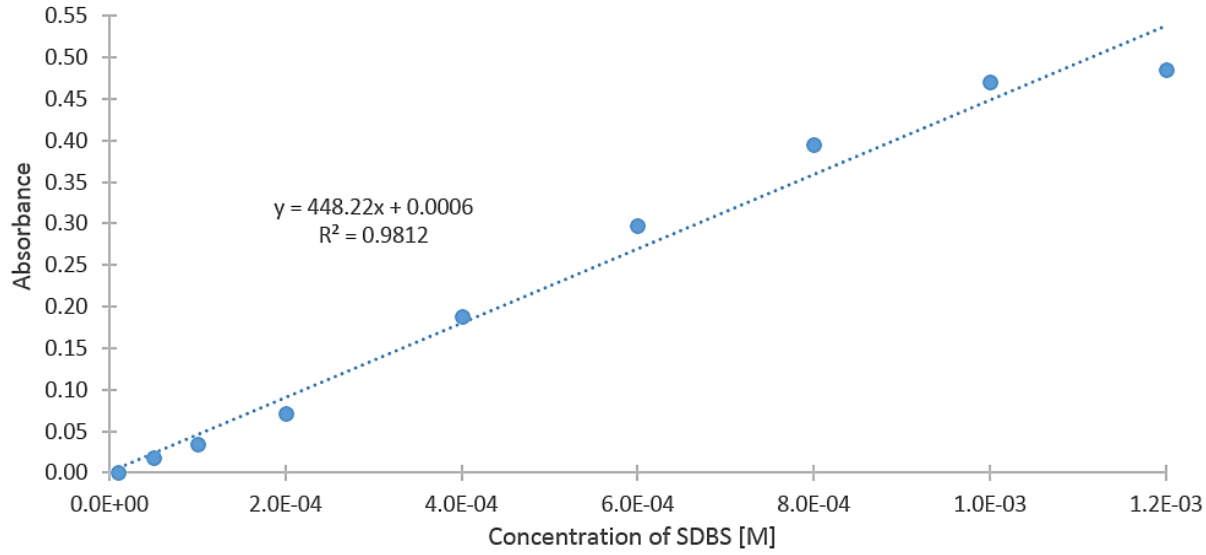

Figure C 4. Calibration curve of SDBS in MS w/Ca^{2+} brine. Absorption at 260 nm as a function of concentration of SDBS.

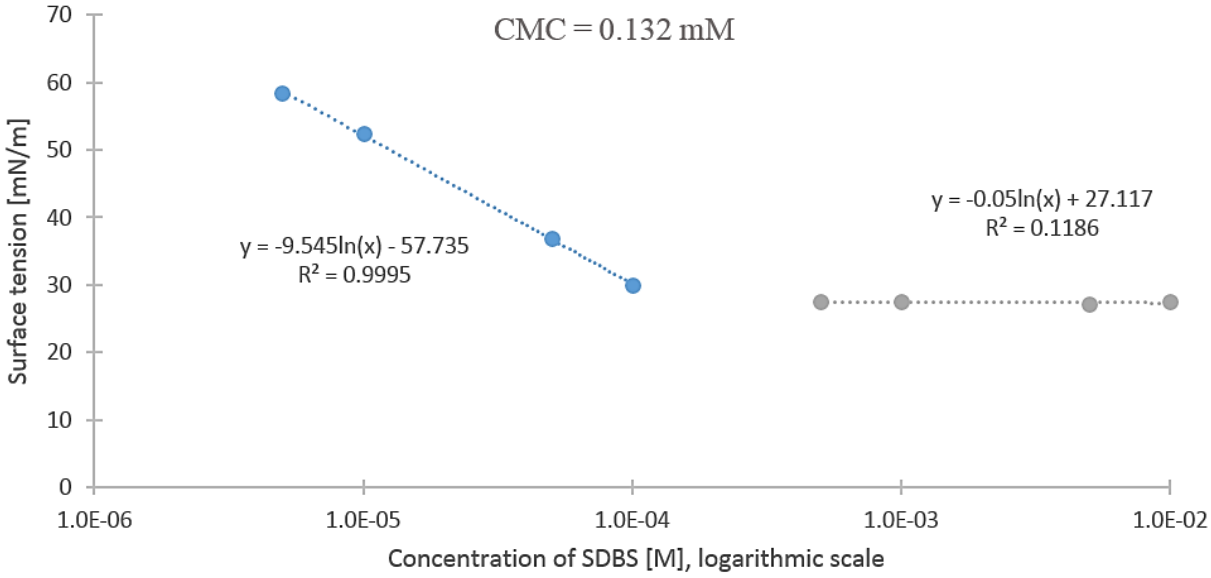

Figure C 5. Calibration curve and determination of CMC of SDBS in MS w/Ca^{2+} brine. Surface tension at 25°C as a function of SDBS concentration.

High Salinity

Measured absorbance, surface tension and density of calibration solutions in HS brine are presented in Table C5. Figures C6 and C7 display the calibration curves of SDBS in HS for measurements of absorbance at 260 nm and surface tension at 25°C, respectively.

Table C 5. SDBS concentration, absorbance at 260nm, surface tension and density at 25°C of high salinity calibration solutions analysed with UV-vis spectrophotometer and ring tensiometer.

SDBS concentration [M]	Absorbance	Surface tension [mN/m]	Density [kg/L]
$1.00 \cdot 10^{-6}$	-	68.2	1.006146
$5.00 \cdot 10^{-6}$	-	55.0	1.006201
$1.00 \cdot 10^{-5}$	0.007	48.9	1.006122
$5.00 \cdot 10^{-5}$	0.016	34.8	1.006221
$1.00 \cdot 10^{-4}$	0.033	29.7	1.006036
$2.00 \cdot 10^{-4}$	0.060	-	-
$4.00 \cdot 10^{-4}$	0.121	-	-
$5.00 \cdot 10^{-4}$	-	27.5	1.006324
$6.00 \cdot 10^{-4}$	0.177	-	-
$8.00 \cdot 10^{-4}$	0.241	-	-
$1.00 \cdot 10^{-3}$	0.298	27.5	1.006258
$1.20 \cdot 10^{-3}$	0.351	-	-
$5.00 \cdot 10^{-3}$	-	27.6	1.006611
$1.00 \cdot 10^{-2}$	-	27.6	1.006999

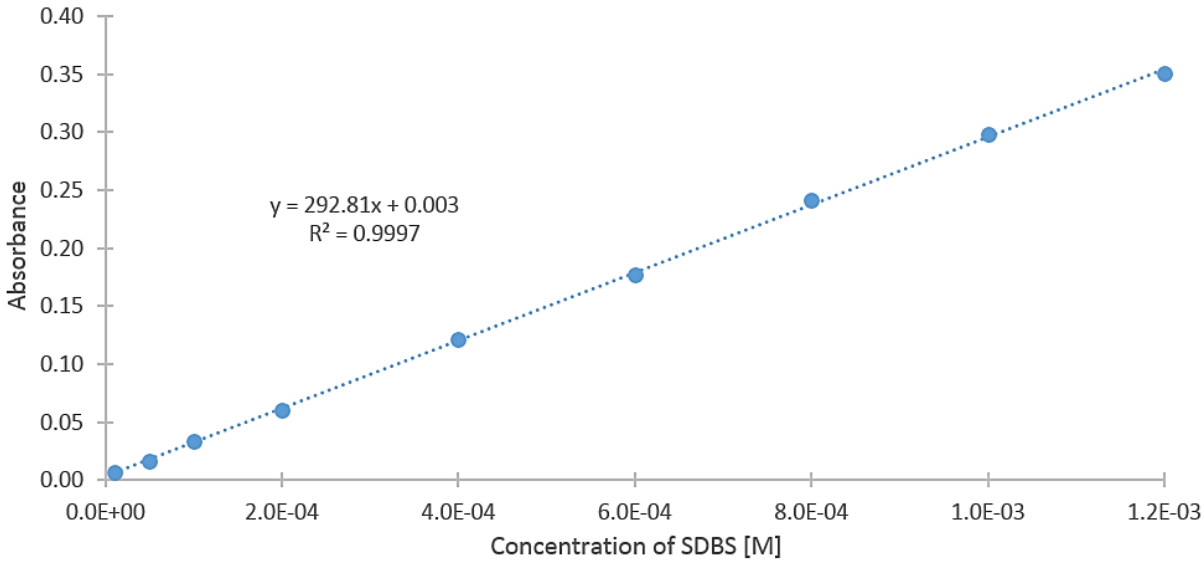

Figure C 6. Calibration curve of SDBS in HS brine. Absorbance at 260 nm as a function of SDBS concentration.

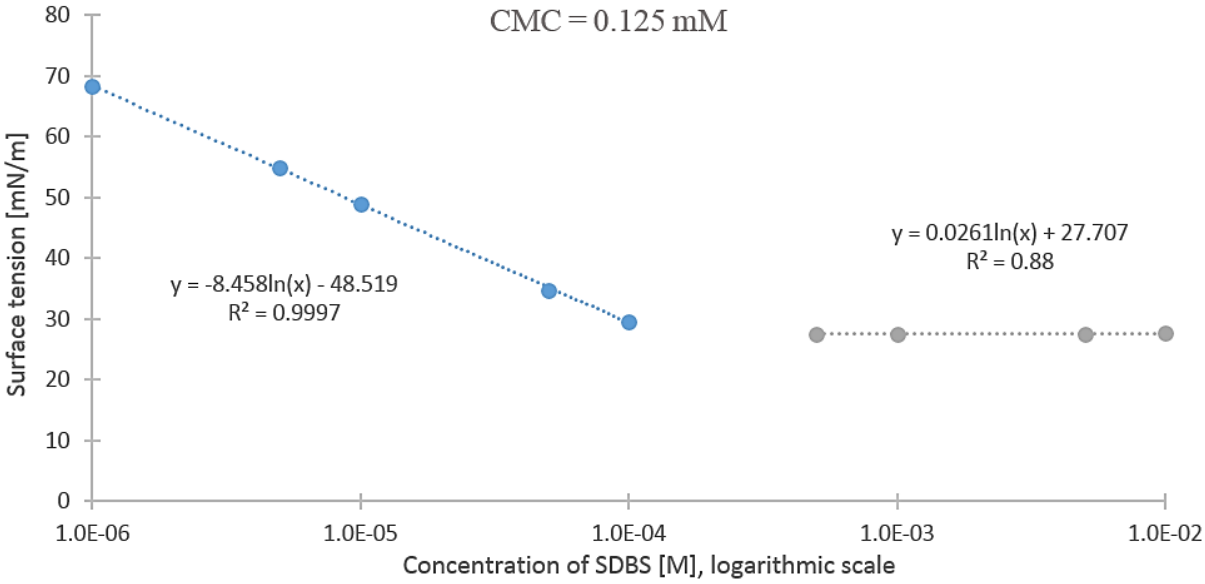

Figure C 7. Calibration curve and determination of CMC of SDBS in HS brine. Surface tension at 25°C as a function of SDBS concentration.

Appendix D. SDBS Absorption Spectra

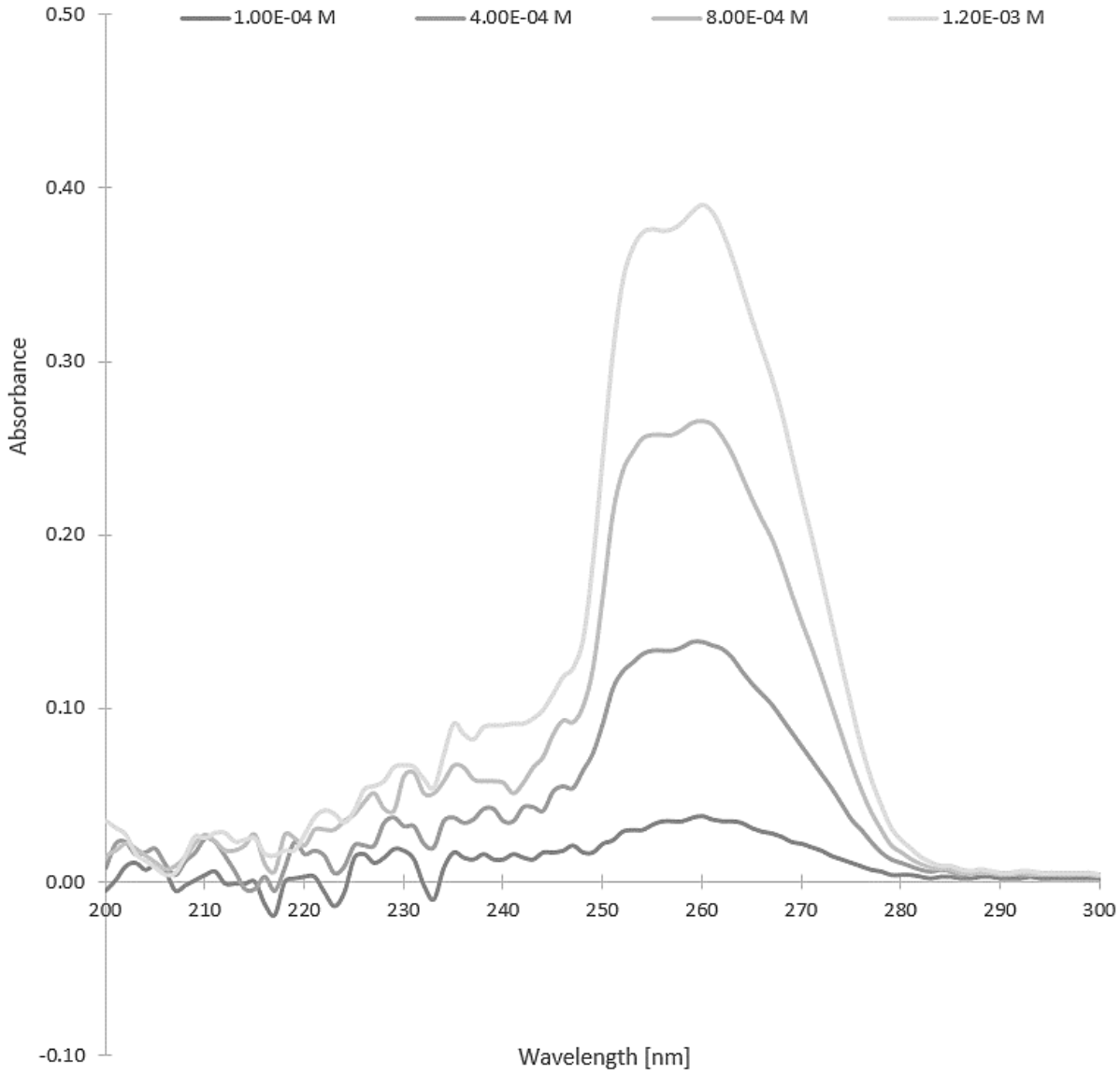

Figure D 1. UV-vis spectrum of SDBS in low salinity water, a selection of four calibration solutions.

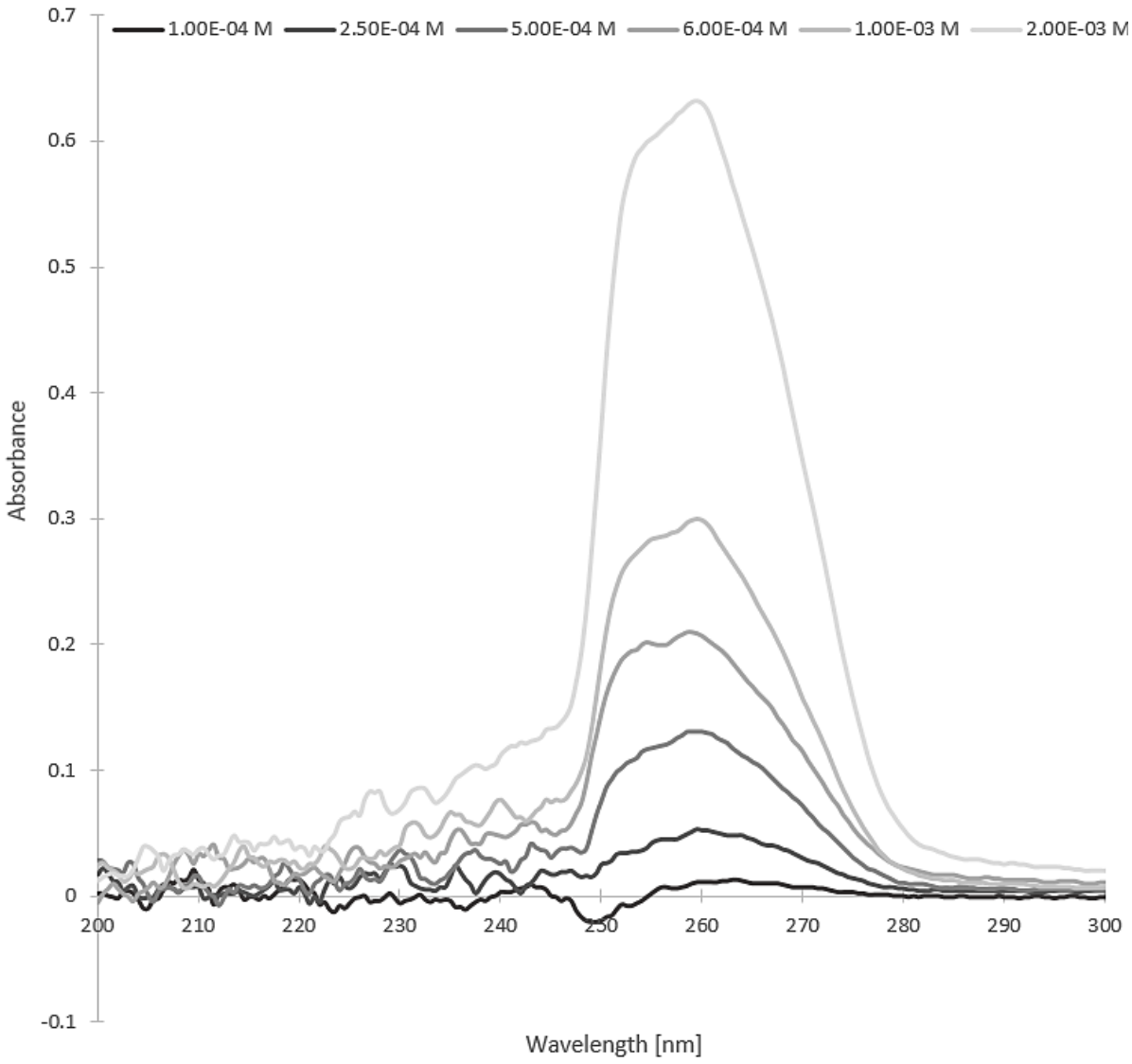

Figure D 2. UV-vis spectrum of SDBS in low salinity water, a selection of six adsorption samples.

Appendix E. Test Experiments – Low Salinity Water

Test Experiment 1

Table E 1. Initial nominal concentration of SDBS, dilution factor, average absorbance at 260 nm and measured initial concentration of SDBS for diluted stock solutions used in the preparation of adsorption samples for Test experiment 1.

Initial nominal concentration of SDBS [M]	Dilution factor	Average absorbance	Initial measured concentration of SDBS [M]
$5.00 \cdot 10^{-5}$	1	0.021	$5.04 \cdot 10^{-5}$
$1.00 \cdot 10^{-4}$	1	0.033	$8.75 \cdot 10^{-5}$
$5.00 \cdot 10^{-4}$	1	0.167	$5.02 \cdot 10^{-4}$
$1.00 \cdot 10^{-3}$	1	0.326	$9.93 \cdot 10^{-4}$
$5.00 \cdot 10^{-3}$	2	0.772	$4.74 \cdot 10^{-3}$

Table E 2. Initial nominal SDBS concentration, mass of clay, dilution factor, measured absorbance at 260 nm, in addition to calculated equilibrium concentration and SDBS adsorption for samples used in adsorption studies of SDBS on kaolinite in Test experiment 1.

Initial nominal concentration of SDBS [M]	Mass of clay [g]	Dilution factor	Absorbance	Equilibrium concentration of SDBS [M]	Adsorption of SDBS [mg/g]
Blank, 0	0.3002	1	0.001	-	-
Blank, 0	0.3003	1	0.004	-	-
$5.00 \cdot 10^{-5}$	0.3004	1	0.024	$5.97 \cdot 10^{-5}$	-0.32
$5.00 \cdot 10^{-5}$	0.3001	1	0.035	$9.37 \cdot 10^{-5}$	-1.51
$1.00 \cdot 10^{-4}$	0.3002	1	0.034	$9.06 \cdot 10^{-5}$	-0.11
$1.00 \cdot 10^{-4}$	0.3002	1	0.035	$9.37 \cdot 10^{-5}$	-0.22
$5.00 \cdot 10^{-4}$	0.3004	1	0.179	$5.39 \cdot 10^{-4}$	-1.29
$5.00 \cdot 10^{-4}$	0.3006	1	0.174	$5.23 \cdot 10^{-4}$	-0.75
$5.00 \cdot 10^{-4}$	0.3001	1	0.173	$5.20 \cdot 10^{-4}$	-0.75
$1.00 \cdot 10^{-3}$	0.3004	1	0.349	$1.04 \cdot 10^{-3}$	-3.23
$1.00 \cdot 10^{-3}$	0.3004	1	0.343	$1.03 \cdot 10^{-3}$	-2.58
$1.00 \cdot 10^{-3}$	0.3000	1	0.341	$1.06 \cdot 10^{-3}$	-1.62
$1.00 \cdot 10^{-3}$	0.3003	1	0.338	$1.05 \cdot 10^{-3}$	-1.29
$5.00 \cdot 10^{-3}$	0.3004	2	0.791	$4.86 \cdot 10^{-3}$	-4.09
$5.00 \cdot 10^{-3}$	0.3003	2	0.786	$4.83 \cdot 10^{-3}$	-3.01

Test Experiment 2

Table E 3. Initial nominal concentration of SDBS, dilution factor, average absorbance at 260 nm and measured initial concentration of SDBS for diluted stock solutions used in the preparation of adsorption samples for Test experiment 2.

Initial nominal concentration of SDBS [M]	Dilution factor	Average absorbance	Initial measured concentration of SDBS [M]
$1.00 \cdot 10^{-4}$	1	0.040	$1.09 \cdot 10^{-4}$
$5.00 \cdot 10^{-3}$	2	0.779	$4.79 \cdot 10^{-3}$

Table E 4. Initial nominal SDBS concentration, mass of clay, dilution factor and measured absorbance at 260 nm of newly made samples used in adsorption studies of SDBS on kaolinite in Test experiment 2.

Initial nominal concentration of SDBS [M]	Mass of clay [g]	Dilution factor	Absorbance General procedure	Absorbance Centrifuged	Absorbance Filtered
$1.00 \cdot 10^{-4}$	0.2996	1	0.036	0.034	0.033
$1.00 \cdot 10^{-4}$	0.2998	1	0.044	0.035	0.034
$1.00 \cdot 10^{-4}$	0.3002	1	0.041	0.037	0.035
$5.00 \cdot 10^{-3}$	0.2998	2	0.795	0.767	0.771
$5.00 \cdot 10^{-3}$	0.3000	2	0.810	0.754	0.779
$5.00 \cdot 10^{-3}$	0.2999	2	0.798	0.756	0.774

Table E 5. Initial nominal SDBS concentration, mass of clay, dilution factor and measured absorbance at 260 nm of one-week-old samples used in adsorption studies of SDBS on kaolinite in Test experiment 2.

Initial nominal concentration of SDBS [M]	Mass of clay [g]	Dilution factor	Absorbance General procedure	Absorbance Centrifuged	Absorbance Filtered
$1.00 \cdot 10^{-4}$	0.2996	1	0.042	-	0.033
$1.00 \cdot 10^{-4}$	0.2998	1	0.046	0.047	0.038
$1.00 \cdot 10^{-4}$	0.3002	1	0.042	0.047	0.030
$5.00 \cdot 10^{-3}$	0.2998	2	0.802	0.773	0.780
$5.00 \cdot 10^{-3}$	0.3000	2	0.811	0.763	0.789
$5.00 \cdot 10^{-3}$	0.2999	2	0.806	0.768	0.782

Table E 6. Calculated SDBS equilibrium concentration ($C_{e\ SDBS}$) and SDBS adsorption (Γ_{SDBS}) for newly made and one-week-old samples used in adsorption studies of SDBS on kaolinite in Test experiment 2.

Experiment	Initial nominal concentration of SDBS [M]	New samples		Samples stored 4 days	
		$C_{e\ SDBS}$ [M]	Γ_{SDBS} [mg/g]	$C_{e\ SDBS}$ [M]	Γ_{SDBS} [mg/g]
General procedure	$1.00 \cdot 10^{-4}$	-0.251	$1.10 \cdot 10^{-4}$	-0.144	$1.19 \cdot 10^{-4}$
Centrifuged	$1.00 \cdot 10^{-4}$	0.287	$9.47 \cdot 10^{-5}$	-0.539	$1.31 \cdot 10^{-4}$
Filtered	$1.00 \cdot 10^{-4}$	0.431	$9.06 \cdot 10^{-5}$	0.898	$8.95 \cdot 10^{-5}$
General procedure	$5.00 \cdot 10^{-3}$	-5.28	$4.93 \cdot 10^{-3}$	-5.93	$4.96 \cdot 10^{-3}$
Centrifuged	$5.00 \cdot 10^{-3}$	3.77	$4.67 \cdot 10^{-3}$	2.37	$4.72 \cdot 10^{-3}$
Filtered	$5.00 \cdot 10^{-3}$	0.647	$4.76 \cdot 10^{-3}$	-1.19	$4.82 \cdot 10^{-3}$

Test Experiment 3

Table E 7. Initial nominal concentration of SDBS, dilution factor, average absorbance at 260 nm and measured initial concentration of SDBS for diluted stock solutions used in the preparation of adsorption samples for Test experiment 3.

Initial nominal concentration of SDBS [M]	Dilution factor	Average absorbance	Initial measured concentration of SDBS [M]
$1.00 \cdot 10^{-4}$	1	0.033	$8.75 \cdot 10^{-5}$
$5.00 \cdot 10^{-4}$	1	0.170	$5.11 \cdot 10^{-4}$
$1.00 \cdot 10^{-3}$	1	0.327	$9.96 \cdot 10^{-4}$
$5.00 \cdot 10^{-3}$	2	0.770	$4.73 \cdot 10^{-3}$

Table E 8. Initial nominal SDBS concentration, mass of clay, dilution factor and measured absorbance at 260 nm with two different spectrophotometric baselines for samples used in adsorption studies of SDBS on kaolinite in Test experiment 3.

Initial nominal concentration of SDBS [M]	Mass of clay [g]	Dilution Factor	Absorbance Baseline – Low salinity water	Absorbance Baseline – Blank sample
0, blank	0.3000	1	0.008	-
0, blank	0.3000	1	0.006	-
$1.00 \cdot 10^{-4}$	0.2998	1	0.038	0.021
$1.00 \cdot 10^{-4}$	0.2999	1	0.04	0.024
$1.00 \cdot 10^{-4}$	0.3004	1	0.033	0.023
$5.00 \cdot 10^{-4}$	0.2997	1	0.167	0.156
$5.00 \cdot 10^{-4}$	0.3003	1	0.178	0.165
$5.00 \cdot 10^{-4}$	0.3004	1	0.159	0.151
$1.00 \cdot 10^{-3}$	0.3002	1	0.312	0.307
$1.00 \cdot 10^{-3}$	0.3002	1	0.305	0.295
$1.00 \cdot 10^{-3}$	0.2999	1	0.308	0.298
$5.00 \cdot 10^{-3}$	0.3003	2	0.754	0.749
$5.00 \cdot 10^{-3}$	0.2999	2	0.753	0.743
$5.00 \cdot 10^{-3}$	0.2999	2	0.756	0.753

Table E 9. Calculated SDBS equilibrium concentration ($C_{e\ SDBS}$) and SDBS adsorption (Γ_{SDBS}) for samples analysed with two different spectrophotometric baselines, used in adsorption studies of SDBS on kaolinite in Test experiment 3.

Initial nominal concentration of SDBS [M]	Baseline – Low salinity water		Baseline – Blank sample	
	$C_{e\ SDBS}$ [M]	Γ_{SDBS} [mg/g]	$C_{e\ SDBS}$ [M]	Γ_{SDBS} [mg/g]
$1.00 \cdot 10^{-4}$	-0.431	$9.98 \cdot 10^{-5}$	1.13	$5.50 \cdot 10^{-5}$
$5.00 \cdot 10^{-4}$	0.215	$5.05 \cdot 10^{-4}$	1.36	$4.72 \cdot 10^{-4}$
$1.00 \cdot 10^{-3}$	2.01	$9.39 \cdot 10^{-4}$	2.91	$9.13 \cdot 10^{-4}$
$5.00 \cdot 10^{-3}$	3.34	$4.64 \cdot 10^{-3}$	4.74	$4.60 \cdot 10^{-3}$

Test Experiment 4

Table E 10. Initial nominal concentration of SDBS, density, dilution factor, average surface tension and measured initial concentration at 25°C of SDBS for diluted stock solutions used in the preparation of adsorption samples prepared by the general procure for Test experiment 4.

Initial nominal concentration of SDBS [M]	Density [kg/L]	Dilution Factor	Average surface tension [mN/m]	Initial measured concentration of SDBS [M]
$5.00 \cdot 10^{-6}$	0.998592	1	65.5	$5.92 \cdot 10^{-6}$
$1.00 \cdot 10^{-5}$	0.998592	1	57.3	$1.73 \cdot 10^{-5}$
$5.00 \cdot 10^{-5}$	0.998595	1	44.3	$9.53 \cdot 10^{-5}$
$1.00 \cdot 10^{-4}$	0.998599	1	38.1	$2.16 \cdot 10^{-4}$
$5.00 \cdot 10^{-4}$	0.998587	5	42.6	$6.00 \cdot 10^{-4}$
$1.00 \cdot 10^{-3}$	0.998606	5	36.0	$1.42 \cdot 10^{-3}$
$5.00 \cdot 10^{-3}$	0.998629	20	36.0	$5.71 \cdot 10^{-3}$

Table E 11. Initial nominal concentration of SDBS, density, dilution factor, average surface tension and measured initial concentration at 25°C of SDBS for diluted stock solutions used in the preparation of adsorption samples prepared by additional centrifugation for Test experiment 4.

Initial nominal concentration of SDBS [M]	Density [kg/L]	Dilution Factor	Average surface tension [mN/m]	Initial measured concentration of SDBS [M]
$5.00 \cdot 10^{-6}$	0.998583	1	65.4	$6.0 \cdot 10^{-6}$
$1.00 \cdot 10^{-5}$	0.998587	1	59.24	$1.3 \cdot 10^{-5}$
$5.00 \cdot 10^{-5}$	0.998582	1	44.89	$8.8 \cdot 10^{-5}$
$1.00 \cdot 10^{-4}$	0.998593	1	42.94	$1.1 \cdot 10^{-4}$

Table E 12. Initial nominal SDBS concentration, mass of clay, density, dilution factor and measured surface tension at 25°C for samples prepared by the general procedure and additional centrifugation used in adsorption studies of SDBS on kaolinite in Test experiment 4.

Initial nominal concentration of SDBS [M]	**Mass of clay [g]**	**Density [kg/L]**	**Dilution factor**	**Surface tension [mN/m]** General procedure	**Surface tension [mN/m]** Additional centrifugation
Blank, 0	0.3002	0.998584	1	71.4	71.3
Blank, 0	0.3003	0.998580	1	71.3	71.6
$5.00 \cdot 10^{-6}$	0.3001	0.998584	1	67.3	69.5
$5.00 \cdot 10^{-6}$	0.3003	0.998586	1	68.7	69.5
$1.00 \cdot 10^{-5}$	0.3005	0.998581	1	65.3	66.5
$1.00 \cdot 10^{-5}$	0.3001	0.998584	1	66.1	64.7
$5.00 \cdot 10^{-5}$	0.3004	0.998590	1	50.1	50.4
$5.00 \cdot 10^{-5}$	0.3001	0.998586	1	51.5	52.7
$1.00 \cdot 10^{-4}$	0.3002	0.998582	1	41.0	45.3
$1.00 \cdot 10^{-4}$	0.3002	0.998485	1	45.0	43.3
$5.00 \cdot 10^{-4}$	0.3004	0.998614	5	41.3	-
$5.00 \cdot 10^{-4}$	0.3006	0.998594	5	42.9	-
$1.00 \cdot 10^{-3}$	0.3004	0.998564	5	37.7	-
$1.00 \cdot 10^{-3}$	0.3004	0.998605	5	36.9	-
$5.00 \cdot 10^{-3}$	0.3004	0.998613	20	35.0	-
$5.00 \cdot 10^{-3}$	0.3003	0.998611	20	34.4	-

Table E 13. Calculated SDBS equilibrium concentration ($C_{e\ SDBS}$) and SDBS adsorption (Γ_{SDBS}) for samples, prepared by the general procedure and additional centrifugation, used in adsorption studies of SDBS on kaolinite in Test experiment 4

Initial nominal concentration of SDBS [M]	**General procedure**		**Additional centrifugation**	
	$C_{e\ SDBS}$ [M]	Γ_{SDBS} [mg/g]	$C_{e\ SDBS}$ [M]	Γ_{SDBS} [mg/g]
$5.00 \cdot 10^{-6}$	0.057	$4.28 \cdot 10^{-6}$	0.086	$3.48 \cdot 10^{-6}$
$1.00 \cdot 10^{-5}$	0.403	$5.75 \cdot 10^{-6}$	0.262	$5.88 \cdot 10^{-6}$
$5.00 \cdot 10^{-5}$	1.89	$4.10 \cdot 10^{-5}$	1.78	$3.72 \cdot 10^{-5}$
$1.00 \cdot 10^{-4}$	3.43	$1.17 \cdot 10^{-4}$	0.609	$9.67 \cdot 10^{-5}$
$5.00 \cdot 10^{-4}$	-1.56	$4.45 \cdot 10^{-4}$	-	-
$1.00 \cdot 10^{-3}$	7.79	$1.20 \cdot 10^{-3}$	-	-
$5.00 \cdot 10^{-3}$	-37.4	$6.79 \cdot 10^{-3}$	-	-

Appendix F. Adsorption Studies

Table F 1. Initial nominal SDBS concentration, dilution factor, average absorbance and measured initial SDBS concentration of diluted stock solutions used in the preparation of filtered adsorption samples in LS brine.

Initial nominal concentration of SDBS [M]	Dilution factor	Average absorbance	Initial measured concentration of SDBS [M]
$1.00 \cdot 10^{-4}$	1	0.032	$8.44 \cdot 10^{-5}$
$2.50 \cdot 10^{-4}$	1	0.084	$2.45 \cdot 10^{-4}$
$5.00 \cdot 10^{-4}$	1	0.162	$4.86 \cdot 10^{-4}$
$7.50 \cdot 10^{-4}$	1	0.257	$7.80 \cdot 10^{-4}$
$1.00 \cdot 10^{-3}$	1	0.337	$1.03 \cdot 10^{-3}$
$2.50 \cdot 10^{-3}$	1	0.781	$2.40 \cdot 10^{-3}$
$5.00 \cdot 10^{-3}$	2	0.766	$4.71 \cdot 10^{-3}$

Table F 2.Initial nominal SDBS concentration, mass of clay, dilution factor, pH and the measured absorbance of filtered samples used in adsorption studies of SDBS on kaolinite in LS brine.

Initial nominal concentration of SDBS [M]	Mass of clay [g]	Dilution factor	pH	Absorbance Baseline – low salinity water	Absorbance Baseline – Blank sample
Blank, 0	0.3004	1	7.28	0.014	-
Blank, 0	0.3005	1	7.16	0.011	-
Blank, 0	0.3006	1	7.26	0.019	-
$1.00 \cdot 10^{-4}$	0.3006	1	7.09	0.029	0.011
$1.00 \cdot 10^{-4}$	0.3000	1	7.17	0.030	0.010
$1.00 \cdot 10^{-4}$	0.3000	1	7.14	0.021	0.011
$2.50 \cdot 10^{-4}$	0.3007	1	7.30	0.065	0.052
$2.50 \cdot 10^{-4}$	0.2999	1	7.37	0.060	0.044
$2.50 \cdot 10^{-4}$	0.3002	1	7.59	0.069	0.056
$5.00 \cdot 10^{-4}$	0.3004	1	7.54	0.145	0.131
$5.00 \cdot 10^{-4}$	0.3003	1	7.56	0.149	0.134
$5.00 \cdot 10^{-4}$	0.3003	1	7.34	0.147	0.131
$7.50 \cdot 10^{-4}$	0.3000	1	7.34	0.252	0.240
$7.50 \cdot 10^{-4}$	0.3001	1	7.92	0.251	0.235
$7.50 \cdot 10^{-4}$	0.2998	1	7.12	0.247	0.237
$1.00 \cdot 10^{-3}$	0.3002	1	7.35	0.322	0.305
$1.00 \cdot 10^{-3}$	0.3003	1	7.27	0.322	0.299
$1.00 \cdot 10^{-3}$	0.3001	1	7.29	0.321	0.299
$2.50 \cdot 10^{-3}$	0.3003	1	7.57	0.775	0.756
$2.50 \cdot 10^{-3}$	0.3002	1	7.67	0.777	0.765
$2.50 \cdot 10^{-3}$	0.3003	1	7.63	0.757	0.742
$5.00 \cdot 10^{-3}$	0.2997	2	7.80	0.752	0.744
$5.00 \cdot 10^{-3}$	0.3002	2	7.91	0.753	0.741
$5.00 \cdot 10^{-3}$	0.3002	2	7.90	0.753	0.743

Table F 3. Initial nominal SDBS concentration, dilution factor, average absorbance and measured initial SDBS concentration of diluted stock solutions used in the preparation of filtered adsorption samples in MS brine.

Initial nominal concentration of SDBS [M]	Dilution factor	Average absorbance	Initial measured concentration of SDBS [M]
$1.00 \cdot 10^{-4}$	1	0.033	$1.43 \cdot 10^{-4}$
$2.50 \cdot 10^{-4}$	1	0.086	$3.14 \cdot 10^{-4}$
$4.00 \cdot 10^{-4}$	1	0.132	$4.62 \cdot 10^{-4}$
$5.00 \cdot 10^{-4}$	1	0.161	$5.56 \cdot 10^{-4}$
$6.00 \cdot 10^{-4}$	1	0.202	$6.88 \cdot 10^{-4}$
$7.50 \cdot 10^{-4}$	1	0.254	$8.55 \cdot 10^{-4}$
$1.00 \cdot 10^{-3}$	1	0.320	$1.07 \cdot 10^{-3}$
$2.50 \cdot 10^{-3}$	1	0.756	$2.47 \cdot 10^{-3}$
$5.00 \cdot 10^{-3}$	2	0.743	$4.86 \cdot 10^{-3}$

Table F 4. Initial nominal SDBS concentration, mass of clay, dilution factor, pH and the measured absorbance of filtered samples used in adsorption studies of SDBS on kaolinite in MS brine.

Initial nominal concentration of SDBS [M]	Mass of clay [g]	Dilution factor	pH	Absorbance Baseline – low salinity water	Absorbance Baseline – Blank sample
Blank, 0	0.3003	1	4.92	0.016	-
Blank, 0	0.3004	1	4.90	0.008	-
Blank, 0	0.3006	1	4.88	0.021	-
$1.00 \cdot 10^{-4}$	0.3005	1	4.79	0.042	0.020
$1.00 \cdot 10^{-4}$	0.3004	1	4.80	0.036	0.011
$1.00 \cdot 10^{-4}$	0.3003	1	4.78	0.037	0.013
$2.50 \cdot 10^{-4}$	0.3004	1	4.96	0.075	0.047
$2.50 \cdot 10^{-4}$	0.3006	1	4.96	0.069	0.045
$2.50 \cdot 10^{-4}$	0.3002	1	4.97	0.075	0.048
$4.00 \cdot 10^{-4}$	0.2997	1	5.39	-	0.101
$4.00 \cdot 10^{-4}$	0.3006	1	5.38	-	0.097
$4.00 \cdot 10^{-4}$	0.3008	1	5.40	-	0.100
$5.00 \cdot 10^{-4}$	0.3008	1	5.69	0.163	0.139
$5.00 \cdot 10^{-4}$	0.3006	1	5.72	0.167	0.139
$5.00 \cdot 10^{-4}$	0.3003	1	5.72	0.166	0.142
$6.00 \cdot 10^{-4}$	0.3002	1	5.93	-	0.173
$6.00 \cdot 10^{-4}$	0.3000	1	6.03	-	0.171
$6.00 \cdot 10^{-4}$	0.3001	1	5.98	-	0.175
$7.50 \cdot 10^{-4}$	0.3003	1	6.19	0.246	0.197
$7.50 \cdot 10^{-4}$	0.3003	1	6.16	0.246	0.197
$7.50 \cdot 10^{-4}$	0.3003	1	6.22	0.237	0.192
$1.00 \cdot 10^{-3}$	0.3003	1	6.38	0.315	0.266
$1.00 \cdot 10^{-3}$	0.3006	1	6.38	0.318	0.267
$1.00 \cdot 10^{-3}$	0.3001	1	6.38	0.310	0.263
$2.50 \cdot 10^{-3}$	0.3005	1	6.73	0.751	0.705
$2.50 \cdot 10^{-3}$	0.3005	1	6.73	0.746	0.701
$2.50 \cdot 10^{-3}$	0.3002	1	6.73	0.754	0.708
$5.00 \cdot 10^{-3}$	0.3003	2	6.97	0.746	0.721
$5.00 \cdot 10^{-3}$	0.3003	2	6.99	0.756	0.730
$5.00 \cdot 10^{-3}$	0.3005	2	7.01	0.752	0.725

Table F 5. Initial nominal SDBS concentration, dilution factor, average absorbance and measured initial SDBS concentration of diluted stock solutions used in the preparation of adsorption samples in LS brine.

Initial nominal concentration of SDBS [M]	Dilution factor	Average absorbance	Initial measured concentration of SDBS [M]
$5.00 \cdot 10^{-5}$	1	0.021	$4.94 \cdot 10^{-5}$
$7.50 \cdot 10^{-5}$	1	0.022	$5.35 \cdot 10^{-5}$
$1.00 \cdot 10^{-4}$	1	0.028	$7.20 \cdot 10^{-5}$
$2.50 \cdot 10^{-4}$	1	0.087	$2.54 \cdot 10^{-4}$
$5.00 \cdot 10^{-4}$	1	0.169	$5.07 \cdot 10^{-4}$
$7.50 \cdot 10^{-4}$	1	0.247	$7.50 \cdot 10^{-4}$
$1.00 \cdot 10^{-3}$	1	0.325	$9.89 \cdot 10^{-4}$
$2.50 \cdot 10^{-3}$	1	0.765	$2.35 \cdot 10^{-3}$

Table F 6. Initial nominal SDBS concentration, mass of clay, dilution factor, pH and the measured absorbance of samples used in adsorption studies of SDBS on kaolinite in LS brine.

Initial nominal concentration of SDBS [M]	Mass of clay [g]	Dilution factor	pH	Absorbance Baseline – low salinity water	Absorbance Baseline – Blank sample
Blank, 0	0.2996	1	5.18	0.015	-
Blank, 0	0.2997	1	5.17	0.009	-
Blank, 0	0.3004	1	5.18	0.017	-
$5.00 \cdot 10^{-5}$	0.3006	1	5.24	0.028	0.005
$5.00 \cdot 10^{-5}$	0.2998	1	5.16	0.026	0.004
$5.00 \cdot 10^{-5}$	0.2998	1	5.15	0.029	0.009
$7.50 \cdot 10^{-5}$	0.3006	1	5.10	0.031	0.014
$7.50 \cdot 10^{-5}$	0.2999	1	5.09	0.037	0.017
$7.50 \cdot 10^{-5}$	0.3000	1	5.09	0.032	0.012
$1.00 \cdot 10^{-4}$	0.2998	1	5.08	0.042	0.022
$1.00 \cdot 10^{-4}$	0.3001	1	5.09	0.040	0.019
$1.00 \cdot 10^{-4}$	0.3002	1	5.09	0.037	0.021
$2.50 \cdot 10^{-4}$	0.3003	1	5.35	0.081	0.065
$2.50 \cdot 10^{-4}$	0.3005	1	5.42	0.082	0.066
$2.50 \cdot 10^{-4}$	0.3004	1	5.42	0.085	0.066
$5.00 \cdot 10^{-4}$	0.3003	1	6.26	0.176	0.154
$5.00 \cdot 10^{-4}$	0.3005	1	6.29	0.174	0.156
$7.50 \cdot 10^{-4}$	0.3001	1	6.48	0.272	0.247
$7.50 \cdot 10^{-4}$	0.2999	1	6.49	0.264	0.242
$7.50 \cdot 10^{-4}$	0.3004	1	6.50	0.265	0.246
$1.00 \cdot 10^{-3}$	0.3004	1	6.63	0.353	0.324
$1.00 \cdot 10^{-3}$	0.3000	1	6.56	0.340	0.317
$1.00 \cdot 10^{-3}$	0.3002	1	6.64	0.342	0.323
$2.50 \cdot 10^{-3}$	0.3003	1	6.93	0.786	0.763
$2.50 \cdot 10^{-3}$	0.3002	1	6.91	0.786	0.764
$2.50 \cdot 10^{-3}$	0.3001	1	6.98	0.802	0.765

Table F 7. Initial nominal SDBS concentration, dilution factor, average absorbance and measured initial SDBS concentration of diluted stock solutions used in the preparation of adsorption samples in MS brine.

Initial nominal concentration of SDBS [M]	Dilution factor	Average absorbance	Initial measured concentration of SDBS [M]
$5.00 \cdot 10^{-5}$	1	0.020	$1.03 \cdot 10^{-4}$
$7.50 \cdot 10^{-5}$	1	0.026	$1.22 \cdot 10^{-4}$
$1.00 \cdot 10^{-4}$	1	0.032	$1.41 \cdot 10^{-4}$
$2.50 \cdot 10^{-4}$	1	0.080	$2.96 \cdot 10^{-4}$
$5.00 \cdot 10^{-4}$	1	0.156	$5.40 \cdot 10^{-4}$
$7.50 \cdot 10^{-4}$	1	0.234	$7.91 \cdot 10^{-4}$
$1.00 \cdot 10^{-3}$	1	0.308	$1.03 \cdot 10^{-3}$
$2.50 \cdot 10^{-3}$	1	0.731	$2.39 \cdot 10^{-3}$

Table F 8. Initial nominal SDBS concentration, mass of clay, dilution factor, pH and the measured absorbance of samples used in adsorption studies of SDBS on kaolinite in MS brine.

Initial nominal concentration of SDBS [M]	Mass of clay [g]	Dilution factor	pH	Absorbance Baseline – low salinity water	Absorbance Baseline – Blank sample
Blank, 0	0.3008	1	4.74	0.013	-
Blank, 0	0.2997	1	4.74	0.008	-
Blank, 0	0.3007	1	4.73	0.010	-
$5.00 \cdot 10^{-5}$	0.3003	1	4.77	0.021	0.001
$5.00 \cdot 10^{-5}$	0.2997	1	4.77	0.019	0.000
$5.00 \cdot 10^{-5}$	0.3001	1	4.76	0.021	0.002
$7.50 \cdot 10^{-5}$	0.3005	1	4.81	0.031	0.026
$7.50 \cdot 10^{-5}$	0.3006	1	4.80	0.027	0.019
$7.50 \cdot 10^{-5}$	0.3004	1	4.80	0.029	0.025
$1.00 \cdot 10^{-4}$	0.3007	1	4.85	0.030	0.030
$1.00 \cdot 10^{-4}$	0.3005	1	4.84	0.035	0.032
$1.00 \cdot 10^{-4}$	0.3003	1	4.83	0.030	0.024
$2.50 \cdot 10^{-4}$	0.3003	1	5.22	0.072	0.059
$2.50 \cdot 10^{-4}$	0.3002	1	5.25	0.069	0.056
$2.50 \cdot 10^{-4}$	0.3006	1	5.29	0.060	0.049
$5.00 \cdot 10^{-4}$	0.3004	1	6.11	0.162	0.148
$5.00 \cdot 10^{-4}$	0.3008	1	6.12	0.163	0.150
$5.00 \cdot 10^{-4}$	0.3001	1	6.06	0.152	0.142
$7.50 \cdot 10^{-4}$	0.3001	1	6.38	0.235	0.227
$7.50 \cdot 10^{-4}$	0.3003	1	6.23	0.229	0.219
$7.50 \cdot 10^{-4}$	0.3008	1	6.40	0.243	0.231
$1.00 \cdot 10^{-3}$	0.3005	1	6.54	0.322	0.311
$1.00 \cdot 10^{-3}$	0.3002	1	6.58	0.314	0.305
$1.00 \cdot 10^{-3}$	0.3005	1	6.55	0.322	0.311
$2.50 \cdot 10^{-3}$	0.3006	1	6.88	0.735	0.725
$2.50 \cdot 10^{-3}$	0.3005	1	6.89	0.729	0.722
$2.50 \cdot 10^{-3}$	0.3005	1	6.90	0.729	0.724

Table F 9. Initial nominal SDBS concentration, dilution factor, average absorbance and measured initial SDBS concentration of diluted stock solutions used in the preparation of adsorption samples in HS brine.

Initial nominal concentration of SDBS [M]	Dilution factor	Average absorbance	Initial measured concentration of SDBS [M]
$5.00 \cdot 10^{-5}$	1	0.014	$3.87 \cdot 10^{-5}$
$7.50 \cdot 10^{-5}$	1	0.026	$7.97 \cdot 10^{-5}$
$1.00 \cdot 10^{-4}$	1	0.031	$9.68 \cdot 10^{-5}$
$2.50 \cdot 10^{-4}$	1	0.078	$2.57 \cdot 10^{-4}$
$5.00 \cdot 10^{-4}$	1	0.156	$5.23 \cdot 10^{-4}$
$7.50 \cdot 10^{-4}$	1	0.227	$7.66 \cdot 10^{-4}$
$1.00 \cdot 10^{-3}$	1	0.306	$1.04 \cdot 10^{-3}$
$2.50 \cdot 10^{-3}$	1	0.722	$2.46 \cdot 10^{-3}$

Table F 10. Initial nominal SDBS concentration, mass of clay, dilution factor, pH and the measured absorbance of samples used in adsorption studies of SDBS on kaolinite in HS brine.

Initial nominal concentration of SDBS [M]	Mass of clay [g]	Dilution factor	pH	Absorbance Baseline – low salinity water	Absorbance Baseline – Blank sample
Blank, 0	0.3003	1	4.66	0.017	-
Blank, 0	0.3001	1	4.66	0.017	-
Blank, 0	0.3004	1	4.67	0.011	-
$5.00 \cdot 10^{-5}$	0.3005	1	4.68	0.028	0.005
$5.00 \cdot 10^{-5}$	0.3001	1	4.69	0.026	0.003
$5.00 \cdot 10^{-5}$	0.3000	1	4.70	0.026	0.008
$7.50 \cdot 10^{-5}$	0.3004	1	4.75	0.031	0.016
$7.50 \cdot 10^{-5}$	0.2996	1	4.74	0.025	0.010
$7.50 \cdot 10^{-5}$	0.2997	1	4.75	0.026	0.012
$1.00 \cdot 10^{-4}$	0.3003	1	4.74	0.034	0.018
$1.00 \cdot 10^{-4}$	0.3003	1	4.75	0.037	0.022
$1.00 \cdot 10^{-4}$	0.3001	1	4.78	0.036	0.019
$2.50 \cdot 10^{-4}$	0.3001	1	5.03	0.069	0.054
$2.50 \cdot 10^{-4}$	0.3005	1	5.03	0.072	0.060
$2.50 \cdot 10^{-4}$	0.3005	1	5.07	0.070	0.048
$5.00 \cdot 10^{-4}$	0.3004	1	5.86	0.141	0.125
$5.00 \cdot 10^{-4}$	0.3005	1	5.95	0.152	0.139
$5.00 \cdot 10^{-4}$	0.2999	1	5.96	0.141	0.131
$7.50 \cdot 10^{-4}$	0.3002	1	6.18	0.246	0.206
$7.50 \cdot 10^{-4}$	0.3004	1	6.22	0.242	0.201
$7.50 \cdot 10^{-4}$	0.3002	1	6.18	0.242	0.212
$1.00 \cdot 10^{-3}$	0.3004	1	6.34	0.312	0.274
$1.00 \cdot 10^{-3}$	0.2998	1	6.33	0.309	0.275
$1.00 \cdot 10^{-3}$	0.3000	1	6.34	0.321	0.280
$2.50 \cdot 10^{-3}$	0.3006	1	6.58	0.724	0.689
$2.50 \cdot 10^{-3}$	0.3002	1	6.57	0.730	0.695
$2.50 \cdot 10^{-3}$	0.3004	1	6.53	0.726	0.691

Table F 11. Initial nominal SDBS concentration (C_0^n SDBS), dilution factor, average absorbance and measured initial SDBS concentration (C^{meas} SDBS) of freshly made and aged diluted stock solutions used in the preparation of adsorption samples in LS w/Ca^{2+} brine.

	Start of adsorption experiment			**End of adsorption experiment**		
C_0^n SDBS [M]	Dilution Factor	Average Absorbance	C^{meas} SDBS [M]	Dilution Factor	Average Absorbance	C^{meas} SDBS [M]
$5.00 \cdot 10^{-5}$	-	-	-	1	0.016	$3.71 \cdot 10^{-5}$
$7.50 \cdot 10^{-5}$	-	-	-	1	0.024	$6.22 \cdot 10^{-5}$
$1.00 \cdot 10^{-4}$	-	-	-	1	0.031	$8.42 \cdot 10^{-5}$
$2.50 \cdot 10^{-4}$	1	0.080	$2.37 \cdot 10^{-4}$	1	0.076	$2.26 \cdot 10^{-4}$
$5.00 \cdot 10^{-4}$	1	0.166	$5.07 \cdot 10^{-4}$	1	0.307	$9.51 \cdot 10^{-4}$
$5.50 \cdot 10^{-4}$	1	0.182	$5.59 \cdot 10^{-4}$	-	-	-
$7.50 \cdot 10^{-4}$	1	0.284	$8.78 \cdot 10^{-3}$	1	0.470	$1.46 \cdot 10^{-3}$
$1.00 \cdot 10^{-3}$	1	0.335	$1.04 \cdot 10^{-3}$	1	0.459	$1.43 \cdot 10^{-3}$
$2.50 \cdot 10^{-3}$	-	-	-	1	0.754	$2.36 \cdot 10^{-3}$
$5.00 \cdot 10^{-3}$	-	-	-	2	0.760	$4.75 \cdot 10^{-3}$

Table F 12. Initial nominal SDBS concentration (C_0^n SDBS), dilution factor, average absorbance and measured initial SDBS concentration (C^{meas} SDBS) of freshly made and aged diluted stock solutions used in the preparation of adsorption samples in MS w/Ca^{2+} brine.

	Start of adsorption experiment			**End of adsorption experiment**		
C_0^n SDBS [M]	Dilution Factor	Average Absorbance	C^{meas} SDBS [M]	Dilution Factor	Average Absorbance	C^{meas} SDBS [M]
$5.00 \cdot 10^{-5}$	-	-	-	1	0.014	$2.99 \cdot 10^{-5}$
$5.50 \cdot 10^{-5}$	1	0.018	$3.81 \cdot 10^{-5}$	1	0.016	$3.51 \cdot 10^{-5}$
$7.50 \cdot 10^{-5}$	-	-	-	1	0.023	$5.00 \cdot 10^{-5}$
$1.00 \cdot 10^{-4}$	-	-	-	1	0.032	$6.93 \cdot 10^{-5}$
$2.50 \cdot 10^{-4}$	1	0.090	$1.99 \cdot 10^{-4}$	1	0.169	$3.75 \cdot 10^{-4}$
$5.00 \cdot 10^{-4}$	-	-	-	1	0.559	$1.25 \cdot 10^{-3}$
$7.50 \cdot 10^{-4}$	1	0.524	$1.17 \cdot 10^{-3}$	2	0.395	$1.76 \cdot 10^{-3}$
$1.00 \cdot 10^{-3}$	-	-	-	2	0.568	$2.53 \cdot 10^{-3}$
$1.50 \cdot 10^{-3}$	1	0.691	$1.54 \cdot 10^{-3}$	2	0.602	$2.68 \cdot 10^{-3}$
$2.50 \cdot 10^{-3}$	-	-	-	4	0.598	$5.33 \cdot 10^{-3}$
$3.00 \cdot 10^{-3}$	2	0.793	$3.54 \cdot 10^{-3}$	4	0.545	$4.86 \cdot 10^{-3}$
$5.00 \cdot 10^{-3}$	-	-	-	2	0.761	$3.39 \cdot 10^{-3}$

Table F 13. Initial nominal SDBS concentration, mass of clay, dilution factor, pH and the measured absorbance of samples used in adsorption studies of SDBS on kaolinite in LS w/Ca^{2+} brine.

Initial nominal concentration of SDBS [M]	**Mass of clay [g]**	**Dilution factor**	**pH**	**Absorbance** Baseline – low salinity water	**Absorbance** Baseline – Blank sample
Blank, 0	0.3000	1	4.88	0.019	-
Blank, 0	0.2997	1	4.84	0.022	-
Blank, 0	0.3002	1	4.86	0.022	-
$5.00 \cdot 10^{-5}$	0.3003	1	4.84	0.025	0.013
$5.00 \cdot 10^{-5}$	0.3006	1	4.85	0.028	0.014
$5.00 \cdot 10^{-5}$	0.3003	1	4.85	0.030	0.015
$7.50 \cdot 10^{-5}$	0.3001	1	4.85	0.034	0.019
$7.50 \cdot 10^{-5}$	0.2999	1	4.84	0.034	0.019
$7.50 \cdot 10^{-5}$	0.3003	1	4.86	0.033	0.018
$1.00 \cdot 10^{-4}$	0.3005	1	4.80	0.036	0.022
$1.00 \cdot 10^{-4}$	0.3002	1	4.81	0.038	0.023
$1.00 \cdot 10^{-4}$	0.3002	1	4.81	0.040	0.025
$2.50 \cdot 10^{-4}$	0.3002	1	5.02	0.076	0.058
$2.50 \cdot 10^{-4}$	0.3003	1	5.02	0.074	0.058
$2.50 \cdot 10^{-4}$	0.3001	1	5.03	0.072	0.056
$5.00 \cdot 10^{-4}$	0.3000	1	5.82	0.149	0.130
$5.00 \cdot 10^{-4}$	0.3003	1	5.79	0.151	0.133
$5.00 \cdot 10^{-4}$	0.3002	1	5.76	0.148	0.129
$5.50 \cdot 10^{-4}$	0.2999	1	5.84	0.167	0.151
$5.50 \cdot 10^{-4}$	0.2997	1	5.92	0.168	0.151
$5.50 \cdot 10^{-4}$	0.3002	1	5.91	0.163	0.148
$7.50 \cdot 10^{-4}$	0.3000	1	6.23	0.241	0.223
$7.50 \cdot 10^{-4}$	0.3005	1	6.19	0.237	0.220
$7.50 \cdot 10^{-4}$	0.3001	1	6.24	0.241	0.225
$1.00 \cdot 10^{-3}$	0.3002	1	6.37	0.315	0.303
$1.00 \cdot 10^{-3}$	0.3002	1	6.38	0.309	0.297
$1.00 \cdot 10^{-3}$	0.3004	1	6.41	0.311	0.300
$2.50 \cdot 10^{-3}$	0.3002	1	6.75	0.765	0.751
$2.50 \cdot 10^{-3}$	0.3005	1	6.75	0.766	0.753
$2.50 \cdot 10^{-3}$	0.3006	1	6.76	0.756	0.738
$5.00 \cdot 10^{-3}$	0.3004	2	7.00	0.763	0.744
$5.00 \cdot 10^{-3}$	0.3000	2	7.00	0.760	0.739
$5.00 \cdot 10^{-3}$	0.3004	2	6.98	0.763	0.746

Table F 14. Initial nominal SDBS concentration, mass of clay, dilution factor, pH and the measured absorbance of samples used in adsorption studies of SDBS on kaolinite in MS w/Ca^{2+} brine.

Initial nominal concentration of SDBS [M]	**Mass of clay [g]**	**Dilution factor**	**pH**	**Absorbance** Baseline – low salinity water	**Absorbance** Baseline – Blank sample
Blank, 0	0.3006	1	4.59	0.025	-
Blank, 0	0.3003	1	4.60	0.016	-
Blank, 0	0.3000	1	4.60	0.017	-
$5.00 \cdot 10^{-5}$	0.3002	1	4.62	0.026	0.003
$5.00 \cdot 10^{-5}$	0.3002	1	4.62	0.019	0.005
$5.00 \cdot 10^{-5}$	0.3006	1	4.62	0.018	0.001
$5.50 \cdot 10^{-5}$	0.3004	1	4.63	0.019	0.008
$5.50 \cdot 10^{-5}$	0.3002	1	4.62	0.018	0.004
$5.50 \cdot 10^{-5}$	0.3005	1	4.63	0.019	0.003
$7.50 \cdot 10^{-5}$	0.3000	1	4.66	0.027	0.007
$7.50 \cdot 10^{-5}$	0.3005	1	4.63	0.029	0.009
$7.50 \cdot 10^{-5}$	0.3004	1	4.64	0.024	0.004
$1.00 \cdot 10^{-4}$	0.3003	1	4.68	0.035	0.014
$1.00 \cdot 10^{-4}$	0.3003	1	4.70	0.030	0.007
$1.00 \cdot 10^{-4}$	0.3003	1	4.70	0.028	0.005
$2.50 \cdot 10^{-4}$	0.2996	1	5.08	0.047	0.048
$2.50 \cdot 10^{-4}$	0.3002	1	5.08	0.053	0.053
$2.50 \cdot 10^{-4}$	0.3001	1	5.10	0.054	0.058
$5.00 \cdot 10^{-4}$	0.3005	1	5.69	0.132	0.115
$5.00 \cdot 10^{-4}$	0.2998	1	5.72	0.126	0.110
$5.00 \cdot 10^{-4}$	0.3000	1	5.69	0.122	0.103
$7.50 \cdot 10^{-4}$	0.2998	1	6.00	0.165	0.145
$7.50 \cdot 10^{-4}$	0.3003	1	6.00	0.174	0.154
$7.50 \cdot 10^{-4}$	0.3002	1	6.06	0.174	0.154
$1.00 \cdot 10^{-3}$	0.3002	1	6.16	0.247	0.225
$1.00 \cdot 10^{-3}$	0.3003	1	6.17	0.248	0.228
$1.50 \cdot 10^{-3}$	0.3007	1	6.15	0.250	0.230
$1.50 \cdot 10^{-3}$	0.3005	1	6.18	0.250	0.230
$2.50 \cdot 10^{-3}$	0.3005	1	6.44	0.706	0.682
$2.50 \cdot 10^{-3}$	0.3005	1	6.45	0.691	0.669
$2.50 \cdot 10^{-3}$	0.3001	1	6.45	0.680	0.659
$3.00 \cdot 10^{-3}$	0.3006	2	6.45	0.719	0.699
$3.00 \cdot 10^{-3}$	0.3003	2	6.47	0.705	0.685
$3.00 \cdot 10^{-3}$	0.3003	2	6.47	0.694	0.674
$5.00 \cdot 10^{-3}$	0.2999	2	6.64	0.736	0.744
$5.00 \cdot 10^{-3}$	0.3002	2	6.63	0.739	0.742
$5.00 \cdot 10^{-3}$	0.3004	2	6.64	0.740	0.745

Appendix G. Results of Adsorption Studies

Table G 1. Calculated SDBS equilibrium concentration ($C_{e\ SDBS}$) and SDBS adsorption (Γ_{SDBS}) with standard deviation, for filtered samples used in adsorption studies of SDBS on kaolinite in LS and MS brine.

Initial nominal concentration of SDBS [M]	**Low salinity**		**Medium salinity**	
	$C_{e\ SDBS}$ [M]	Γ_{SDBS} [mg/g]	$C_{e\ SDBS}$ [M]	Γ_{SDBS} [mg/g]
$1.00 \cdot 10^{-4}$	$1.84 \cdot 10^{-5}$	2.30 ± 0.06	$8.43 \cdot 10^{-5}$	2.1 ± 0.5
$2.50 \cdot 10^{-4}$	$1.42 \cdot 10^{-4}$	3.6 ± 0.7	$1.87 \cdot 10^{-4}$	4.4 ± 0.2
$4.00 \cdot 10^{-4}$	-	-	$3.57 \cdot 10^{-4}$	3.7 ± 0.2
$5.00 \cdot 10^{-4}$	$3.94 \cdot 10^{-4}$	3.2 ± 0.2	$4.88 \cdot 10^{-4}$	2.4 ± 0.2
$6.00 \cdot 10^{-4}$	-	-	$5.94 \cdot 10^{-4}$	3.3 ± 0.2
$7.50 \cdot 10^{-4}$	$7.19 \cdot 10^{-4}$	2.1 ± 0.3	$6.66 \cdot 10^{-4}$	6.6 ± 0.3
$1.00 \cdot 10^{-3}$	$9.16 \cdot 10^{-4}$	3.8 ± 0.4	$8.92 \cdot 10^{-4}$	6.1 ± 0.2
$2.50 \cdot 10^{-3}$	$2.32 \cdot 10^{-3}$	3 ± 1	$2.31 \cdot 10^{-3}$	5.8 ± 0.4

Table G 2.Calculated SDBS equilibrium concentration ($C_{e\ SDBS}$) and SDBS adsorption (Γ_{SDBS}) with standard deviation, for samples used in adsorption studies of SDBS on kaolinite in LS, MS and HS brine.

Initial nominal concentration of SDBS [M]	**Low salinity**		**Medium salinity**		**High salinity**	
	$C_{e\ SDBS}$ [M]	Γ_{SDBS} [mg/g]	$C_{e\ SDBS}$ [M]	Γ_{SDBS} [mg/g]	$C_{e\ SDBS}$ [M]	Γ_{SDBS} [mg/g]
$5.00 \cdot 10^{-5}$	$4.02 \cdot 10^{-6}$	1.6 ± 0.3	$3.81 \cdot 10^{-5}$	2.2 ± 0.2	$7.97 \cdot 10^{-6}$	1.1 ± 0.3
$7.50 \cdot 10^{-5}$	$2.98 \cdot 10^{-5}$	0.8 ± 0.3	$1.12 \cdot 10^{-4}$	0.3 ± 0.4	$2.96 \cdot 10^{-5}$	1.8 ± 0.6
$1.00 \cdot 10^{-4}$	$4.94 \cdot 10^{-5}$	0.8 ± 0.2	$1.29 \cdot 10^{-4}$	0.4 ± 0.5	$6.26 \cdot 10^{-5}$	1.2 ± 0.6
$2.50 \cdot 10^{-4}$	$1.88 \cdot 10^{-4}$	2.30 ± 0.06	$2.13 \cdot 10^{-4}$	2.9 ± 0.6	$1.74 \cdot 10^{-4}$	2.9 ± 0.7
$5.00 \cdot 10^{-4}$	$4.65 \cdot 10^{-4}$	1.5 ± 0.2	$5.10 \cdot 10^{-4}$	1.0 ± 0.5	$4.36 \cdot 10^{-4}$	3.0 ± 0.5
$7.50 \cdot 10^{-4}$	$7.43 \cdot 10^{-4}$	0.25 ± 0.08	$7.64 \cdot 10^{-4}$	0.9 ± 0.3	$6.92 \cdot 10^{-4}$	2.6 ± 0.3
$1.00 \cdot 10^{-3}$	$9.79 \cdot 10^{-4}$	0.36 ± 0.08	$1.02 \cdot 10^{-3}$	0.2 ± 0.2	$9.33 \cdot 10^{-4}$	3.6 ± 0.4
$2.50 \cdot 10^{-3}$	$2.35 \cdot 10^{-3}$	1.6 ± 0.2	$2.37 \cdot 10^{-3}$	0.86 ± 0.08	$2.35 \cdot 10^{-3}$	3.6 ± 0.2

Table G 3. Calculated SDBS equilibrium concentration ($C_{e\ SDBS}$) SDBS adsorption (Γ_{SDBS}) with standard deviation, used in adsorption studies of SDBS on kaolinite in LS w/Ca^{2+} brine.

Initial nominal concentration of SDBS [M]	**Start of adsorption experiment**		**End of adsorption experiment**	
	$C_{e\ SDBS}$ [M]	Γ_{SDBS} [mg/g]	$C_{e\ SDBS}$ [M]	Γ_{SDBS} [mg/g]
$5.00 \cdot 10^{-5}$	-	-	$3.08 \cdot 10^{-5}$	0.2 ± 0.1
$7.50 \cdot 10^{-5}$	-	-	$4.54 \cdot 10^{-5}$	0.58 ± 0.06
$1.00 \cdot 10^{-4}$	-	-	$6.06 \cdot 10^{-5}$	0.8 ± 0.2
$2.50 \cdot 10^{-4}$	$2.10 \cdot 10^{-4}$	0.9 ± 0.4	$1.67 \cdot 10^{-4}$	2.0 ± 0.1
$5.00 \cdot 10^{-4}$	$4.60 \cdot 10^{-4}$	1.6 ± 0.5	$3.98 \cdot 10^{-4}$	19.3 ± 0.3
$5.50 \cdot 10^{-4}$	$5.08 \cdot 10^{-4}$	3.5 ± 0.2	$6.86 \cdot 10^{-4}$	27.1 ± 0.3
$7.50 \cdot 10^{-4}$	$8.01 \cdot 10^{-4}$	5.7 ± 0.3	-	-
$1.00 \cdot 10^{-3}$	$1.02 \cdot 10^{-3}$	3.5 ± 0.8	$9.29 \cdot 10^{-4}$	17.4 ± 0.3

Table G 4. Calculated SDBS equilibrium concentration ($C_{e\ SDBS}$) SDBS adsorption (Γ_{SDBS}) with standard deviation, used in adsorption studies of SDBS on kaolinite in MS w/Ca^{2+} brine.

Initial nominal concentration of SDBS [M]	**Start of adsorption experiment**		**End of adsorption experiment**	
	$C_{e\ SDBS}$ [M]	Γ_{SDBS} [mg/g]	$C_{e\ SDBS}$ [M]	Γ_{SDBS} [mg/g]
$5.00 \cdot 10^{-5}$	-	-	$5.35 \cdot 10^{-6}$	0.9 ± 0.2
$5.50 \cdot 10^{-5}$	$9.82 \cdot 10^{-6}$	1.0 ± 0.2	$9.82 \cdot 10^{-6}$	0.9 ± 0.2
$7.50 \cdot 10^{-5}$	-	-	$1.35 \cdot 10^{-5}$	1.3 ± 0.2
$1.00 \cdot 10^{-4}$	-	-	$1.80 \cdot 10^{-5}$	1.8 ± 0.4
$2.50 \cdot 10^{-4}$	$1.17 \cdot 10^{-4}$	2.9 ± 0.4	$1.17 \cdot 10^{-4}$	9.0 ± 0.4
$5.00 \cdot 10^{-4}$	-	-	$2.43 \cdot 10^{-4}$	35.0 ± 0.5
$7.50 \cdot 10^{-4}$	$3.36 \cdot 10^{-4}$	29.0 ± 0.4	$3.36 \cdot 10^{-4}$	49.6 ± 0.4
$1.00 \cdot 10^{-3}$	-	-	$5.04 \cdot 10^{-4}$	70.6 ± 0.2
$1.50 \cdot 10^{-3}$	$5.12 \cdot 10^{-4}$	35.80 ± 0.04	$5.12 \cdot 10^{-4}$	75.58 ± 0.04
$2.50 \cdot 10^{-3}$	-	-	$1.49 \cdot 10^{-3}$	133.5 ± 0.7
$3.00 \cdot 10^{-3}$	$3.06 \cdot 10^{-3}$	17 ± 2	$3.06 \cdot 10^{-3}$	62.5 ± 2

Appendix H. SDBS Adsorption Isotherms

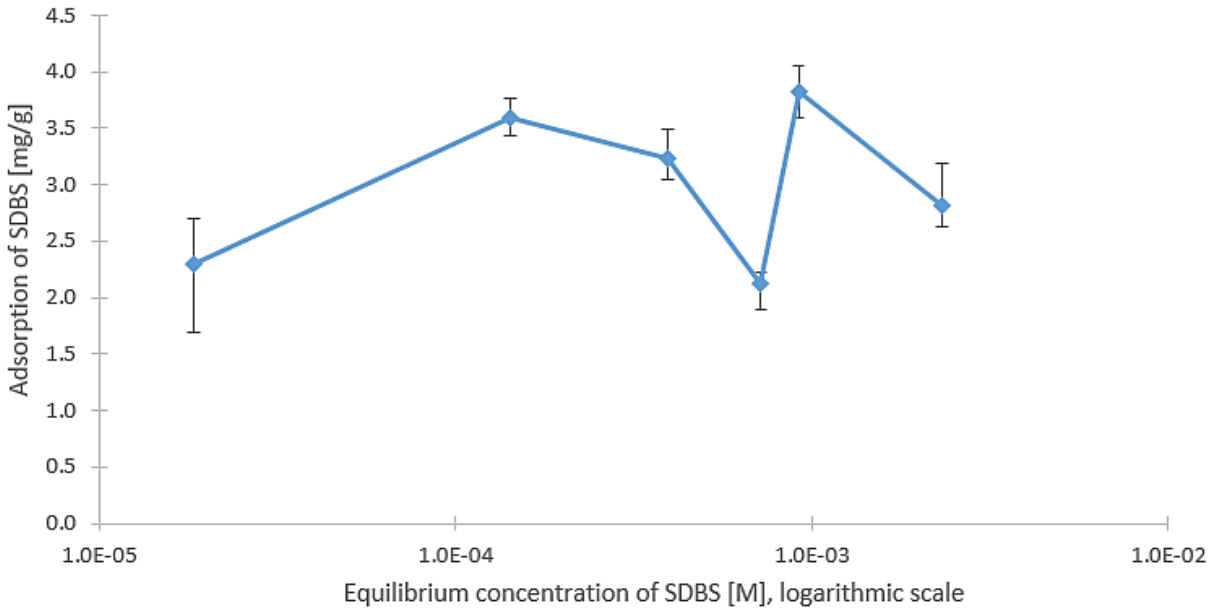

Figure H 1. Adsorption isotherm of SDBS in filtered LS samples. Adsorption of SDBS on kaolinite as a function of equilibrium SDBS concentration (logarithmic) based on analysis conducted with an UV-vis spectrophotometer at 260 nm.

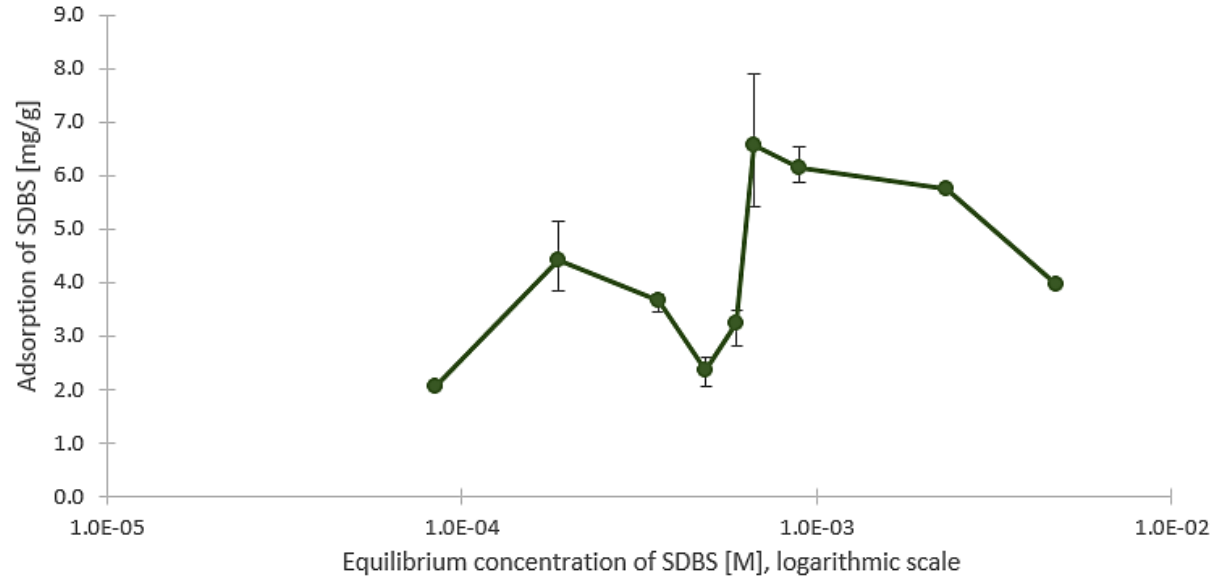

Figure H 2. Adsorption isotherm of SDBS in filtered MS samples. Adsorption of SDBS on kaolinite as a function of equilibrium SDBS concentration (logarithmic) based on analysis conducted with an UV-vis spectrophotometer.

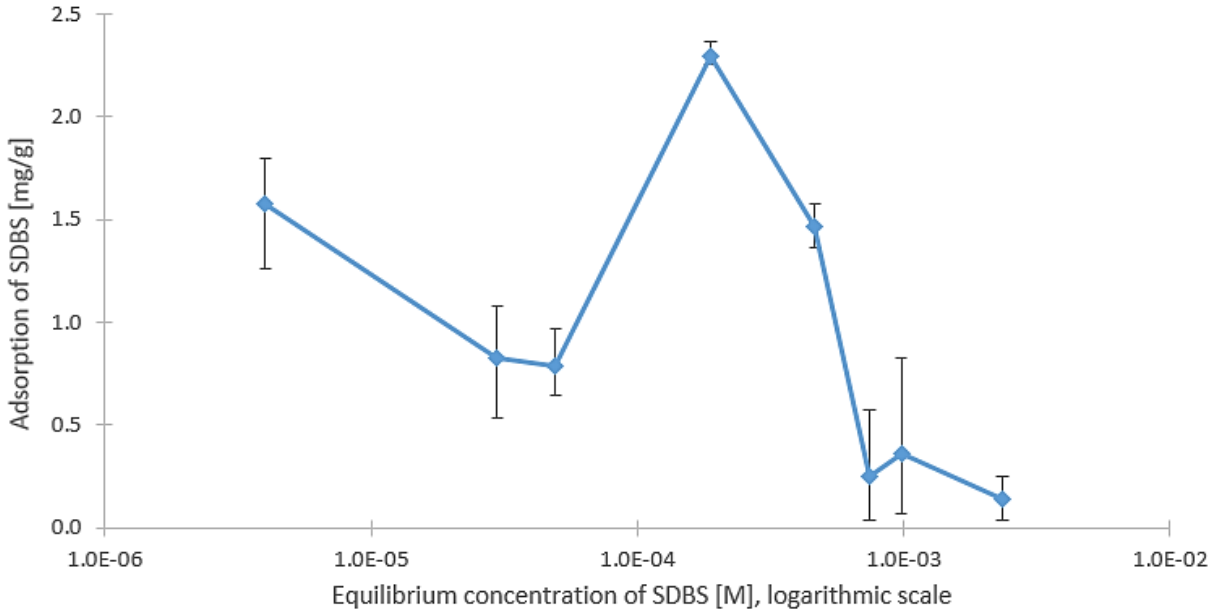

Figure H 3. Adsorption isotherm of SDBS in LS brine. Adsorption of SDBS on kaolinite as a function of equilibrium SDBS concentration based on analysis conducted with an UV-vis spectrophotometer at 260 nm.

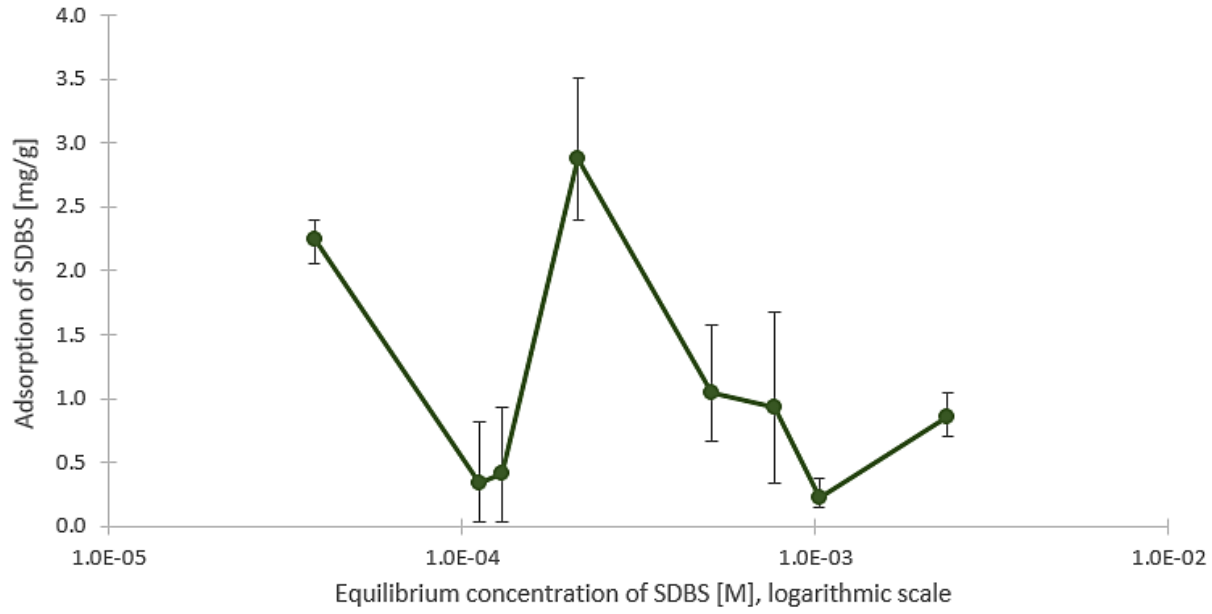

Figure H 4. Adsorption isotherm of SDBS in MS brine. Adsorption of SDBS on kaolinite as a function of equilibrium SDBS concentration based on analysis conducted with an UV-vis spectrophotometer at 260 nm.

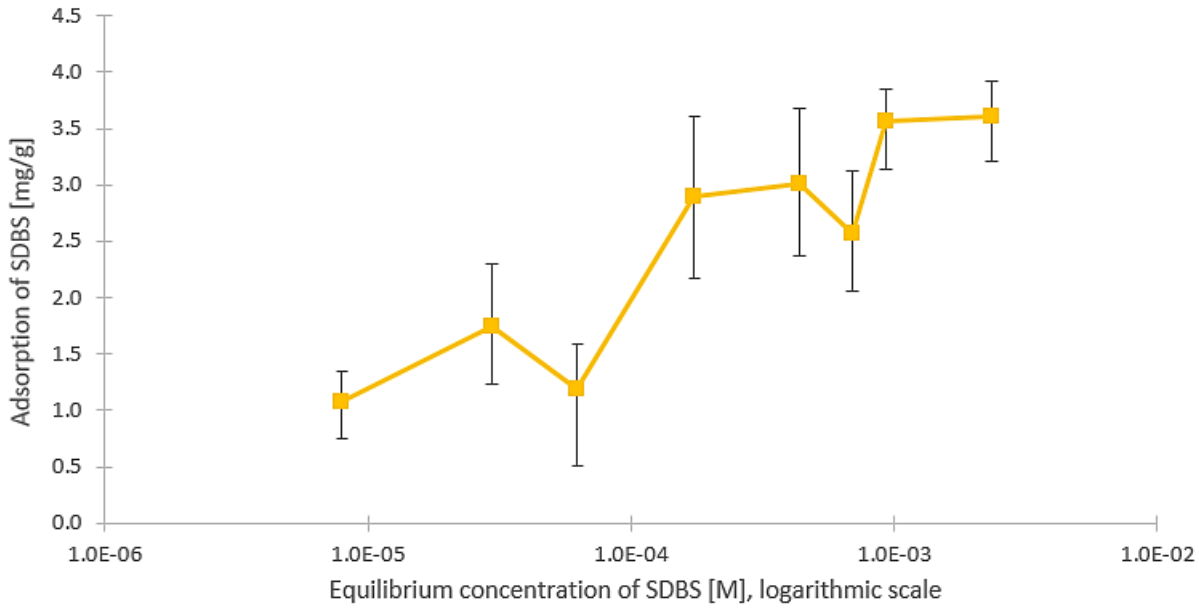

Figure H 5. Adsorption isotherm of SDBS in HS brine. Adsorption of SDBS on kaolinite as a function of equilibrium SDBS concentration based on analysis conducted with an UV-vis spectrophotometer at 260 nm.

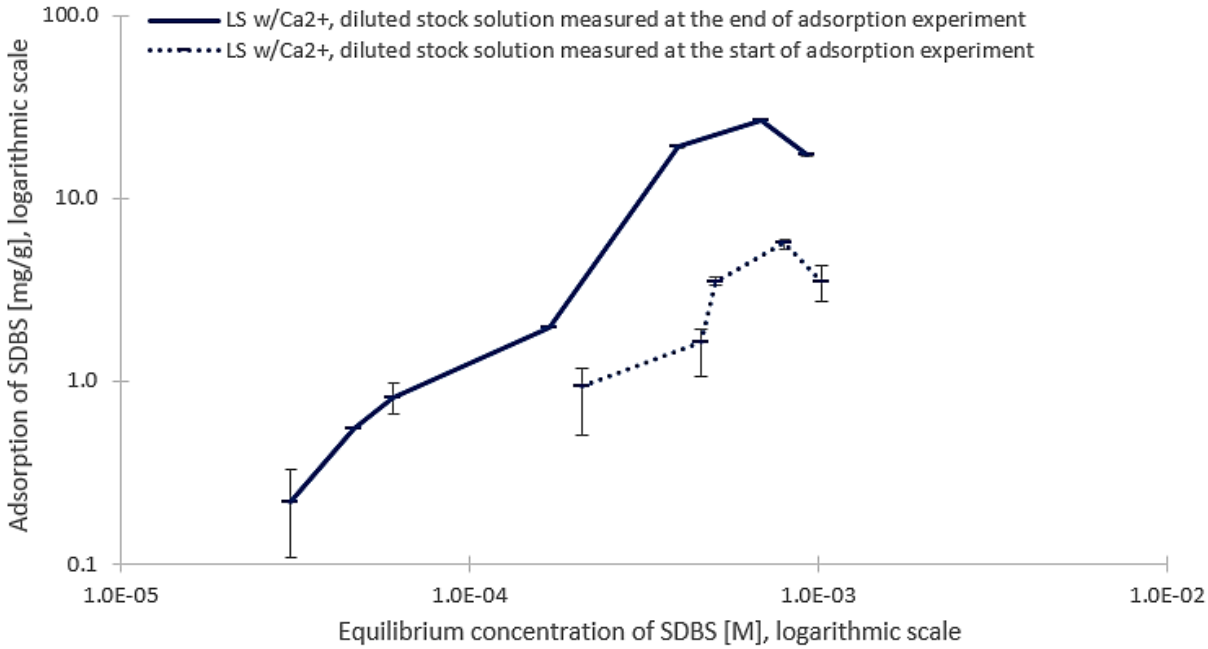

Figure H 6. Adsorption isotherm of SDBS in LS w/Ca^{2+} brine. Adsorption of SDBS on kaolinite as a function of equilibrium SDBS concentration based on analysis conducted with an UV-vis spectrophotometer at 260 nm. Both scales are logarithmic.

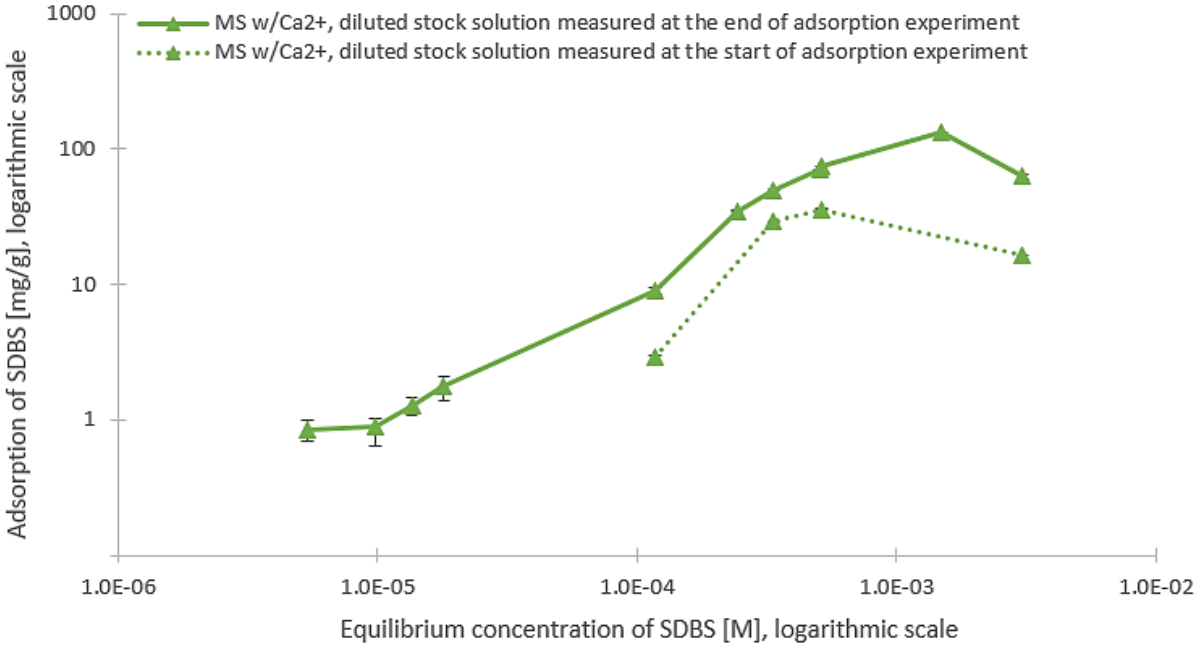

Figure H 7. Adsorption isotherm of SDBS in MS w/Ca^{2+} brine. Adsorption of SDBS on kaolinite as a function of equilibrium SDBS concentration based on analysis conducted with an UV-vis spectrophotometer at 260 nm. Both scales are logarithmic.